T.R.
GEBZE TECHNICAL UNIVERSITY
GRADUATE SCHOOL OF NATURAL AND APPLIED SCIENCES

EVALUATION OF NONLINEAR PERFORMANCE ASSESSMENT METHODS FOR BUILDINGS WITH FLEXIBLE SLABS

OSLEINER ENRIQUE GONZALEZ VALDEZ

A THESIS SUBMITTED FOR THE DEGREE OF
MASTER OF SCIENCE
DEPARTMENT OF CIVIL ENGINEERING
EARTHQUAKE AND STRUCTURAL ENGINEERING PROGRAM

GEBZE
2017

T.R.
GEBZE TECHNICAL UNIVERSITY
GRADUATE SCHOOL OF NATURAL AND APPLIED SCIENCES

EVALUATION OF NONLINEAR PERFORMANCE ASSESSMENT METHODS FOR BUILDINGS WITH FLEXIBLE SLABS

OSLEINER ENRIQUE GONZALEZ VALDEZ

A THESIS SUBMITTED FOR THE DEGREE OF
MASTER OF SCIENCE
DEPARTMENT OF CIVIL ENGINEERING
EARTHQUAKE AND STRUCTURAL ENGINEERING PROGRAM

THESIS SUPERVISOR
PROF. DR. YASIN FAHJAN
II. THESIS SUPERVISOR
ASSIST. PROF. DR. FERHAT PAKDAMAR

GEBZE
2017

T.C.
GEBZE TEKNİK ÜNİVERSİTESİ
FEN BİLİMLERİ ENSTİTÜSÜ

BOŞLUKLU DÖŞEMELİ BİNALARIN DOĞRUSAL OLMAYAN PERFORMANS DEĞERLENDİRME YÖNTEMLERİNİN İNCELENMESİ

OSLEINER ENRIQUE GONZALEZ VALDEZ

YÜKSEK LİSANS TEZİ

İNŞAAT MÜHENDİSLİĞİ ANABİLİM DALI
DEPREM VE YAPI MÜHENDİSLİĞİ PROGRAMI

DANIŞMANI
PROF. DR. YASİN FAHJAN
II. DANIŞMANI
YRD. DOÇ. FERHAT PAKDAMAR

GEBZE
2017

GEBZE TEKNİK ÜNİVERSİTESİ	**YÜKSEK LİSANS JÜRİ ONAY FORMU**

GTÜ Fen Bilimleri Enstitüsü Yönetim Kurulu'nun 21/06/2017 tarih ve 2017/33 sayılı kararıyla oluşturulan jüri tarafından 21/07/2017 tarihinde tez savunma sınavı yapılan Osleiner Enrique Gonzalez Valdez'ın tez çalışması İnşaat Mühendisliği Anabilim Dalı Deprem ve Yapı Mühendisliği Programında YÜKSEK LİSANS tezi olarak kabul edilmiştir.

JÜRİ

ÜYE
(TEZ DANIŞMANI) : Prof.Dr. Yasin FAHJAN

ÜYE
(II DANIŞMANI) : Yrd. Doç. Dr. Ferhat PAKDAMAR

ÜYE : Yrd. Doç. Dr. Abdullah Can ZÜLFİKAR

ÜYE : Yrd. Doç. Dr. Ahmet Anıl DİNDAR

ÜYE : Yrd. Doç. Dr. Erkan AKPINAR

ONAY

Gebze Teknik Üniversitesi Fen Bilimleri Enstitüsü Yönetim Kurulu'nun
……./……./……… tarih ve ………/…….. sayılı kararı.

İMZA/MÜHÜR

Doç. Dr. Arif Çağdaş AYDINOĞLU
Gebze Teknik Üniversitesi
Fen Bilimleri Enstitüsü Müdürü

SUMMARY

The traditional method used to design structures subjected to earthquakes is the force method that applies forces along the height of the building to simulate the effect of earthquakes. However, recent investigations have developed more realistic methods, such as linear dynamic, nonlinear static and nonlinear dynamic methods.

In this research, nonlinear static method (Pushover) was tested with irregular buildings. Discontinuity in diaphragm was the irregularity selected.

The buildings selected are six-story reinforced concrete buildings. The slabs in all the stories have open areas between 20% and 60% of the total area.

Each building was designed using linear method, modal response spectrum analysis, and then analyzed using nonlinear static method (Pushover), using the procedures specified in ASCE-41-13, EN 1998-3 and TBDY-16. Performance levels were assigned to each element and to the whole structures.

The Structures were modeled using SAP2000 for the analysis, the models had to be necessarily 3 dimensional and must consider the flexibility of diaphragms, because of the discontinuities in them. The slabs were modeled as membranes, as specified in seismic codes, considering the effective stiffness for cracked sections.

Although a membrane is a good approach to consider the slab flexibility, for the structures analyzed membranes showed a behavior almost rigid, furthermore; it was found that if the shear stiffness in membranes (F12) is reduced, the flexibility desired is fulfilled and the results obtained are more realistic.

In terms of performance level, the results according to the three codes show that structures with discontinuity in diaphragms, designed with linear methods, and subjected to the design earthquake, may experience extensive damage, repairs may be required before reoccupancy but they remain stable and have reserve capacity. Although the performance levels obtained in the three codes are equivalent, according to percentage of elements on each performance level, TBDY-16 is the one which shows more damage. Therefore, for seismic performance assessment TBDY-16 is found as more conservative than ASCE-41-13 and EN 1998-3.

Key Words: Earthquake, Reinforced Concrete, Pushover, Structural Irregularity, Flexible Diaphragm, Membrane, Performance Level.

ÖZET

Deprem etkisinde olan binaların tasarımında en yaygın kullanılan yöntem kuvvete dayalı bir yöntemdir. Bu yöntem ile depremin etkisini simülize etmek için binanın yüksekliği boyunca kuvvetler uygulanmaktadır. Fakat, son yıllardaki araştırmalar sayesinde daha gerçekçi yöntemler oluşturulmuştur. Doğrusal olmayan itme ve zaman tanım alanında doğrusal olmayan yöntemler birer örnektir.

Bu araştırmada, doğrusal olmayan itme yöntemi düzensiz binalarla test edilmiştir. Seçilen düzensizlik, süreksizlik diyaframıdır.

Seçilen binalar altı katlı betonarme binalardır. Bütün döşemelerde toplam alanın %20'si ile %60'ı arasında boşluk alan vardır.

Her bina, doğrusal olan mod birleştirme yöntemi kullanılarak tasarlanmıştır ve sonrasında ASCE-41-13, EN 1998-3 ve TBDY-16'ya göre doğrusal olmayan itme yöntemi ile analiz edilmiştir. Her elemanın ver her binanın performans seviyesi belirlenmiştir ve sonunda bu sonuçlar karşılaştırılmıştır.

SAP2000 kullanılarak yapılar modellenmiştir, diyaframda süreksizlik bulunduğu için, modellerin 3 boyutlu olması ve diyaframların rijit olmayan davranışının göz önüne alınması gerekli olmuştur. Deprem yönetmeliklerinde belirtildiği gibi, çatlamış kesitler için etkin rijitliği kullanılarak, döşemeler membran olarak modellenmiştir.

Membran yöntemi, rijit olmayan davranışı elde etmek için uygun bir yöntem olmasına rağmen, analiz edilmiş olan yapılar neredeyse rijit davranış göstermiştir, ayrıca, membranın kesme rijitliği (F12) azaltılarak gerçekte beklenen rijit olmayan davranışın elde edilebildiği gözlemlenmiştir.

Performans seviyesinin sonuçları konusunda, üç yönetmeliğe göre, doğrusal yöntem kullanılarak tasarlanmış olan binalar, tasarım depremi etkisi altında hasar görebilir ve kullanmadan önce güçlendirilmesi gerekli olabilir, fakat, göçme olmayacaktır. Üç yönetmeliğe göre performans durumu denk olmasına rağmen, her performans düzeyinde bulunan elemanların sayısına göre, en fazla hasar gösteren TBDY-16'dır. Sonuç olarak, TBDY-16 daha güvenli tarafta kalmaktadır.

Anahtar Kelimeler: Deprem, Betonarme, İtme analizi, Yapı düzensizliği, Rijit Olmayan Diyafram, Membran, Performans seviyesi.

ACKNOWLEDGEMENTS

To my supervisors, Prof. Dr. Yasin FAHJAN and Asst. Prof. Dr. Ferhat PAKDAMAR.

To the jury committee members, Asst. Prof. Dr. Abdullah Can ZÜLFİKAR, Asst. Prof. Dr. Ahmet Anıl DİNDAR and Asst. Prof. Dr. Erkan AKPINAR.

To my parents, brother, sisters and to my fiancee.

TABLE of CONTENTS

	Page
SUMMARY	v
ÖZET	vi
ACKNOWLEDMENTS	vii
TABLE of CONTENTS	viii
LIST of ABBREVIATIONS and ACRONYMS	x
LIST of FIGURES	xii
LIST of TABLES	xi
1. INTRODUCTION	1
1.1. Literature review	2
1.2. Purpose and Scope	4
2. GENERAL REQUIREMENTS FOR NONLINEAR PERFORMANCE ASSESSMENT	5
2.1 ASCE-41-13	5
2.1.1. Performance Objectives	5
2.1.2. Structural Model	11
2.1.3. Nonlinear Static (Pushover) Procedure	14
2.1.4. Acceptance criteria	17
2.2 Eurocode EN 1998-3	21
2.2.1. Target Building Performance Levels	21
2.2.2. Seismic Hazard	21
2.2.3. Response Spectrum	22
2.2.4. Structural Model	24
2.2.5. Nonlinear Static (Pushover) Procedure	26
2.2.6. Acceptance criteria	31
2.3 Turkish Seismic Code (TBDY-16)	34
2.3.1. Performance Objectives	34
2.3.2. Structural Model	38
2.3.3. Nonlinear Static (Pushover) Procedure	40
2.3.4. Performance Levels	45

2.4 Comparison of General Requirements for Nonlinear Performance Assessment 50
2.4.1. Target Building Performance levels 50
2.4.2. Seismic Hazard 51
2.4.3. Response Spectrum 51
2.4.4. Structural Model 53
2.4.5. Nonlinear Static (Pushover) Procedure 55
2.4.6. Acceptance Criteria 58
3. STUDY CASE 59
3.1. Description of the studied Buildings 59
3.1.1. Geometry 59
3.1.2. Material 60
3.1.3. Loading 60
3.2. Analysis Methodology 68
3.2.1. Seismic Hazard 68
3.2.2. Response Spectrum 68
3.2.3. Structural Model 69
3.2.4. Modal Analysis 70
3.2.5. Flexibility in slabs 78
3.2.6. Force-Displacement curves 80
3.2.7. Target displacements 84
3.2.8. Pushover until target displacements 99
3.2.9. Performance Levels 103
3.3. Analysis Results 114
4. CONCLUSION 116

REFERENCES 118
BIOGRAPHY 120
APPENDICES 121

LISTof ABBREVIATIONS and ACRONYMS

Abbreviations and Acronyms		**Explanations**
A_g	:	Gross area of element, ASCE-41-13
A_v	:	Area of shear reinforcement, ASCE-41-13
a_1	:	Spectral acceleration of the equivalent single degree of freedom (SDOF) system, TBDY-16
a	:	Site class factor, ASCE-41-13
a_g	:	Ground acceleration, EN 1998-3
a_{y1}	:	Effective yielding equivalent acceleration, TBDY-16
b_w	:	Web width, ASCE-41-13, TBDY-16
B_1	:	Damping coefficient used to adjust spectral response for the effect of viscous damping, ASCE-41-13
CG	:	Life safety performance level, TBDY-16
CP	:	Collapse prevention performance level, ASCE-41-13
C_0	:	Modification factor to relate spectral displacement of an equivalent single degree of freedom (SDOF) system to the roof displacement of the building multi degree of freedom (MDOF) system, ASCE-41-13
C_1	:	Modification factor to relate expected maximum inelastic displacement to displacements calculated for linear elastic response, ASCE-41-13
C_2	:	Modification factor to represent the effect of pinched hysteresis shape and cyclic stiffness degradation, ASCE-41-13
C_m	:	Modal mass participation factor, ASCE-41-13
C_R		Spectral displacement ratio, TBDY-16
c_u	:	Undrained shear strength of the upper 30 m of soils at the site, ASCE-41-13, EN 1998-3, TBDY-16
DL	:	Damage limitation performance level, EN 1998-3
d	:	Distance from extreme compression fiber to centroid of tension reinforcement, ASCE-41-13, EN 1998-3, TBDY-16

$d_{1,max}$	:	Target displacement, TBDY-16
d'	:	Distance from extreme tension fiber to centroid of compression reinforcement, EN 1998-3
d_{bL}	:	Mean diameter of the tension reinforcement, EN 1998-3
d_n	:	Displacement of the control node of the multi degree of freedom (MDOF) system, EN 1998-3
d^*	:	Displacement of the equivalent single degree of freedom (SDOF) system, EN 1998-3
d_{et}^*	:	Elastic target displacement, EN 1998-3
d_m^*	:	Displacement at the formation of plastic mechanism, EN 1998-3
d_t^*	:	Inelastic target displacement, EN 1998-3
d_y^*	:	Yield displacement, EN 1998-3
E_c	:	Modulus of elasticity of concrete, ASCE-41-13
E_m^*	:	Actual deformation energy up to the formation of the plastic mechanism, EN 1998-3
F_a	:	Factor to adjust spectral acceleration in the short-period range for site class, ASCE-41-13
F_S	:	Factor to adjust spectral acceleration in the short-period range for site class, TBDY-16
F11	:	Internal axial force along axis 1 in membranes
F22	:	Internal axial force along axis 2 in membranes
F12, F21	:	Internal shear forces in membranes
F_b	:	Base shear force, EN 1998-3
F_v	:	Factor to adjust spectral acceleration at 1 s for site class, ASCE-41-13
F_1	:	Factor to adjust spectral acceleration at 1 s for site class, TBDY-16
F^*	:	Base shear force of the equivalent single degree of freedom (SDOF) system, EN 1998-3
F_y^*	:	Yield force, EN 1998-3
f_{ctm}	:	Tension Strength of concrete, TBDY-16
f_y	:	Yield stress of reinforcing steel, EN 1998-3
f'_c	:	Compressive strength of concrete, ASCE-41-13, EN 1998-3
G	:	Permanent action, EN 1998-3

GC	:	Collapse performance level, TBDY-16
GO	:	Collapse prevention performance level, TBDY-16
GV	:	Safety performance level, TBDY-16
g	:	Acceleration of gravity, ASCE-41-13
HK	:	Immediate occupancy performance level, TBDY-16
h	:	Height of the member along which deformations are measured, EN 1998-3, TBDY-16
h	:	Story height, Chapter 7
IO	:	Immediate occupancy performance level, ASCE-41-13
I_{cr}	:	Moment of inertia of cracked concrete section, EN 1998-3
I_g	:	Moment of inertia of gross concrete section about centroidal axis, neglecting reinforcement, ASCE-41-13, EN 1998-3
KK	:	Operational Performance Level, TBDY-16
K_e	:	Effective stiffness of the building, ASCE-41-13
K_i	:	Elastic lateral stiffness of the building, ASCE-41-13
L	:	Length of the element, EN 1998-3
L_F	:	Orthogonal distance to the nearest fault, TBDY-16
L_p	:	Plastic hinge length, TBDY-16
L_{pL}	:	Plastic hinge length, EN 1998-3
LS	:	Life safety performance level, ASCE-41-13
L_V	:	Shear span, moment/shear ratio, EN 1998-3
l	:	Span length of one-way ribbed slab
M	:	Design moment from Nonlinear Static Procedure (Pushover), EN 1998-3
MN	:	Minimum damage performance level, TBDY-16
M_{nb}	:	Nominal moment strength at beam section, ASCE-41-13
M_{nc}	:	Nominal moment strength at column section, ASCE-41-13
M_y	:	Yielding moment, EN 1998-3
m_i	:	Mass at level i, EN 1998-3
m_t	:	Mass of the equivalent single degree of freedom (SDOF), TBDY-16
m^*	:	Mass of the equivalent single degree of freedom (SDOF), EN 1998-3

N	:	Average standard penetration test (SPT) of the upper 30 m of soils at the site, ASCE-41-13, EN 1998-3, TBDY-16
NC	:	Near collapse performance level, EN 1998-3
n	:	Live load mass contribution coefficient, TBDY-16
P	:	Axial load in concrete column, ASCE-41-13
Q	:	Variable action, EN 1998-3
Q_D	:	Action caused by dead load, ASCE-41-13
Q_G	:	Action caused by gravity loads, ASCE-41-13
Q_L	:	Action caused by live load, ASCE-41-13
q_u	:	Ratio between the acceleration in the structure with unlimited elastic behaviour, $S_e(T^*)$, and in the structure with limited strength, F^*_y / m*, EN 1998-3
R	:	Seismic response modification coefficient
R_y	:	Strength reduction factor, TBDY-16
S	:	Soil factor, EN 1998-3
S_1	:	Spectral response acceleration parameter at a one-second period, ASCE-41-13, TBDY-16
SD	:	Significant damage performance level, EN 1998-3
S_a	:	Spectral response acceleration, ASCE-41-13
S_{ae}	:	Spectral response acceleration, TBDY-16
$S_{ae}(T_1)$	:	Response spectrum acceleration at the fundamental period, TBDY-16
$S_a(T_e)$	:	Response spectrum acceleration at the effective fundamental period, ASCE-41-13
S_{D1}	:	Spectral response acceleration parameter at a one-second period, adjusted for site class, TBDY-16
S_{DS}	:	Spectral response acceleration parameter at short periods, adjusted for site class, TBDY-16
$S_{de}(T_1)$	:	Elastic response spectrum displacement at the fundamental period, TBDY-16
$S_{di}(T_1)$	:	Inelastic response spectrum displacement at the fundamental period, TBDY-16
S_e	:	Spectral response acceleration, EN 1998-3

$S_e(T^*)$	:	Elastic acceleration response spectrum displacement at the equivalent period, T*, EN 1998-3
S_S	:	Spectral response acceleration parameter at short periods, ASCE-41-13, TBDY-16
S_{XS}	:	Spectral response acceleration parameter at short periods, adjusted for site class, ASCE-41-13
S_{X1}	:	Spectral response acceleration parameter at a one-second period, adjusted for site class, ASCE-41-13
s	:	Spacing of shear reinforcement, ASCE-41-13
T	:	Fundamental period of the building in the direction of consideration, ASCE-41-13, EN 1998-3, TBDY-16
T_0	:	Lower limit of the period of the constant spectral acceleration branch, ASCE-41-13
T_A	:	Lower limit of the period of the constant spectral acceleration branch, TBDY-16
T_B	:	Lower limit of the period of the constant spectral acceleration branch, EN 1998-3
T_B	:	Upper limit of the period of the constant spectral acceleration branch, TBDY-16
T_C	:	Upper limit of the period of the constant spectral acceleration branch, EN 1998-3
T_D	:	Period for which horizontal displacement spectrum become constant, EN 1998-3
T_e	:	Effective fundamental period of the building in the direction under consideration, ASCE-41-13
T_i	:	Elastic fundamental period in the direction under consideration calculated by elastic dynamic analysis, ASCE-41-13
T_S	:	Upper limit of the period of the constant spectral acceleration branch, ASCE-41-13
T_L	:	Period for which horizontal displacement spectrum become constant, ASCE-41-13, TBDY-16
T^*	:	Period of the equivalent single degree of freedom (SDOF) system, EN 1998-3

u_N : Displacement of the control node of the multi degree of freedom (MDOF) system, TBDY-16

V : Design shear force from Nonlinear Static Procedure (Pushover), ASCE-41-13, EN 1998-3, TBDY-16

V_0 : Shear strength of column, ASCE-41-13

V_d : Base shear at Δ_d, ASCE-41-13

V_p : Shear force at the development of the flexural capacity, ASCE-41-13

V_t : Base shear force, TBDY-16

V_y : Effective yield strength of the building, ASCE-41-13

v_s : Average shear wave velocity of the upper 30 m of soils at the site, ASCE-41-13, EN 1998-3, TBDY-16

W : Effective seismic weigth, ASCE-41-13

w : Action caused by gravity loads, TBDY-16

w_G : Action caused by dead load, TBDY-16

w_Q : Action caused by live load, TBDY-16

Δ : Story drift

Δ_avg : Average Story Drift, ASCE-41-13

Δ_d : Lesser of the target displacement or displacement corresponding to the maximum base shear, ASCE-41-13

Δ_dia : Diaphragm deformation

Δ_y : Displacement at effective yield strength, ASCE-41-13

$(\Delta_\mathrm{i})_\mathrm{max}$: Maximum Story drift in floor i, TBDY-16

$(\Delta_\mathrm{i})_\mathrm{min}$: Minimum Story drift in floor i, TBDY-16

$(\Delta_\mathrm{i})_\mathrm{ort}$: Average Story drift in floor i, TBDY-16

Γ : Modal participation factor, EN 1998-3, TBDY-16

β : Effective viscous damping ratio, ASCE-41-13

γ_F : Distance to fault coefficient, TBDY-16

δ_t : Target displacement, ASCE-41-13

ε_y : Yield strain of reinforcing steel, EN 1998-3

$(\varepsilon_\mathrm{cg})$: Compression strain in extreme confined concrete fiber, TBDY-16

$(\varepsilon_\mathrm{cu})$: Compression strain in extreme concrete fiber, TBDY-16

(ε_s)	:	Strain in the extreme layer of longitudinal tension reinforcement, TBDY-16
ξ	:	Viscous damping ratio, expressed as a percentage, EN 1998-3
η	:	Damping correction factor, EN 1998-3
η_{bi}	:	Torsion irregularity coefficient in floor i, TBDY-16
θ_P	:	Plastic rotation
θ_{um}	:	Near collapse performance total chord rotation (elastic + plastic), EN 1998-3
θ_{SD}	:	Significant damage performance total chord rotation (elastic + plastic), EN 1998-3
θ_y	:	Chord rotation at yield, EN 1998-3
μ	:	Seismic ductility demand, TBDY-16
$\mu_{strength}$	:	Ratio of elastic strength demand to yield strength, ASCE-41-13
ρ	:	Ratio of tension reinforcement, ASCE-41-13
ρ_{bal}	:	Reinforcement ratio producing balanced strain conditions, ASCE-41-13
ρ'	:	Ratio of compression reinforcement, ASCE-41-13
Φ_i	:	Modal displacement at level i, EN 1998-3, TBDY-16
Φ_N	:	Modal displacement at the last floor, TBDY-16
ϕ_u	:	Ultimate curvature, EN 1998-3
ϕ_t	:	Total curvature, TBDY-16
ϕ_y	:	Yield curvature, EN 1998-3, TBDY-16
ω_1	:	Fundamental angular frequency, TBDY-16
ω_B	:	Characteristic angular frequency of the response spectrum, TBDY-16
Ω	:	Overstrength Factor

LIST of FIGURES

FigureNo:		**Page**
1.1:	Typical floor plan of Eight-Span Three-Story Structure.	2
1.2:	Typical floor plan of Three-Story Building.	3
2.1:	Target building Performance Levels.	7
2.2:	General Horizontal Response Spectrum.	8
2.3:	Deformations in Diaphragms.	13
2.4:	Idealized Force-Displacement Curve.	15
2.5:	Performance Assessment Procedure in ASCE-41-13.	20
2.6:	Shape of the Elastic Response Spectrum.	22
2.7:	Bilinear equivalent SDOF Force-Displacement curve.	28
2.8:	Determination of target displacement for the equivalent SDOF system (Medium and long period range).	30
2.9:	Determination of target displacement for the equivalent SDOF system (Short range).	31
2.10:	Chord Rotation.	31
2.11:	Performance Assessment Procedure in EN 1998-3.	33
2.12:	General Horizontal Response Spectrum.	35
2.13:	Internal forces in membranes.	40
2.14:	Determination of Inelastic displacement demand ($T_1 > T_B$).	43
2.15:	Bilinear SDOF Force-Displacement Curve.	44
2.16:	Determination of Inelastic displacement demand ($T_1 < T_B$).	45
2.17:	Damage levels in sections and elements.	46
2.18:	Performance Assessment Procedure in TBDY-16.	49
2.19:	Response Spectrum Comparison (S_S=1.06, S_1=0.39, a_g=0.4, Soil: Rock).	52
2.20:	Response Spectrum Comparison (S_S=1.06, S_1=0.39, a_g=0.4, Soil: Sand).	53
3.1:	Typical floor plan for 6 story Structure 1 (20%).	61
3.2:	Sections of the elements in Structure 1 (20%).	61
3.3:	Typical floor plan for 6 story Structure 2 (30%).	62

3.4: Sections of the elements in Structure 2 (30%). 62
3.5: Typical floor plan for 6 story Structure 3 (40%). 63
3.6: Sections of the elements in Structure 3 (40%). 63
3.7: Typical floor plan for 6 story Structure 4 (50%). 64
3.8: Sections of the elements in Structure 4 (50%). 64
3.9: Typical floor plan for 6 story Structure 5 (60%). 65
3.10: Sections of the elements in Structure 5 (60%). 65
3.11: Typical Slab Plan. 66
3.12: Slab section in Structure 1, Structure 2 and Structure 3. 66
3.13: Slab section in Structure 4 and Structure 5. 66
3.14: Three dimensional SAP models. 67
3.15: Response Spectrum. 69
3.16: Load distribution in slabs. 69
3.17: Modal participating mass ratios, Structure 3. 71
3.18. Shear Story resulting from first mode, Structure 3, direction x. 72
3.19: Shear Story resulting from ten modes, Structure 3, direction x. 72
3.20: Pushover curve from SAP2000, Structure 1, direction x, ASCE-41-13. 80
3.21: Pushover curve, Structure 1, Mode 1 (y direction). 81
3.22: Pushover curve, Structure 1, Mode 2 (x direction). 81
3.23: Pushover curve, Structure 2, Mode 1 (x direction). 82
3.24: Pushover curve, Structure 2, Mode 2 (y direction). 82
3.25: Pushover curve, Structure 3, Mode 1 (x direction). 82
3.26: Pushover curve, Structure 3, Mode 2 (y direction). 83
3.27: Pushover curve, Structure 4, Mode 1 (y direction). 83
3.28: Pushover curve, Structure 4, Mode 2 (x direction). 83
3.29: Pushover curve, Structure 5, Mode 1 (y direction). 84
3.30: Pushover curve, Structure 5, Mode 2 (x direction). 84
3.31: Bilinear Pushover curve, Structure 3, direction x, first iteration. 85
3.32: Bilinear Pushover curve, Structure 3, direction x, second iteration. 86
3.33: Bilinear Pushover curve, Structure 1, direction x, first iteration. 88
3.34: Target displacement computation, Structure 1, direction x, first iteration. 89

3.35: Bilinear Pushover curve, Structure 1, direction x, first, second and third iteration. 89
3.36: Target displacement computation, Structure 1, direction x, second iteration. 90
3.37: Target displacement computation, Structure 1, direction x, third iteration. 90
3.38: Target displacement computation, EN 1998-3, Structure 1, direction x. 91
3.39: Target displacement computation, EN 1998-3, Structure 1, direction y. 91
3.40: Target displacement computation, EN 1998-3, Structure 2, direction x. 91
3.41: Target displacement computation, EN 1998-3, Structure 2, direction y. 92
3.42: Target displacement computation, EN 1998-3, Structure 3, direction x. 92
3.43: Target displacement computation, EN 1998-3, Structure 3, direction y. 92
7.44: Target displacement computation, EN 1998-3, Structure 4, direction x. 93
3.45: Target displacement computation, EN 1998-3, Structure 4, direction y. 93
3.46: Target displacement computation, EN 1998-3, Structure 5, direction x. 93
3.47: Target displacement computation, EN 1998-3, Structure 5, direction y. 94
3.48: Target displacement computation, TBDY-16, Structure 1, direction x. 95
3.49: Target displacement computation, TBDY-16, Structure 1, direction y. 95
3.50: Target displacement computation, TBDY-16, Structure 2, direction x. 95

3.51: Target displacement computation, TBDY-16, Structure 2, direction y 96
3.52: Target displacement computation, TBDY-16, Structure 3, direction x. 96
3.53: Target displacement computation, TBDY-16, Structure 3, direction y. 96
3.54: Target displacement computation, TBDY-16, Structure 4, direction x. 97
3.55: Target displacement computation, TBDY-16, Structure 4, direction y. 97
3.56: Target displacement computation, TBDY-16, Structure 5, direction x. 97
3.57: Target displacement computation, TBDY-16, Structure 5, direction y. 98
3.58: Drift (Δ/h), Structure 1, x direction. 100
3.59: Drift (Δ/h), Structure 1, y direction. 100
3.60: Drift (Δ/h), Structure 2, x direction. 100
3.61: Drift (Δ/h), Structure 2, y direction. 101
3.62: Drift (Δ/h), Structure 3, x direction. 101
3.63: Drift (Δ/h), Structure 3, y direction. 101
3.64: Drift (Δ/h), Structure 4, x direction. 102
3.65: Drift (Δ/h), Structure 4, y direction. 102
3.66: Drift (Δ/h), Structure 5, x direction. 102
3.67: Drift (Δ/h), Structure 5, y direction. 103
3.68: Deformed shape, Structure 3, Frame B. 104
3.69: Deformed shape and internal forces in element 443. 104
3.70: Plastic rotations in element 443. 105
3.71: Deformed shape and internal forces in element 448. 106
3.72: Moment-curvature diagram in 40x60cm section beam. 107
3.73: Deformed shape and internal forces in element 659. 109
3.74: Strains in concrete and steel for 0.037rad/m curvature. 110

LIST of TABLES

Table No:		**Page**
2.1:	Target building Performance Levels.	6
2.2:	Probability of exceedance and Mean Return Period.	8
2.3:	Spectral acceleration coefficient at Period 0.2 s (F_a).	9
2.4:	Spectral acceleration coefficient at Period 1.0 s (F_v).	9
2.5:	Site Classes.	10
2.6:	Effective Stiffness Values.	12
2.7:	Numerical Acceptance Criteria – Reinforced Concrete Beams.	18
2.8:	Numerical Acceptance Criteria – Reinforced Concrete Columns.	19
2.9:	Probability of exceedance and Mean Return Period.	21
2.10:	Ground Types.	23
2.11:	Soil Characteristic values describing the response spectra.	24
2.12:	Probability of exceedance and Mean Return Period.	35
2.13:	Spectral acceleration coefficient at Short-Period (F_s).	36
2.14:	Spectral acceleration coefficient at Period 1.0 s (F_1).	37
2.15:	Site Classes.	37
2.16:	Live load mass contribution coefficient.	39
2.17:	Effective Stiffness Factor.	39
2.18:	Target Building Performance Levels.	50
2.19:	Seismic Hazards.	51
2.20:	Parameters for Response Spectrum.	52
2.21:	Effective stiffness values.	54
2.22:	Plastic hinge length.	54
2.23:	Classification of diaphragms.	55
2.24:	Nonlinear Static (Pushover) Procedure limitations.	55
2.25:	Idealized Bilinear Force-Displacement curve.	56
2.26:	Target displacements.	57
2.27:	Parameters for acceptance criteria.	58
3.1:	Open Areas in Studied Structures.	59
3.2:	Modal Characteristics, Structure 1, ASCE-41-13.	73

3.3: Modal Characteristics, Structure 2, ASCE-41-13. 73
3.4: Modal Characteristics, Structure 3, ASCE-41-13. 73
3.5: Modal Characteristics, Structure 4, ASCE-41-13. 73
3.6: Modal Characteristics, Structure 5, ASCE-41-13. 74
3.8: Modal Characteristics, Structure 1, EN 1998-3. 74
3.9: Modal Characteristics, Structure 2, EN 1998-3. 74
3.9: Modal Characteristics, Structure 3, EN 1998-3. 75
3.10: Modal Characteristics, Structure 4, EN 1998-3. 75
3.11: Modal Characteristics, Structure 5, EN 1998-3. 75
3.12: Modal Characteristics, Structure 1, TBDY-16. 76
3.13: Modal Characteristics, Structure 2, TBDY-16. 76
3.14: Modal Characteristics, Structure 3, TBDY-16. 76
3.15: Modal Characteristics, Structure 4, TBDY-16. 76
3.16: Modal Characteristics, Structure 5, TBDY-16. 77
3.17: Normalized Modal Shapes, ASCE-41-13. 77
3.18: Normalized Modal Shapes, EN 1998-3. 78
3.19: Normalized Modal Shapes, TBDY-16. 78
3.20: Flexibility on slabs, Structure 1. 79
3.21: Flexibility on slabs, Structure 2. 79
3.22: Flexibility on slabs, Structure 3. 79
3.23: Flexibility on slabs, Structure 4. 80
3.24: Flexibility on slabs, Structure 5. 80
3.25: Target displacement computation, ASCE-41-13, direction x. 87
3.26: Target displacement computation, ASCE-41-13, direction y. 87
3.27: Target displacement computation, EN 1998-3, direction x (summary). 94
3.28: Target displacement computation, EN 1998-3, direction y (summary). 94
3.29: Target displacement computation, TBDY-16, direction x (summary). 98
3.30: Target displacement computation, TBDY-16, direction y (summary). 98
3.31: Target displacements, x direction (cm). 99
3.32: Target displacements, y direction (cm). 99

3.33: Maximum plastic rotation in beams, Structure 3, Frame B, ASCE-41-13. 104
3.34: Maximum plastic rotation in beams, Structure 3, Frame B, TBDY-16. 108
3.35: Percentage of Beams by Performance level, Structure 1, x direction. 111
3.36: Percentage of Beams by Performance level, Structure 1, y direction. 111
3.37: Percentage of Beams by Performance level, Structure 2, x direction. 111
3.38: Percentage of Beams by Performance level, Structure 2, y direction. 112
3.39: Percentage of Beams by Performance level, Structure 3, x direction. 112
3.40: Percentage of Beams by Performance level, Structure 3, y direction. 112
3.41: Percentage of Beams by Performance level, Structure 4, x direction. 113
3.42: Percentage of Beams by Performance level, Structure 4, y direction. 113
3.43: Percentage of Beams by Performance level, Structure 5, x direction. 113
3.44: Percentage of Beams by Performance level, Structure 5, y direction. 114

1. INTRODUCTION

The force methods for seismic structural design; both Equivalent Lateral Force Analysis and Modal Response Spectrum Analysis, have been used very widely providing earthquake resistant designs with a good reliability, however, around the 90's started the idea that those methods were not enough, because severe damages were found in many buildings that had been designed to resist earthquake actions.

After being aware of the magnitude of damages in buildings caused by recent earthquakes, United States of America was one of the first countries that established in official documents the need of performing seismic assessment of buildings and retrofitting of existing buildings. Applied Technology Council (ATC) published "Seismic evaluation and retrofit of concrete buildings" in 1996, additionally the Federal Emergency Management (FEMA) published "NEHRP Guidelines for the seismic rehabilitation of buildings" in 1997 and "Prestandard and commentary for the seismic rehabilitation of buildings" in 2000. The American Society of Civil Engineering (ASCE) published in 2006 the standard "Seismic Rehabilitation of Existing Buildings" and its most recent version in 2013 "Seismic Evaluation and Retrofit of Existing Buildings".

In the European Union, the European Committee for Standardization published 10 Eurocodes between 1998 and 2006, each one divided in several parts, in total there are 58 Eurocodes. Eurocode8, "Design of structures for earthquake resistance", includes 6 parts, its Part 3 corresponds to the Assessment and retrofitting of building, which shows that also in European countries the traditional force methods are being changed for performance based methods.

In turkey, after the earthquake in Kocaeli in 1999, the need of updating the seismic design methods came up, therefore the previous seismic code "ABYYHY-98" was changed for the one published in 2007, DBYBHY-07 "Deprem Bölgelerinde Yapılacak Binalar Hakkında Yönetmelik Hakkında Yönetmelik". The chapter 7 in this new code, "Evaluation and Retrofit of Existing Buildings", includes several performance assessment methods, such as nonlinear static (Pushover) and nonlinear dynamic (Time-History). In 2016 the newest Turkish Seismic code was released, TBDY-16 "Türkiye Bina Deprem Yönetmeliği", as a draft version, updating its design techniques to the latest investigations.

The new methods that are developed continuously by engineering organizations around the world should be studied, analyzed and tried with different types of buildings, different hazards, etc.

These types of buildings can include several irregularities, which can be vertical irregularities like; Stiffness soft story irregularity, Weight irregularity, Vertical geometry irregularity, or horizontal irregularities like; torsional irregularity, Nonparallel system irregularity or Diaphragm discontinuity irregularity.

This thesis will be focused in buildings with diaphragm discontinuity. Several buildings with open areas in all their stories will be studied. This discontinuity affects the rigidity of the diaphragms, which in many cases are assumed rigid. The assumption of rigid floor diaphragms is often used to simplify engineering analysis, but this might affect the accuracy of the results.

1.1. Literature Review

Previous researches have demonstrated the need of considering flexible diaphragms in order to keep a good enough accuracy,

Kunnath (1991) analyzed four, six, and eight-span single-story structures and eight-span two and three-story structures (see figure 1.1) and found that for structures such as long and narrow buildings the effect of diaphragm flexibility cannot be disregarded.

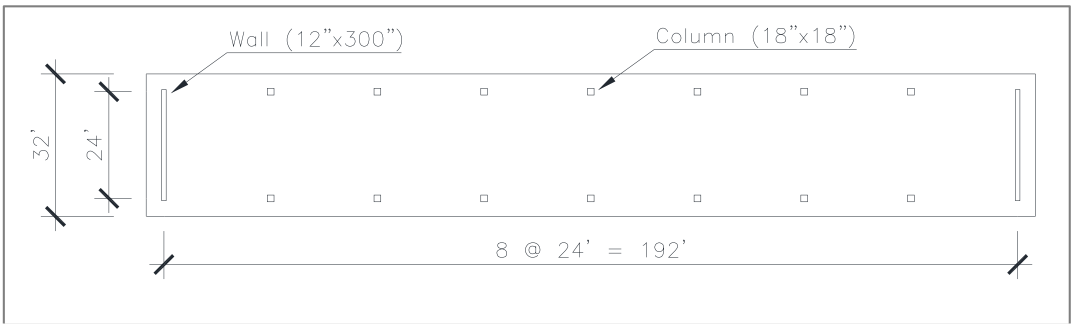

Figure 1.1: Typical floor plan of Eight-Span Three-Story Structure.

S. H. Ju (1999) investigated the difference between the rigid-floor and flexible-floor analysis of buildings. The finite-element was used to analyze U-shaped and T-shaped buildings with and without shear walls. It was found that the rigid-floor model is accurate enough for regular and nonregular buildings without shear walls. However, the difference between the rigid-floor and flexible-floor analyses can be large for the buildings without shear walls.

More recently, Basu (2004) analyzed an asymmetric three-story building (see figure 1.2) with flexible floor diaphragms to study its torsional response; the aspect ratio of the floor plan (50m x 10m) was chosen as 5, higher than that of typical buildings to show the effect of floor flexibility.

The building was analyzed using SAP2000, beams and columns were modeled as line elements and slabs were considered as membrane elements. The results showed that treating the diaphragm of such buildings as rigid for torsional analysis may cause considerable error.

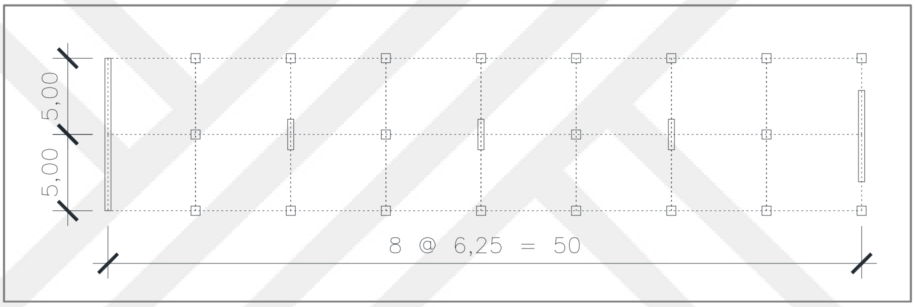

Figure 1.2: Typical floor plan of Three-Story Building.

Joel (2004) used FEMA 273-NEHRP performance-based approach to assess three-story and five-story reinforced concrete buildings with end shear walls and two aspect ratios (approximately 2:1 and 3:1). Those buildings were previously designed assuming rigid diaphragm behavior. It was found that the use of a flexible diaphragm model had the largest impact on the three-story, 3:1 aspect ratio buildings.

Roskelley B. (2010) performed an assessment of the validity of idealizing a concrete diaphragm as rigid through the modal analysis of three existing buildings.

Modal analysis was performed both by physical experimentation and computational analysis. It was found that the design seismic demands were higher when modeled with semi-rigid diaphragms than with rigid diaphragms.

Flexible diaphragms have been analyzed in several types of buildings, like narrow buildings, L shape buildings among others, however, discontinuity in diaphragms can be a common irregularity in buildings that should be also studied

1.2. Purpose and Scope

The purpose of this thesis is to assess performance of structures with diaphragm discontinuity, using the methods stated in the codes ASCE-41-13 “Seismic Rehabilitation of Existing Buildings”, Eurocode EN 1998-3 (2005) “Assessment and retrofitting of buildings” and Turkish Seismic code TBDY-16, whose procedures and results will be also compared.

The chosen method to evaluate is nonlinear static method (pushover) and this will be applied to different reinforced concrete buildings.

The studied buildings are 6 stories concrete reinforced moment resistant frames. Those buildings have open areas in all their slabs, this open area corresponds to 20%, 30%, 40%, 50% and 60% of the total area of the slab. Different techniques for modelling slabs will be also analyzed.

Those buildings were designed using linear method, Modal response spectrum analysis, as Moment frames with high ductility.

Nonlinear static (Pushover) method will be applied and performance levels will be assigned to each section, each element and to each structure.

2. GENERAL REQUIREMENTS FOR NONLINEAR PERFORMANCE ASSESSMENT

This chapter defines the requirements for nonlinear performance assessment in the standards used in this research (ASCE-41-13, EN 1998-3 and TBDY-16).

2.1. ASCE-41-13

This section shows the nonlinear performance assessment procedure stated in the standard ASCE-41-13, "Seismic Evaluation and Retrofit of Existing Buildings", published in 2013 by The American Society of Civil Engineering (ASCE). Figure 2.5 sketches this procedure and shows specific chapter references.

2.1.1. Performance Objectives

A Performance Objective shall consist of one or more pairings of a selected Seismic Hazard Level with a target Structural Performance Level and a target Nonstructural Performance Level.

- Target Building Performance Levels

- Structural Performance Levels

The structural Performance Level of a building shall be selected from six discrete Structural Performance Levels defined.

The discrete Structural Performance Levels are Immediate Occupancy (S-1), Damage Control (S-2), Life Safety (S-3), Limited Safety (S-4), Collapse Prevention (S-5), and Not Considered (S-6).

- Nonstructural Performance Levels

The target Nonstructural Performance Levels for a building shall be selected from four discrete Nonstructural Performance Levels.

Those performance levels are Operational (N-A), Position Retention (N-B), Life Safety (N-C), and Not Considered (N-D).

- Designation of Target Building Performance Levels

A target Building Performance Level is designated alphanumerically with a numeral representing the Structural Performance Level and a letter representing the Nonstructural Performance Level, such as 1-B, 3-C, 5-E or 6-C. Several common target Building Performance Levels are shown in Figure 2.1. Many combinations are possible because structural performance can be selected at any level in the two Structural Performance Ranges. Table 2.1 indicates some of the possible combinations of target Building Performance Levels and provides names for those most likely to be selected as the basis for design.

Table 2.1: Target building Performance Levels.

Nonstructural Performance Levels	Structural Performance Levels					
	Immediate Occupancy (S-1)	Damage Control (S-2)	Life Safety (S-3)	Limited Safety (S-4)	Collapse Prevention (S-5)	Not Considered (S-6)
Operational (N-A)	Operational 1-A	2-A	NR	NR	NR	NR
Position Retention (N-B)	Immediate Occupancy 1-B	2-B	3-B	4-B	NR	NR
Life Safety (N-C)	1-C	2-C	Life Safety 3-C	4-C	5-C	6-C
Not Considered (N-D)	NR	NR	3-D	4-D	Collapse Prevention 5-D	6-D No Evaluation or Retrofit

- NR = Not recommended.

- Seismic Hazard

Several probabilistic Seismic Hazard Levels are used to describe ground motions for which performance evaluations are made. Such ground motions are often referred to either as a probability of exceedance in a specific time period, or as a return period for exceedance of the specified ground motion. Table 2.2 shows the ground motions probabilities of exceedance and corresponding return period used.

The seismic hazard caused by ground shaking is defined for any Seismic Hazard Level using approved 5%-damped response spectrum ordinates for short (0.2 s) and long (1 s) periods.

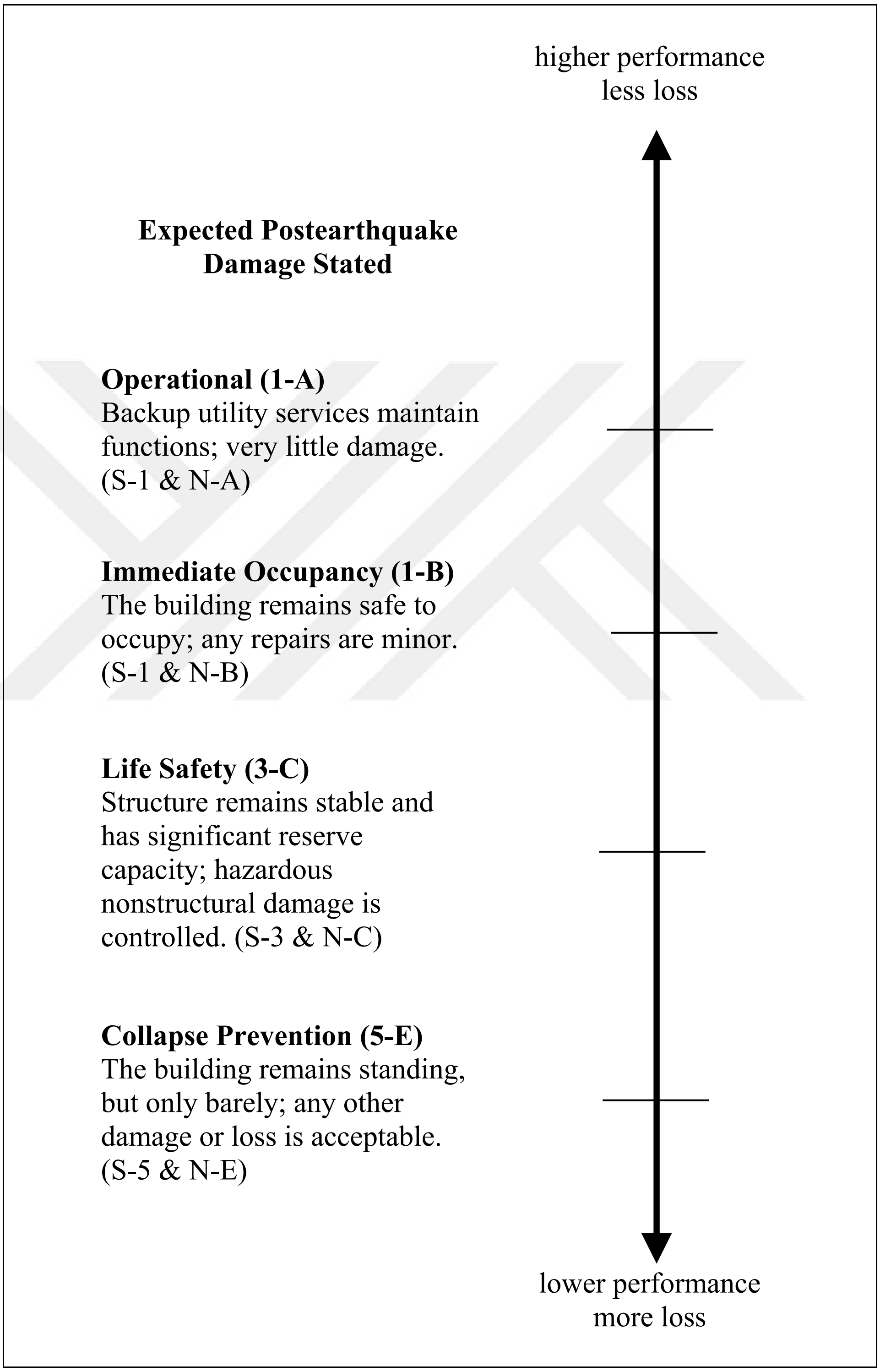

Figure 2.1: Target building Performance Levels.

Table 2.2: Probability of Exceedance and Mean Return Period.

Probability of Exceedance	**Mean Return Period (years)**
50% / 50 years	72
20% / 50 years	225
10% / 50 years	475
5% / 50 years	975
2% / 50 years	2475

- Response Spectrum

A general horizontal response spectrum, as shown in figure 2.2, is developed for spectral acceleration, S_a, versus structural period, T, in the horizontal direction.

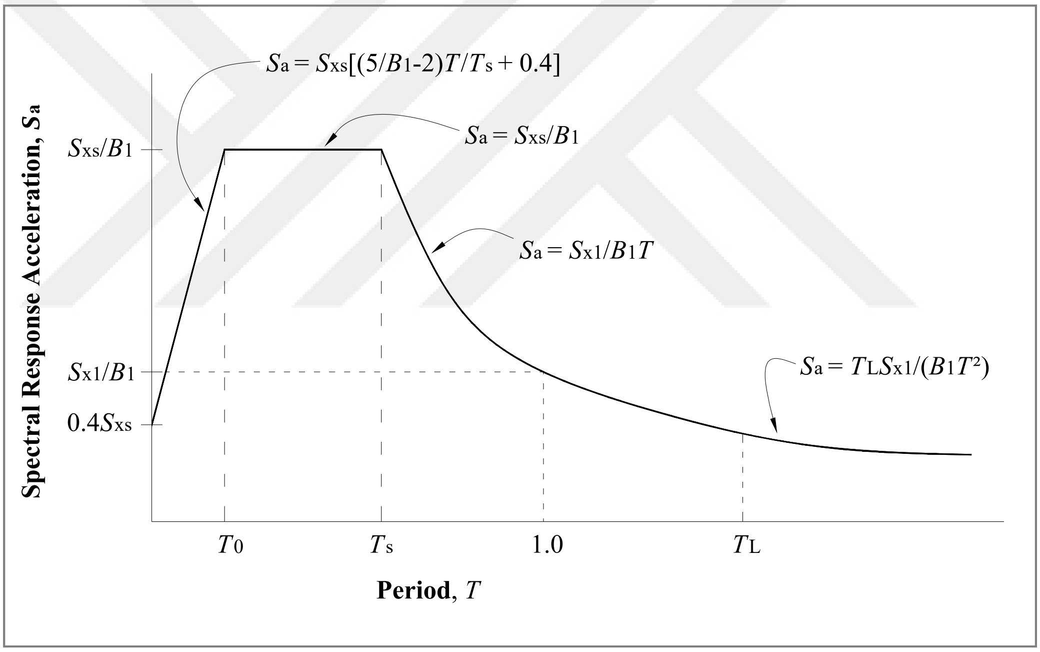

Figure 2.2: General Horizontal Response Spectrum.

The design short-period spectral response acceleration parameter, S_{XS}, and the design spectral response acceleration parameter at a 1-s period, S_{X1}, for the BSE-2N (MCE_R) Seismic Hazard Level will be taken as values from approved 2%/50-year maximum direction spectral response acceleration contour maps (denoted S_S and S_1).

The design short-period spectral response acceleration parameter, S_{XS}, and the design spectral response acceleration parameter at 1 s, S_{X1}, will be obtained from the next equations:

$$S_{XS} = F_a S_S \tag{2.1}$$

$$S_{X1} = F_v S_1 \tag{2.2}$$

Where Fa and Fv are site coefficients determined respectively from tables 2.3 and 2.4, based on based on the site class and the values of the response acceleration parameters SS and S1 for the selected return period.

Table 2.3: Spectral acceleration coefficient at period 0.2 s (F_a).

Site Class	**Mapped Spectral Acceleration at Short-Period S_S**				
	$S_S \leq 0.25$	**$S_S = 0.50$**	**$S_S = 0.75$**	**$S_S = 1.0$**	**$S_S \geq 1.25$**
A	0.80	0.80	0.80	0.80	0.80
B	1.00	1.00	1.00	1.00	1.00
C	1.20	1.20	1.10	1.00	1.00
D	1.60	1.40	1.20	1.10	1.00
E	2.50	1.70	1.20	0.90	0.90
F	Site-specific geotechnical investigation shall be performed				

Table 2.4: Spectral acceleration coefficient at period 1.0 s (F_v).

Site Class	**Mapped Spectral Acceleration at 1-s Period S_1**				
	$S_1 \leq 0.1$	**$S_1 = 0.2$**	**$S_1 = 0.3$**	**$S_1 = 0.4$**	**$S_1 \geq 0.5$**
A	0.80	0.80	0.80	0.80	0.80
B	1.00	1.00	1.00	1.00	1.00
C	1.70	1.60	1.50	1.40	1.30
D	2.40	2.00	1.80	1.60	1.50
E	3.50	3.20	2.80	2.40	2.40
F	Site-specific geotechnical investigation shall be performed				

Straight-line interpolation shall be used for intermediate values of S_S and S_1.

Soil class will be defined according to the table 2.5.

Table 2.5: Site Classes.

Site Class	v_s (ft/s)	N	c_u (lb/ft^2)
A. Hard Rock with average shear velocity.	> 5000	-	-
B. Rock	2500 - 5000	-	-
C. Very dense soil and soft rock	1200 - 2500	> 50	> 2000
D. Stiff soil	600 - 1200	15 - 50	1000 - 2000
E. Any profile with more than 10 ft of soft clay	< 600		< 500

Where:

- v_s = Average shear wave velocity of the upper 100 ft of soils at the site.
- N = Average standard penetration test of the upper 100 ft of soils at the site.
- c_u = Undrained shear strength of the upper 100 ft of soils at the site.

T_0 and T_S are given by the next equations:

$$T_S = S_{X1} / S_{XS} \tag{2.3}$$

$$T_0 = 0.2 T_S \tag{2.4}$$

The period for which horizontal displacement spectrum become constant, T_L, will be obtained from published maps.

The damping coefficient used to adjust spectral response for the effect of viscous damping, B_1, is given by the next equation:

$$B_1 = 4 / [5.6 - \ln(100\beta)] \tag{2.5}$$

Where:

- β = Effective viscous damping ratio.

2.1.2. Structural Model

Building shall be modeled, analyzed, and evaluated as a three-dimensional assembly of components.

- Damping

For linear static, linear dynamic, and nonlinear static procedures, 5% damped response spectra shall be used for the analysis of all buildings.

- Gravity loads

For nonlinear procedures, the following actions caused by gravity loads, Q_G, in accordance with equation 2.6 shall be considered for combination with actions caused by seismic forces.

$$Q_G = Q_D + 0.25Q_L \tag{2.6}$$

Where:

- Q_G = Action caused by gravity loads.
- Q_D = Action caused by dead load.
- Q_L = *Action caused by live load.*

- Effective Stiffness

Component stiffness shall be calculated considering shear, flexure, axial behavior, and reinforcement slip deformations.

Component effective stiffness shall correspond to the secant value to the yield point of the component. Alternatively, effective stiffness values in Table 2.6 shall be permitted.

For columns with axial compression falling between the limits provided, flexural rigidity should be determined by linear interpolation. If interpolation is not performed, the more conservative effective stiffness should be used.

Table 2.6: Effective Stiffness Values.

Component	Flexural Rigidity	Shear Rigidity
Beams-nonprestressed	$0.3E_cI_g$	$0.4\ E_cA_g$
Beams-prestressed	E_cI_g	$0.4\ E_cA_g$
Column with compression caused by design gravity loads $\geq 0.5A_g f'_c$	$0.7E_cI_g$	$0.4\ E_cA_g$
Column with compression caused by design gravity loads $\leq 0.1A_g f'_c$ or with tension	$0.3E_cI_g$	$0.4\ E_cA_g$
Walls-cracked	$0.5E_cI_g$	$0.4\ E_cA_g$
Flat slabs	$0.5E_cI_g$	$0.4\ E_cA_g$

Where:

- E_c = Modulus of elasticity of concrete.
- I_g = Moment of inertia of gross concrete section about centroidal axis, neglecting reinforcement.
- A_g = Gross area of element.
- f'_c = Compressive strength of concrete.

- Joint Model

Where joint stiffness is not modeled explicitly, it shall be permitted to be modeled implicitly by adjusting a center line model:

- For $\Sigma M_{nc} / \Sigma M_{nb} > 1.2$, column offsets are rigid and beam offsets are not.
- For $\Sigma M_{nc} / \Sigma M_{nb} < 0.8$, beam offsets are rigid and column offsets are not.
- For $0.8 \leq \Sigma M_{nc} / \Sigma M_{nb} \leq 1.2$, half of the beam and column offsets are considered rigid.

- M_{nc} = Nominal moment strength at column section.
- M_{nb} = Nominal moment strength at beam section.

M_{nc} shall be calculated considering axial force from gravity loads ($Q_D + 0.25Q_L$).

• Hinge Model

Beams and columns shall be modeled using concentrated or distributed plastic hinge models. Other models whose behavior represents the behavior of reinforced concrete beam and column components subjected to seismic loading shall be permitted. The beam and column model shall be capable of representing inelastic response along the component length, except where it is shown by equilibrium that yielding is restricted to the component ends.

• Slab model in irregular buildings

Diaphragms shall be classified as flexible where the maximum horizontal deformation of the diaphragm along its length is more than twice the average story drift of the vertical seismic-force-resisting elements of the story immediately below the diaphragm (see figure 2.3).

Diaphragms shall be classified as rigid where the maximum lateral deformation of the diaphragm is less than half the average story drift of the vertical seismic-force-resisting elements of the story immediately below the diaphragm (see figure 2.3).

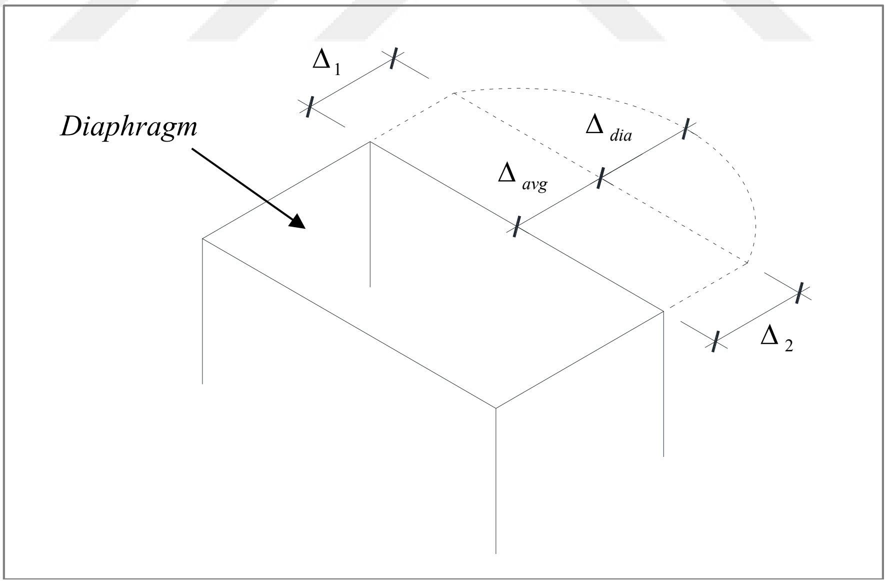

Figure 2.3: Deformation in diaphragms.

• Δ_{avg} = Average story drift.

• Δ_{dia} = Diaphragm deformation.

2.1.3. Nonlinear Static (Pushover) Procedure

Nonlinear static procedure shall be applied according to the requirements in this section. Mathematical model directly incorporating the nonlinear load-deformation characteristics of components of the buildings shall be subjected to increasing lateral loads representing inertia forces in an earthquake until a target displacement is exceeded.

- Nonlinear Static Procedure (Pushover) limitations

The pushover shall be permitted for structures which higher modes are not significant. To determine if higher modes are significant, a modal response spectrum analysis shall be performed for the structure using sufficient modes to produce 90% mass participation. A second response spectrum analysis shall also be performed, considering only the first mode participation. Higher mode effects shall be considered significant if the shear in any story resulting from the modal analysis considering modes required to obtain 90% mass participation exceeds 130% of the corresponding story shear considering only the first response.

- Idealized Force-Displacement Curve

The nonlinear force-displacement relationship between base shear and displacement of the control node will be replaced with an idealized relationship to calculate the effective lateral stiffness, K_e, and the effective yield strength, V_y, of the building, as shown in Figure 2.4.

The first segment of the idealized force-displacement curve will begin at the origin and have a slope equal to the effective lateral stiffness, K_e. The effective lateral stiffness, K_e, will be taken as the secant stiffness calculated at a base shear force equal to 60% of the effective yield strength of the structure. The effective yield strength, V_y, will not be taken as greater than the maximum base shear force at any point along the force-displacement curve.

The second line segment will represent the positive post-yield slope, determined by a point (V_d, Δ_d) and a point at the intersection with the first line segment such that the areas above and below the actual curve are approximately balanced. (V_d, Δ_d) will be a point on the actual force-displacement curve at the calculated target displacement, or at the displacement corresponding to the maximum base shear, whichever is least.

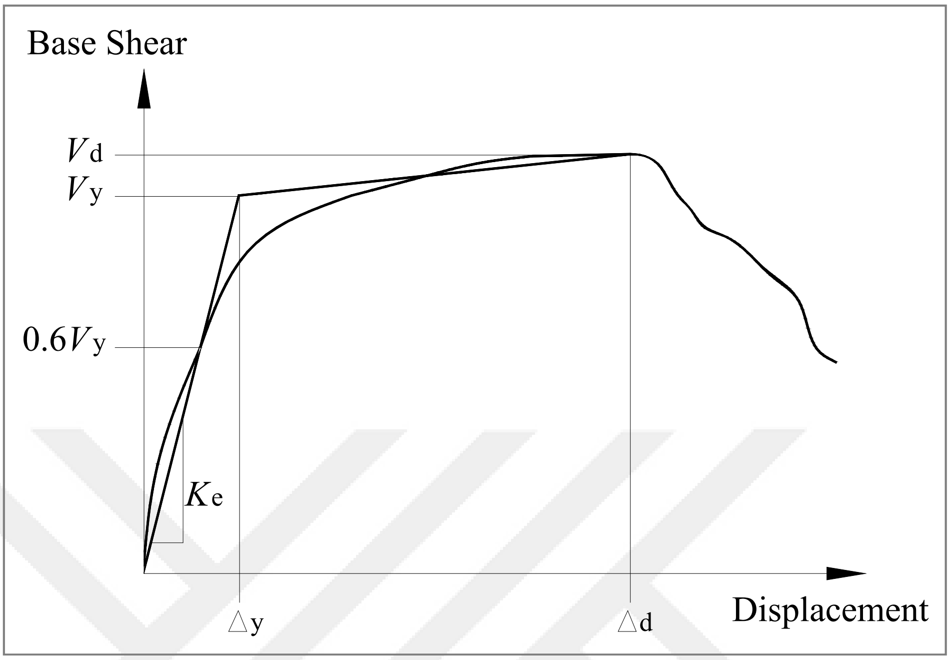

Figure 2.4: Idealized Force-Displacement Curve.

Where:

- Δ_y = Displacement at effective yield strength.
- Δ_d = Lesser of the target displacement or displacement corresponding to the maximum base shear defined in Figure 2.4.
- V_y = Effective yield strength of the building.
- V_d = Base shear at Δ_d.
- K_e = Effective stiffness of the building.

- Target displacement

The target displacement, δ_t, at the control node will be calculated in accordance with equation 2.7:

$$\delta_t = C_0 C_1 C_2 S_a(T_e) \frac{T_e^{\,2}}{4\pi^2} g \tag{2.7}$$

Where:

- $S_a(T_e)$ = Response spectrum acceleration at the effective fundamental period.
- g = Acceleration of gravity.
- C_0 = Modification factor to relate spectral displacement of an equivalent single degree of freedom (SDOF) system to the roof displacement of the building multi degree of freedom (MDOF) system, calculated as the first mode mass participation factor multiplied by the ordinate of the first mode shape at the control node.
- C_1 = Modification factor to relate expected maximum inelastic displacements to displacements calculated for linear elastic response. For periods less than 0.2 s, C_1 need not to be taken greater than the value at T = 0.2 s. For periods greater than 1.0 s, C_1 = 1.0.

$$C_1 = 1 + \frac{\mu_{strength} - 1}{a.T_e^{\,2}} \tag{2.8}$$

- a = Site class factor; 130 Site Class A or B, 90 Site Class C; 60 Site Class D, E, or F.
- T_e = Effective fundamental period of the building in the direction under consideration.

$$T_e = T_i \sqrt{\frac{K_i}{K_e}} \tag{2.9}$$

Where:

- T_i = Elastic fundamental period (in seconds) in the direction under consideration calculated by elastic dynamic analysis.
- K_i = Elastic lateral stiffness of the building.
- K_e = Effective lateral stiffness of the building. See Figure 2.4.
- $\mu_{strength}$ = Ratio of elastic strength demand to yield strength.

$$\mu_{strength} = \frac{S_a}{V_y / W}.C_m \qquad (2.10)$$

Where:

- V_y = Yield strength of the building from the idealized nonlinear force-displacement curve.
- W = Effective seismic weight, (Q_D + 0.25Q_L)
- C_m = Modal mass participation factor. If the fundamental period is greater than 1.0 s, C_m will be taken as 1.0.
- C_2 = Modification factor to represent the effect of pinched hysteresis shape and cyclic stiffness degradation. For periods greater than 0.7 s, C_2 = 1.0.

$$C_2 = 1 + \frac{1}{800}\left(\frac{\mu_{strength} - 1}{T_e}\right)^2 \qquad (2.11)$$

2.1.4. Acceptance criteria

Actions in a structure shall be classified as being either deformation controlled or force controlled. For deformation-controlled actions performance level shall be established according to maximum plastic rotation values indicated in tables 2.7 and 2.8. For force-controlled actions their strength will checked, ACI318 will be used to calculate the design strengths.

Table 2.7: Numerical Acceptance Criteria - Reinforce Concrete Beams.

Conditions			Acceptance Criteria		
			Plastic Rotations Angle (radians)		
			Performance Level		
			IO	LS	CP
Condition i. Beams controlled by flexure					
$\frac{\rho - \rho'}{\rho_{bal}}$	Transverse reinforcement	$\frac{V}{b_w d \sqrt{f'_c}}$			
≤0.0	C	≤ 0.25	0.010	0.025	0.05
≤0.0	C	≥ 0.50	0.005	0.02	0.04
≥0.5	C	≤ 0.25	0.005	0.02	0.03
≥0.5	C	≥ 0.50	0.005	0.015	0.02
≤0.0	NC	≤ 0.25	0.005	0.02	0.03
≤0.0	NC	≥ 0.50	0.0015	0.01	0.015
≥0.5	NC	≤ 0.25	0.005	0.01	0.015
≥0.5	NC	≥ 0.50	0.0015	0.005	0.01
Condition ii. Beams controlled by shear					
Stirrup spacing ≤ *d/2*			0.0015	0.01	0.02
Stirrup spacing > *d/2*			0.0015	0.005	0.01

"C" and "NC" are abbreviations for conforming and nonconforming transverse reinforcement, respectively. Transverse reinforcement is conforming if, within the flexural plastic hinge region, hoops are spaced at ≤ $d/3$.

- b_w = Web width.
- d = Distance from extreme compression fiber to centroid of tension reinforcement.
- V = Design shear force from Nonlinear Static Procedure (Pushover).
- f'_c = Compressive strength of concrete (MPa).
- ρ = Ratio of tension reinforcement.
- ρ' = Ratio of compression reinforcement.
- ρ_{bal} = Reinforcement ratio producing balanced strain conditions.
- IO = Immediate occupancy performance level.
- LS = Life safety performance level.
- CP = Collapse prevention performance level.

Table 2.8: Numerical Acceptance Criteria - Reinforce Concrete Columns.

Conditions			**Acceptance Criteria**		
			Plastic Rotations Angle (radians)		
			Performance Level		
			IO	**LS**	**CP**
Condition i. $V_p/V_o \leq 0.6$					
$\frac{P}{A_g f'_c}$	$\rho = \frac{A_v}{b_w s}$				
≤0.1	≥0.006		0.005	0.045	0.060
≥0.6	≥0.006		0.003	0.009	0.010
≤0.1	=0.002		0.005	0.027	0.034
≥0.6	=0.002		0.002	0.004	0.005
Condition ii. $1.0 \geq V_p/V_o > 0.6$					
$\frac{P}{A_g f'_c}$	$\rho = \frac{A_v}{b_w s}$	$\frac{V}{b_w d \sqrt{f'_c}}$			
≤0.1	≥0.006	≤ 0.25	0.005	0.045	0.060
≤0.1	≥0.006	≥ 0.50	0.005	0.045	0.060
≥0.6	≥0.006	≤ 0.25	0.003	0.009	0.010
≥0.6	≥0.006	≥ 0.50	0.003	0.007	0.008
≤0.1	≤0.0005	≤ 0.25	0.005	0.010	0.012
≤0.1	≤0.0005	≥ 0.50	0.004	0.005	0.006
≥0.6	≤0.0005	≤ 0.25	0.002	0.003	0.004
≥0.6	≤0.0005	≥ 0.50	0.0	0.0	0.0

Values between those listed in the table should be determined by linear interpolation.

- V_p = Shear force at the development of the flexural capacity.
- V_0 = Shear strength of column.
- P = Axial load in concrete column.
- A_g = Gross area of column.
- A_v = Area of shear reinforcement.
- b_w = Web width.
- s = Spacing of shear reinforcement.
- V = Design shear force from Nonlinear Static Procedure (Pushover).

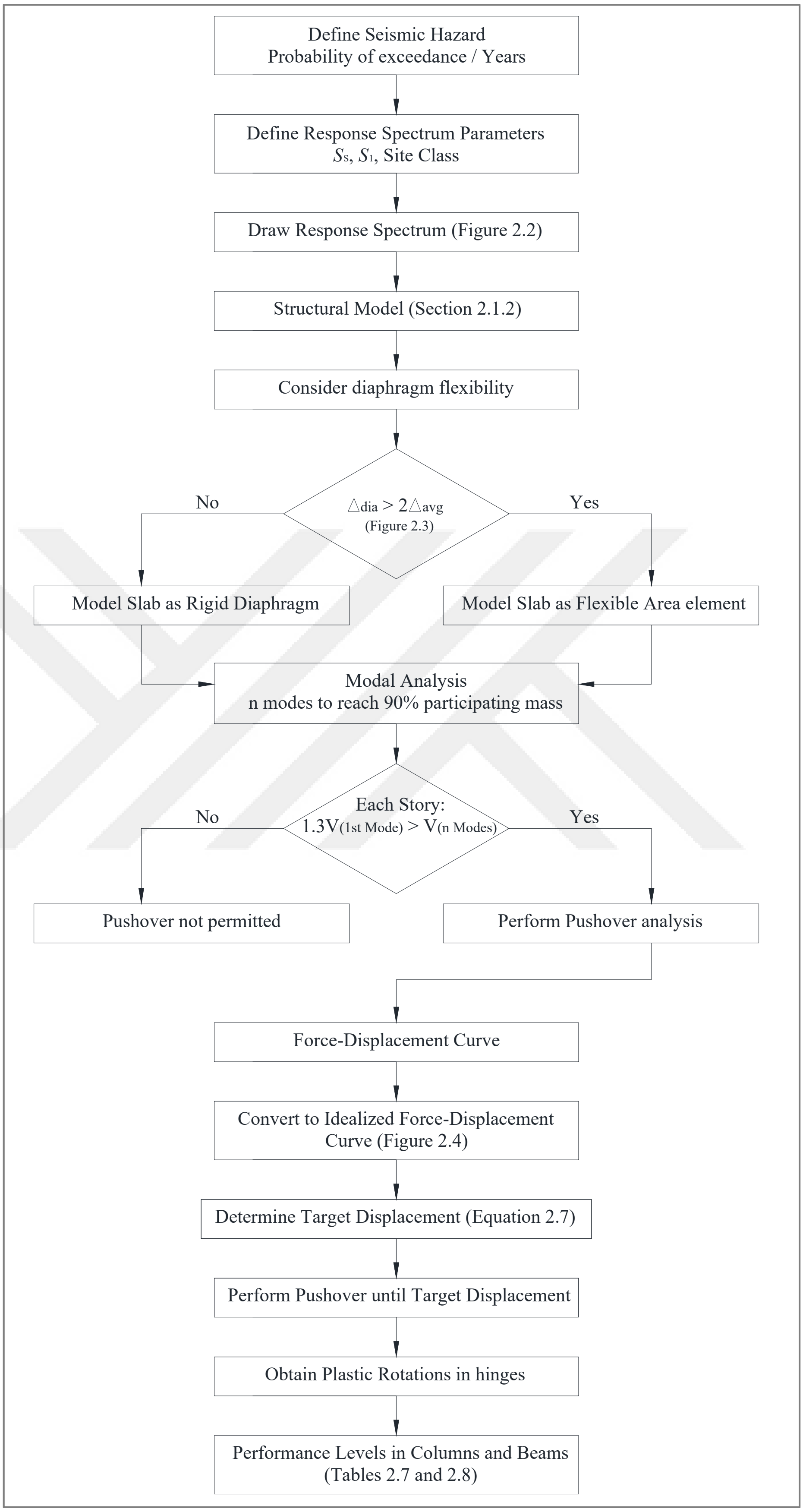

Figure 2.5: Performance Assessment Procedure in ASCE-41-13.

2.2. Eurocode EN 1998-3

This section shows the nonlinear performance assessment procedure stated in Eurocode 8, “Design of structures for earthquake resistance” - Part 3: “Assessment and retrofitting of building” published in 2005 by the European Committee for Standardization. Figure 2.11 sketches this procedure and shows specific chapter references.

2.2.1. Target Building Performance Levels

The Performance Level of a building shall be selected from three discrete levels defined.

The discrete Performance Levels are Near Collapse (NC), Significant Damage (SD), and Damage Limitation (DL).

2.2.2. Seismic Hazard

Table 2.9 shows the ground motions probabilities of exceedance and corresponding return period recommended in this standard. In order to obtain different levels of seismic hazard, the seismic action must be multiplied by importance factors. An importance factor equal to 1.0 is associated with 10%/50years; an importance factor equal to 1.5 is associated with 2%/50years.

Table 2.9: Probability of exceedance and Mean Return Period.

Probability of Exceedance	**Mean Return Period (years)**
10% / 50years	475
10% / 10 years	95

2.2.3. Response Spectrum

For the horizontal components of the seismic action, the elastic response spectrum $S_e(T)$ is defined by equations 2.12, 2.13, 2.14, and 2.15. (See figure 2.6)

$$0 \le T \le T_B, \qquad S_e(T) = a_g S\left[1 + \frac{T}{T_B}(\eta.2.5 - 1)\right] \tag{2.12}$$

$$T_B \le T \le T_C, \qquad S_e(T) = 2.5 a_g S.\eta \tag{2.13}$$

$$T_C \le T \le T_D, \qquad S_e(T) = 2.5 a_g S.\eta\left[\frac{T_C}{T}\right] \tag{2.14}$$

$$T_D \le T \le 4s, \qquad S_e(T) = 2.5 a_g S.\eta\left[\frac{T_C T_D}{T^2}\right] \tag{2.15}$$

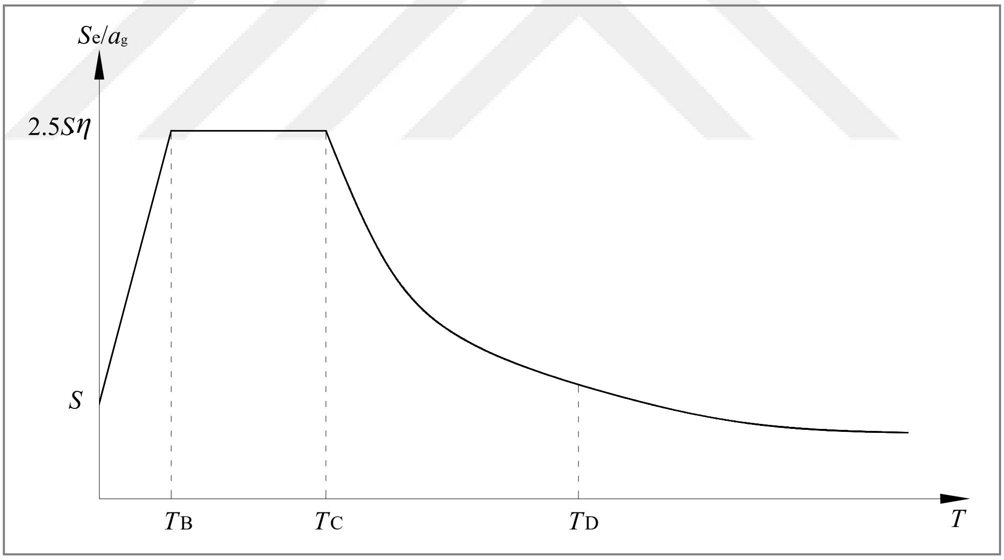

Figure 2.6: Shape of the Elastic Response Spectrum.

- T = Fundamental period of the building in the direction under consideration.
- a_g = Ground acceleration.
- T_B = Lower limit of the period of the constant spectral acceleration branch.
- T_C = Upper limit of the period of the constant spectral acceleration branch.
- T_D = Value defining the beginning of the constant displacement response range.

• S = Soil factor.

• η = Damping correction factor.

$$\eta = \sqrt{10/(5+\xi)} \geq 0.55 \tag{2.16}$$

ξ = Viscous damping ratio, expressed as a percentage.

Soil class will be defined according to table 2.10.

The parameters T_B, T_C, T_D, and S, will be determined from table 2.11.

Table 2.10: Ground Types.

Ground Type	Description of stratigraphic profile	Parameters		
		v_s (m/s)	***N*** **(blows/30cm)**	c_u (kPa)
A	Rock or other rock-like geological formation, including at most 5 m of weaker material at the surface.	> 800	-	-
B	Deposits of very dense sand, gravel, or very stiff clay, at least several tens of meters in thickness, characterized by a gradual increase of mechanical properties with depth.	360 - 800	> 50	> 250
C	Deep deposits of dense or medium-dense sand, gravel or stiff clay with thickness from several tens to many hundreds of meters.	180 - 360	15 - 50	70 - 250
D	Deposits of loose-to-medium cohesionless soil (with or without some soft cohesive layers), or of predominantly soft-to-firm cohesive soil.	< 180	< 15	< 70
E	Deposits consisting, or containing a layer at least 10 thick, of soft clays/silts with a high plasticity index (PI>40) and high water content.	-	-	-

- v_s = Average shear wave velocity of the upper 30m of soils at the site.
- N = Average standard penetration test(SPT) of the upper 30m of soils at the site.
- c_u = Undrained shear strength of the upper 30m of soils at the site.

Table 2.11: Soil Characteristic values describing the response spectra.

Ground Type	S	T_B (s)	T_C (s)	T_D (s)
A	1.0	0.15	0.4	2
B	1.2	0.15	0.5	2
C	1.15	0.2	0.6	2
D	1.35	0.2	0.8	2
E	1.4	0.15	0.5	2

2.2.4. Structural Model

Building shall be modeled, analyzed, and evaluated as a three-dimensional assembly of components. The strength and the stiffness of secondary seismic elements against lateral actions may in general be neglected in the analysis.

- Gravity loads

The inertial effects of the seismic action shall be evaluated by taking into account the presence of the masses associated with the gravity loads in equation 2.17.

$$\Sigma G + \Sigma 0.24Q \tag{2.17}$$

- G = Permanent action.
- Q = Variable action.

- Effective Stiffness

Flexural stiffness of each element must be taken equal to the mean value of the effective inertia obtained in equation 2.18, at the two ends of the element. Shear stiffness properties may be taken to be equal to one-half of the corresponding stiffness of the uncracked elements.

$$I_{cr} = \frac{M_y L}{6\theta_y} \tag{2.18}$$

Where:

- I_{cr} = Moment of inertia of cracked concrete section.
- θ_y = Chord rotation at yield.
- M_y = Yielding Moment.
- L = Length of the element.

- Joint Model

The model should account for the contribution of joints regions to the deformability of the building, like the end zones in beams or columns of frame type structures.

- Hinge Model

Beams, columns and walls shall be modeled using concentrated plastic hinges in their edges. The plastic hinge length shall be calculated according to the equation 2.19.

$$L_{pl} = \frac{L_V}{30} + 0.20h + 0.11\frac{d_{bL} f_y (MPa)}{\sqrt{f'_c (MPa)}} \qquad (2.19)$$

The shear span at member end, L_V, shall be obtained from equation 2.20.

$$L_V = M / V \qquad (2.20)$$

Where:

- h = Height of the member along which deformations are measured.
- d_{bL}: Mean diameter of the tension reinforcement.
- f'_c = Concrete compressive strength (MPa).
- f_y = Stirrup yield strength (MPa).
- V = Design shear force from Nonlinear Static Procedure (Pushover).
- M = Design moment from Nonlinear Static Procedure (Pushover).

- Slab model in irregular buildings

For a building to be categorized as being regular in plan, the in-plan stiffness of the floors shall be sufficiently large in comparison with the lateral stiffness of the vertical structural elements, so that the deformation of the floor shall have a small effect on the distribution of the forces among the vertical structural elements. In this respect, the L, C, H, I, and X plan shapes should be carefully examined, specially the stiffness of lateral branches, which should be comparable to that of the central part, in order to satisfy the rigid diaphragm condition.

The diaphragm is taken as being rigid, if, when it is modelled with its actual in-plane flexibility, its horizontal displacements nowhere exceed those resulting from the rigid diaphragm assumption by more than 10%.

A solid reinforced concrete slab might be considered to serve as a diaphragm, if it has a thickness of not 1ess than 70 mm and is reinforced in both horizontal directions.

2.2.5. Nonlinear Static (Pushover) Procedure

Nonlinear static (pushover) analysis is a non-linear static analysis under constant gravity loads and monotonically increasing horizontal loads. This section shows the procedure to apply this method.

- Nonlinear Static Procedure (Pushover) limitations

The pushover method may be applied to buildings whose response is not significantly affected by contributions from modes of vibration higher than the fundamental mode in each principal direction.

This can be satisfied in buildings which have fundamental periods of vibration T_1 in the two main directions which are smaller than 2.0s or $4T_C$.

T_C = upper limit of the period of the constant spectral acceleration branch.

Furthermore the building must meet the following criteria for regularity in elevation:

- All the lateral load resisting systems, frames or walls, shall run without interruption from their foundations to the top of the building.

- Both the lateral stiffness and the mass of the individual stories shall remain constant or reduce gradually, without abrupt changes, from the base to the top of a particular building.

• Equivalent SDOF Force-Displacement Curve

The pushover curve, which represents the base shear force and displacement in the control node, shall be converted in an equivalent SDOF curve, the transformation factor is equivalent to the modal participation factor and is given by equation 2.21.

$$\Gamma = \frac{m_i \Phi_i}{\sum m_i \Phi_i^2} \tag{2.21}$$

• Φ_i = Modal displacement of floor i.

• m_i = Mass at level i.

The modal shape shall be normalized in such a way that the displacement in the control node (usually the roof level) is equal to 1.0.

The force, F^*, and displacement, d^*, of the equivalent SDOF system are computed as:

$$F^* = \frac{F_b}{\Gamma} \tag{2.22}$$

$$d^* = \frac{d_n}{\Gamma} \tag{2.23}$$

Where:

• F_b = Base shear force.

• d_n = Displacement of the control node of the Multi Degree of Freedom (MDOF) system.

• Idealized Force-Displacement Curve

The equivalent SDOF Force-Displacement relationship will be replaced with an idealized bilinear curve to define the yield force, F_y^*, and yield displacement, d_y^*.

The yield force F_y*, which represents also the ultimate strength of the idealized system, shall be equal to the base shear force at the formation of the plastic mechanism. The initial stiffness of the idealized system is determined in such a way that the areas under the actual and the idealized force-deformation curves are equal as shown in figure 2.7. The second line shall be a horizontal line with an ordinate equal to F_y*.

Based on this assumption, the yield displacement of the idealized SDOF system d_y* is given by:

$$d_y* = 2\left(d_m * - \frac{E_m *}{F_y *} \right) \tag{2.24}$$

Where:

- E_m* = Actual deformation energy up to the formation of the plastic mechanism.
- d_y* = Yield displacement.
- d_m* = Displacement at the formation of plastic mechanism.
- F_y* = Yield force.

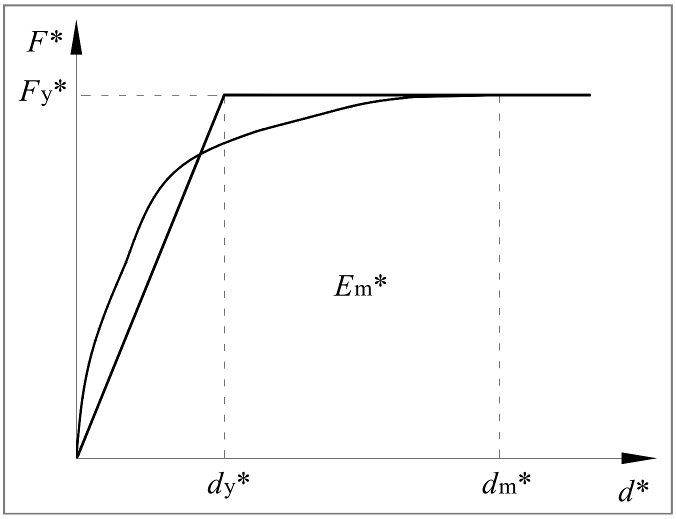

Figure 2.7: Bilinear equivalent SDOF Force-Displacement curve.

The period of the equivalent bilinear SDOF system, T*, shall be calculated in accordance with equation 2.25:

$$T^* = 2\pi\sqrt{\frac{m^* d_y{}^*}{F_y{}^*}} \tag{2.25}$$

The mass of an equivalent SDOF system, m^*, is determined as:

$$m^* = \Sigma m_i \Phi_i \tag{2.26}$$

- Target displacement

The target displacement is determined from the elastic response spectrum and the capacity curve, which represents the relation between base shear and force control node displacement.

$$d_{et}^* = S_e(T^*)\left[\frac{T^*}{2\pi}\right]^2 \tag{2.27}$$

Where:

- $S_e(T^*)$ = Elastic acceleration response spectrum displacement at the equivalent period, T^*.
- d_{et}^* = Elastic target displacement.

There are two possible cases to determine the Inelastic target displacement, d^*_t, those cases will depend on the equivalent period, T^*, and on one of the characteristics period of the soil, T_C.

- Case 1: $T_1 > T_C$ (Medium and long period range)

In this case the inelastic target displacement, d_t^*, will be as given by equation 2.28.

$$d_t^* = d_{et}^* \tag{2.28}$$

- T_C = Upper limit of the period of the constant spectral acceleration branch.

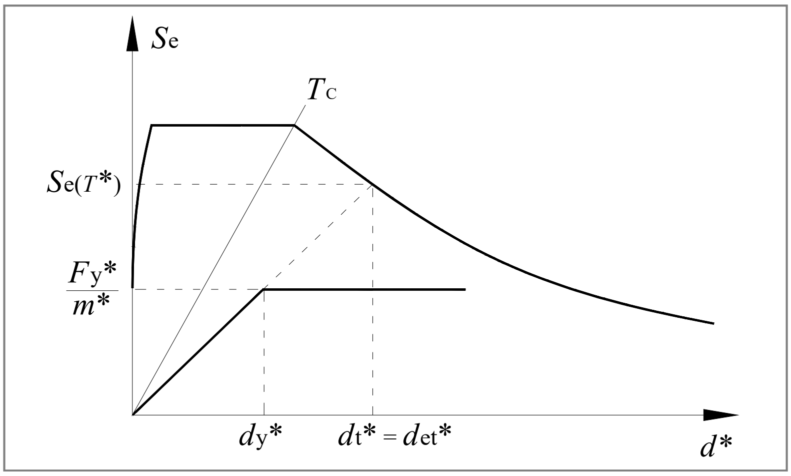

Figure 2.8: Determination of target displacement for the equivalent SDOF system (Medium and long period range).

- Case 2: $T_1 < T_C$ (Short period range)

In this case the inelastic target displacement will be determined according to equation 2.29.

$$d_t^* = \frac{d_{et}^*}{q_u}\left(1 + (q_u - 1)\frac{T_C}{T^*}\right) \geq d_{et}^* \tag{2.29}$$

• q_u = Ratio between the acceleration in the structure with unlimited elastic behaviour, $S_e(T^*)$, and in the structure with limited strength, F^*_y / m*.

$$q_u = \frac{S_e(T^*)m^*}{F_y^*} \tag{2.30}$$

d_t* need not exceed $3d_{et}$*.

If the target displacement, d_t*, is much different from the displacement at the formation of plastic mechanism, d_m*, an iterative procedure may be applied, in which the idealized bilinear curve is repeated by using d_t* (and the corresponding F_y*) instead of d_m*.

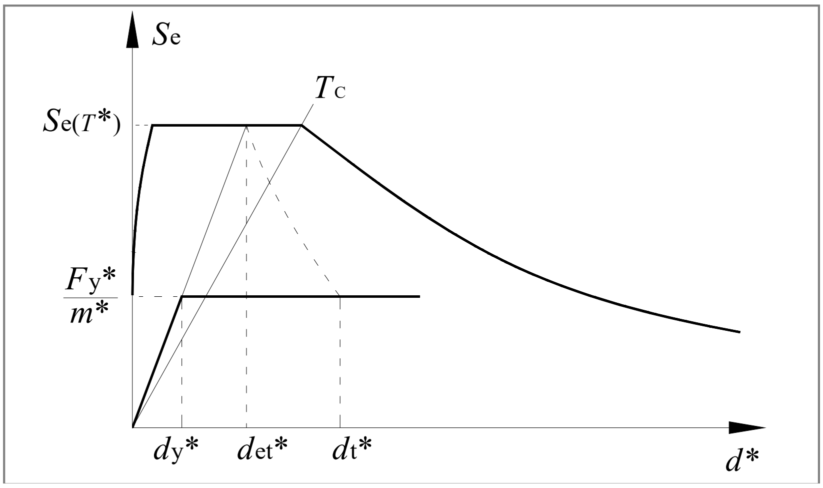

Figure 2.9: Determination of target displacement for the equivalent SDOF system (Short period range).

2.2.6. Acceptance criteria

Components shall be classified as being either ductile or brittle. Beams, columns and walls under flexure with and without axial force shall be classified as ductile. Shear mechanism of beams, columns and walls shall be classified as brittle.

For deformation-controlled components performance level shall be established according to the total chord rotation limits given in equations 2.31, 2.32 and 2.33. Chord rotation, θ (see figure 2.10), is the angle between the tangent to the axis at the yielding end and the chord connecting that end with the end of the shear span ($L_v = M/V$).

For brittle components their strength shall be checked.

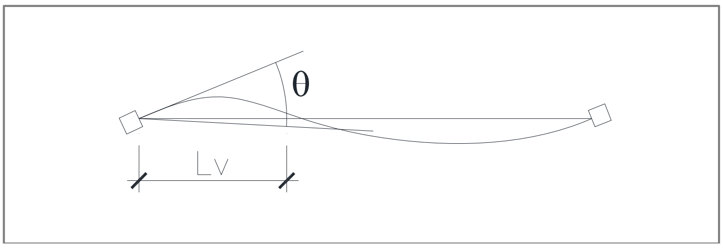

Figure 2.10: Chord Rotation.

• Limit State of near collapse (NC)

$$\theta_{um} = \frac{2}{3}\left(\theta_y + (\varphi_u - \varphi_y)L_{pl}\left(1 - \frac{0.5L_{pl}}{L_V}\right)\right) \quad (2.31)$$

• θ_{um} = Near collapse performance total chord rotation (elastic + plastic).

• θ_y = Chord rotation at yield.

• ϕ_u = Ultimate curvature.

• ϕ_y = Yield curvature.

The shear span at member end, L_V, and the plastic hinge length, L_{pl}, shall be obtained from equations 3.23 and 3.24.

• Limit State of Significant Damage (SD)

$$\theta_{SD} = \frac{3}{4}\theta_{um} \quad (2.32)$$

• θ_{SD} = significant damage performance total chord rotation (elastic + plastic).

• Limit State of Damage Limitation (DL)

$$\theta_y = \phi_y \frac{L_V}{3} + 0.0014\left(1 + 1.5\frac{h}{L_V}\right) + \frac{\varepsilon_y}{d - d'}\frac{d_{bL} f_y}{6\sqrt{f'_c}} \quad (2.33)$$

$$L_V = M / V \quad (2.34)$$

$$L_{pl} = \frac{L_V}{30} + 0.20h + 0.11\frac{d_{bL} f_y}{\sqrt{f'_c}} \quad (2.35)$$

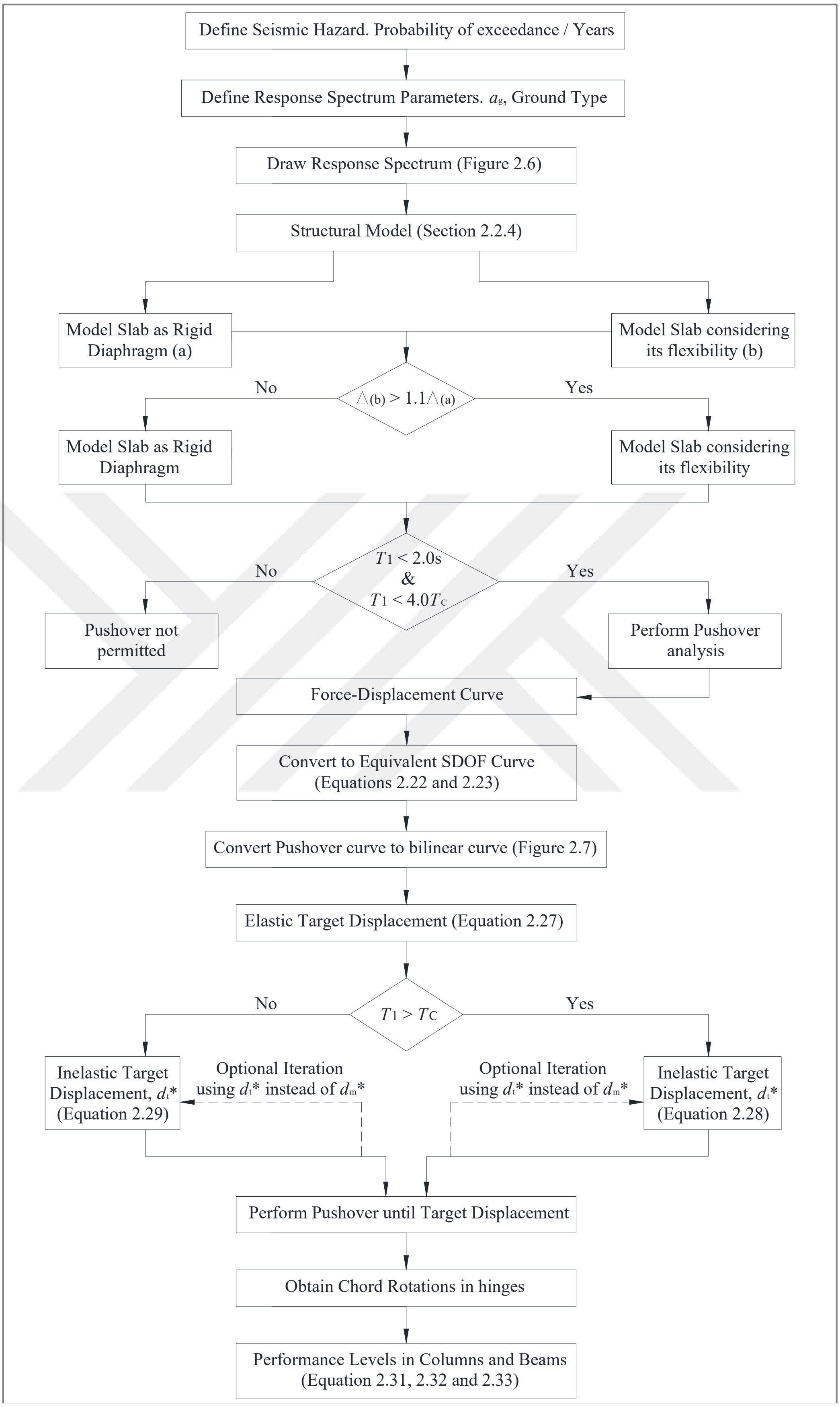

Figure 2.11: Performance Assessment Procedure in EN 1998-3.

- θ_y = Chord rotation at yield.
- ε_y = Stirrup yield strain.
- d = Distance from extreme compression fiber to centroid of tension reinforcement.
- d' = Distance from extreme tension fiber to centroid of compression reinforcement.
- h = Height of the member along which deformations are measured.
- d_{bL}: Mean diameter of the tension reinforcement.
- f'_c = Compressive strength of concrete (MPa).
- f_y = Yield stress of reinforcing steel (MPa).
- L_V = Shear span.
- V = Design shear force from Nonlinear Static Procedure (Pushover).
- M = Design moment from Nonlinear Static Procedure (Pushover).

2.3. Turkish Seismic Code (TBDY-16)

This section shows the nonlinear performance assessment procedure stated in Turkish Seismic Code (TBDY-16), published in 2016 as draft version. Figure 2.18 sketches this procedure and shows specific chapter references.

2.3.1. Performance Objectives

A performance Objective shall consist of one or more pairings of a selected Seismic Hazard level with a target Building Performance Level.

- Target Building Performance Levels

The Performance Level of a building shall be selected from four discrete Levels defined.

The discrete Performance Levels are Operational (KK), Immediate Occupation (HK), Life Safety (CG), and Collapse Prevention (GO).

• Seismic Hazard

Table 2.12 shows the four ground motions probabilities of exceedance and corresponding return periods used in this standard.

Table 2.12: Probability of Exccedance and Mean Return Period.

Hazard level	Probability of Exceedance	Mean Return Period (years)
DD-1	2% / 50 years	2475
DD-2	10% / 50 years	475
DD-3	50% / 50years	72
DD-4	50% / 30years	43

• Response Spectrum

A general horizontal response spectrum, as shown in figure 2.12, will be developed for a defined seismic hazard and using a 5% damping.

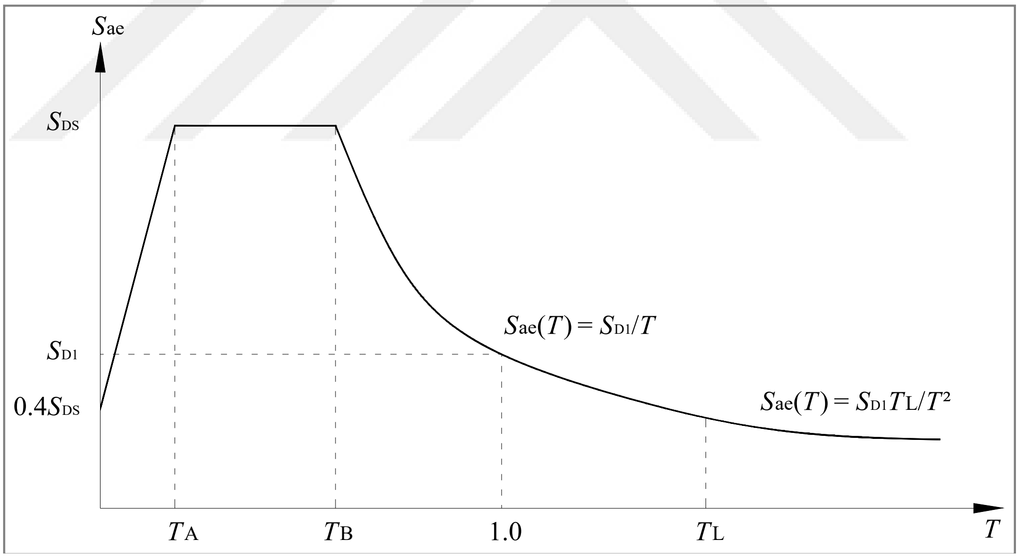

Figure 2.12: General Horizontal Response Spectrum.

The short-period response acceleration parameter, S_S, and the response acceleration parameter at a 1-s period, S_1, for the DD-1 Seismic Hazard Level will be taken as values from approved 2%/50-year maximum direction spectral response acceleration contour maps.

The design spectral response acceleration parameters, S_{DS} and S_{D1}, will be obtained from the next equations:

$$S_{DS} = S_S F_S \tag{2.36}$$

$$S_{D1} = S_1 \gamma_F F_1 \tag{2.37}$$

F_s and F_1 are site coefficients determined respectively from tables 2.13 and 2.14, based on based on the site class and the values of the response acceleration parameters S_S and S_1 for the selected return period.

The distance to fault coefficient, γ_F, will be obtained from equation 2.38:

$$\gamma_F = 1.2 - 0.02(L_F - 15) \tag{2.38}$$

Where:

- L_F = Orthogonal distance to the nearest fault.

For distances greater than 25 km, γ_F = 1.0. For distances less than 15 km, γ_F = 1.2.

Table 2.13: Spectral acceleration coefficient at short period (F_s).

Local Site Class	**Mapped Spectral Acceleration at Short-Period S_S**					
	$S_S \leq 0,25$	**$S_S = 0,50$**	**$S_S = 0,75$**	**$S_S = 1,0$**	**$S_S = 1,25$**	**$S_S \geq 1,50$**
ZA	0.80	0.80	0.80	0.80	0.80	0.80
ZB	0.90	0.90	0.90	0.90	0.90	0.90
ZC	1.30	1.30	1.20	1.20	1.20	1.20
ZD	1.60	1.40	1.20	1.10	1.00	1.00
ZE	2.40	1.70	1.30	1.10	0.90	0.80
ZF	Site-specific geotechnical investigation shall be performed					

Straight-line interpolation shall be used for intermediate values of S_S.

Table 2.14: Spectral acceleration coefficient at period 1.0 s (F_1).

Local Site Class	Mapped Spectral Acceleration at 1-s Period S_1					
	$S_1 \leq 0,1$	$S_1 = 0,2$	$S_1 = 0,3$	$S_1 = 0,4$	$S_1 = 0,5$	$S_1 \geq 0,6$
ZA	0.80	0.80	0.80	0.80	0.80	0.80
ZB	0.80	0.80	0.80	0.80	0.80	0.80
ZC	1.50	1.50	1.50	1.50	1.50	1.40
ZD	2.40	2.20	2.00	1.90	1.80	1.70
ZE	4.20	3.30	2.80	2.40	2.20	2.00
ZF	Site-specific geotechnical investigation shall be performed					

Straight-line interpolation shall be used for intermediate values of S_1.

Local site class will be defined according to table 2.15.

Table 2.15: Site Classes.

Site Class	Type of soil	Average of the upper 30 m of soil		
		v_s [m/s]	N	c_u [kPa]
ZA	Solid, hard rock.	> 1500	-	-
ZB	Sedimentary, moderately solid rock	760 - 1500	-	-
ZC	Very dense sand, gravel and hard clay layers or sedimentary, very fissured soft rock	360 - 760	> 50	> 250
ZD	Medium dense or dense sand, gravel or very stiff clay layers.	180 - 360	15 - 50	70 - 250
ZE	Loose sand, gravel or soft clay layers	< 180	< 15	< 70

- v_s = Average shear wave velocity of the upper 30m of soils at the site.
- N = Average standard penetration test (SPT) of the upper 30m of soils at the site.
- c_u = Undrained shear strength of the upper 30m of soils at the site.

T_A and T_B are given by the next equations:

$$T_A = 0.2\frac{S_{D1}}{S_{DS}} \tag{2.39}$$

$$T_B = \frac{S_{D1}}{S_{DS}} \tag{2.40}$$

The period for which horizontal displacement spectrum become constant, T_L, will be taken as 6 s.

2.3.2. Structural Model

The structural system of the building shall be modeled in three dimensions. The effect of the seismic loads shall be considered in the two orthogonal horizontal directions.

- Damping

Linear Critical damping ratio will be taken as 5%.

- Gravity loads

The following actions caused by gravity loads, w_j, in accordance with equation 2.41 shall be combined with actions caused by seismic forces.

$$w = w_G + n.w_Q \tag{2.41}$$

Where:

- w = Action caused by gravity loads.
- $w_{G,}$ = Action caused by dead load.
- w_Q = Action caused by live load.

The live load coefficient, n, will be defined according to the table 2.16.

Table 2.16: Live load mass contribution Coefficient.

Use or occupancy of the building	***n***
Areas of storage	0.80
Schools, cinemas, theatres, restaurants, shops and similar	0.60
Residential buildings, offices, hotels, hospitals, parking lots and similar	0.30

- Effective Stiffness

The stiffness of the structural member shall be multiplied by the factors given in table 2.17.

Table 2.17: Effective Stiffness Factor.

Element	**Effective Section Stiffness Factor**	
	Flexural	**Shear**
Connection Beams	0.15	1.00
Beam in Frames	0.35	1.00
Columns	0.70	1.00
Walls	0.50	0.50
Slabs	0.25	0.25

- Joint Model

In Beam-Column joints, the column offsets can be modeled rigid or partially rigid.

- Hinge Model

In elements that can be modeled as a frame, such as beam, columns and walls, the nonlinear beahavior can be modeled using concentrated hinge models. The hinges shall be placed inmediately next to joints in columns and beams, however, in the center of beams could also be considered or any other place where is expected nonlinear beahavior caused by the gravity loads.

The plastic hinge length shall be set equal 0.5 times the flexural depth of the element.

$$L_p = 0.5h \tag{2.42}$$

- L_p = Plastic hinge length.
- h = Height of the member along which deformations are measured.

- Slab model in irregular buildings

If in any story, the open area in the slab including stairs and elevators exceeds one third of the total area, the structure shall be classified as irregular in plan, this irregularity is called discontinuity in diaphragm.

In this type of structures the slabs shall be modeled as a membrane, in order to show that is safely capable of transferring seismic forces between vertical elements. (Not rigid diaphragm can be assigned).

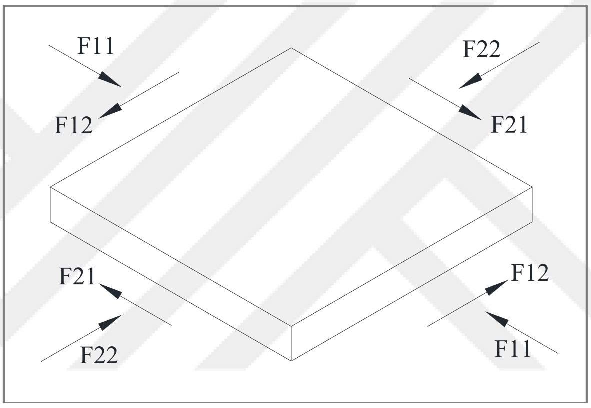

Figure 2.13: Internal forces in membranes.

- F11 = Internal axial force along axis 1.
- F22 = Internal axial force along axis 2.
- F12 = F21 = Internal shear force.

2.3.3. Nonlinear Static (Pushover) Procedure

This section shows the procedure to be applied in nonlinear static procedure.

Buildings shall be subjected to monotonically increasing lateral loads, which will be proportional to the Dominant vibration modal shape in the direction considered. This procedure will be applied until a step equivalent to a target displacement.

• Nonlinear Static Procedure (Pushover) limitations

To be able to use the pushover method, in each floor the torsion irregularity coefficient, η_{bi}, must be smaller than 1.4. Moreover, the ratio of the participating mass of the fundamental vibration mode to the total mass of the building should be at least 0.70.

$$\eta_{bi} = (\Delta_i)_{\max} / (\Delta_i)_{ort} \tag{2.43}$$

$$(\Delta_i)_{ort} = 1/2\left[(\Delta_i)_{\max} + (\Delta_i)_{\min}\right] \tag{2.44}$$

- $(\Delta_i)_{max}$ = maximum Story drift in floor i.
- $(\Delta_i)_{min}$ = minimum Story drift in floor i.

• Equivalent SDOF Force-Displacement Curve

The pushover curve, which represents the base shear force and the displacement in the control node, will be converted in an equivalent SDOF curve, representing spectral acceleration and displacement.

The spectral acceleration, a_1, and displacement, *d,* of the equivalent SDOF system are computed as:

$$a_1 = \frac{V_t}{m_t} \tag{2.45}$$

$$d = \frac{u_N}{\Phi_N \Gamma} \tag{2.46}$$

Where:

- V_t = Base shear force.
- u_N = Displacement of the control node of the Multi Degree of Freedom (MDOF) system.

The modal participating factor, Γ, and the effective modal mass, m_t, are given by equations 2.47 and 2.48:

$$\Gamma = \frac{\sum m_i \Phi_i}{\sum m_i \Phi_i^{\ 2}} \tag{2.47}$$

$$m_t = \sum m_i \Phi_i \Gamma \tag{2.48}$$

- Φ_i = Modal displacement of floor i.
- Φ_N = Modal displacement of the last floor.
- m_i = Mass at level i.

- Target displacement

The target displacement, d_1, will be given by the equation 2.49:

$$d_{1,\max} = S_{di}(T_1) \tag{2.49}$$

$$S_{di}(T_1) = C_R S_{de}(T_1) \tag{2.50}$$

$$S_{de}(T_1) = S_{ae}(T_1)\left(\frac{T_1}{2\pi}\right)^2 \tag{2.51}$$

Where:

- $S_{de}(T_1)$ = Elastic response spectrum displacement at the fundamental period.
- $S_{ae}(T_1)$ = Elastic response spectrum acceleration at the fundamental period.
- $S_{di}(T_1)$ = Inelastic response spectrum displacement at the fundamental period.
- C_R = Spectral displacement Ratio.

There are two possible cases to calculate the spectral displacement ratio, C_R, those cases will depend on the fundamental period of the structure, T_1, and one of the characteristic periods of the soil, T_B.

- Case 1: $T_1 > T_B$

- $C_R = 1.0$

$$S_{di}(T_1) = S_{de}(T_1) \quad (2.52)$$

Where:

- T_1 = Fundamental period of the building.
- T_B = Characteristic period of the response spectrum at which the constant acceleration segment transitions to the constant velocity segment.
- ω_1 = Fundamental angular frequency.

$$\omega_1 = \frac{2\pi}{T_1} \quad (2.53)$$

$$\omega_B = \frac{2\pi}{T_B} \quad (2.54)$$

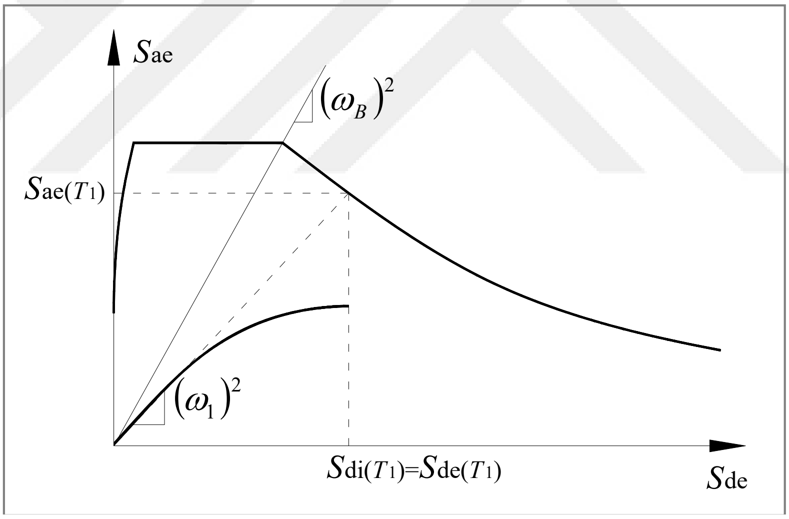

Figure 2.14: Determination of Inelastic displacement demand ($T_1 > T_B$).

- Case 2: $T_1 < T_B$

In this case the spectral displacement ratio, C_R, will be calculated using an iterative process; first the equivalent SDOF force-displacement curve will be replaced with an idealized bilinear relationship, from this curve the effective yielding equivalent acceleration, a_{y1}, will be obtained, as shown in Figure 2.15.

The first segment of the idealized curve will begin at the origin and have a slope equal to the square of the fundamental angular frequency, $(\omega_1)^2$. The second line segment will be a horizontal line, determined by a point (a_{y1}, $S_{de}(T_1)$) and a point at the intersection with the first line segment such that the areas above and below the actual curve are approximately balanced.

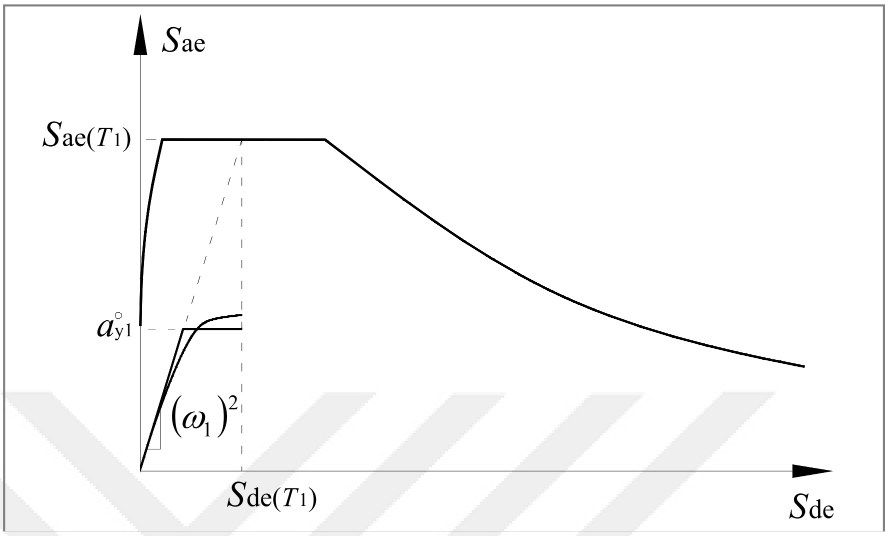

Figure 2.15: Bilinear SDOF Force-Displacement Curve.

Then the strength reduction factor, R_y, is calculated as follows:

$$R_y = \frac{S_{ae}(T_1)}{a_{y1}} \tag{2.55}$$

The next step is to calculate the Seismic ductility demand, μ, which is given by equation 2.56.

$$\mu(R_y, T_1) = 1 + (R_y - 1)\frac{T_B}{T_1} \tag{2.56}$$

The spectral displacement ratio is given by:

$$C_R = \frac{\mu(R_y, T_1)}{R_y} \tag{2.57}$$

Using this spectral displacement ratio, C_R, the inelastic displacement demand, $S_{di}(T_1)$, is estimated using equation 2.58:

$$S_{di}(T_1) = C_R S_{de}(T_1) \tag{2.58}$$

Using this inelastic displacement demand, S_{di}, a new bilinear curve is built until a displacement equal to S_{di} and a new yielding equivalent acceleration, a_{y1}, is found, as shown in figure 2.16.

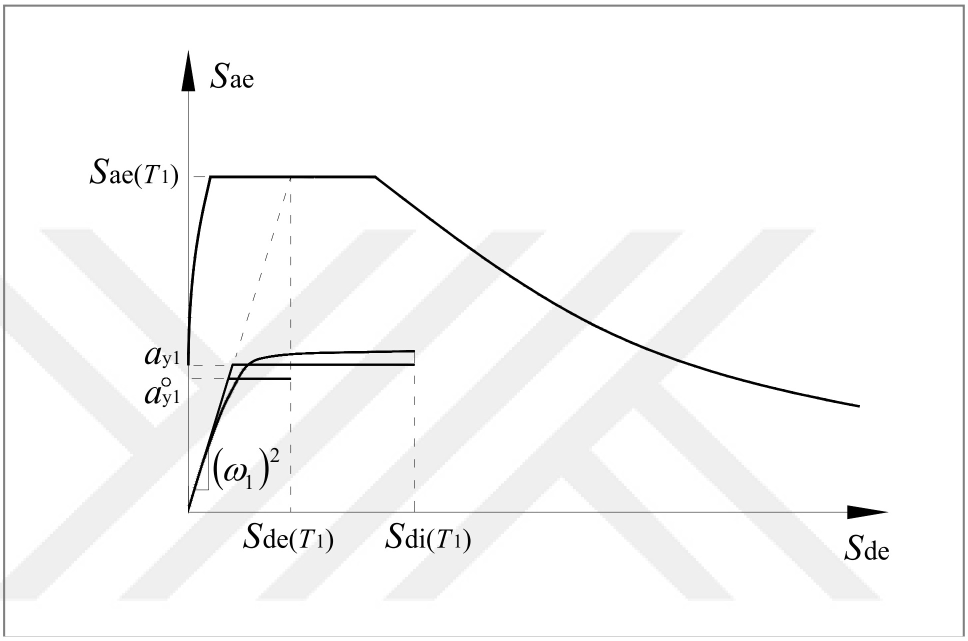

Figure 2.16: Determination of Inelastic displacement demand ($T_1 < T_B$).

Finally the spectral displacement ratio, C_R, and the displacement demand are calculated again. If the current and the previous displacement demand calculated are very different, iterations can be done.

2.3.4. Performance Levels:

Three limit conditions have been defined for ductile elements. These are Minimum Damage Limit (MN), Safety Limit (GV) and Collapse Limit (GC). This classification does not apply to elements damaged in a brittle condition.

• Performance levels in Sections

Performance levels in sections shall be established according to maximum strain values indicated in equations 2.60, 2.61 and 2.62 and assigned to one of the four regions shown in figure 2.17.

Strains in concrete and steel shall be obtained from the Moment-curvature diagram of the element, using the total curvature in the sections of the elements in the deformed structure.

Total curvature shall be obtained using the plastic rotations from the structural analysis and equation 2.59

$$\phi_t = \frac{\theta_p}{L_p} + \phi_y \qquad (2.59)$$

- θ_p = Plastic rotation.
- ϕ_y = Yielding curvature.
- ϕ_t = Total curvature.
- L_p = Plastic hinge length.

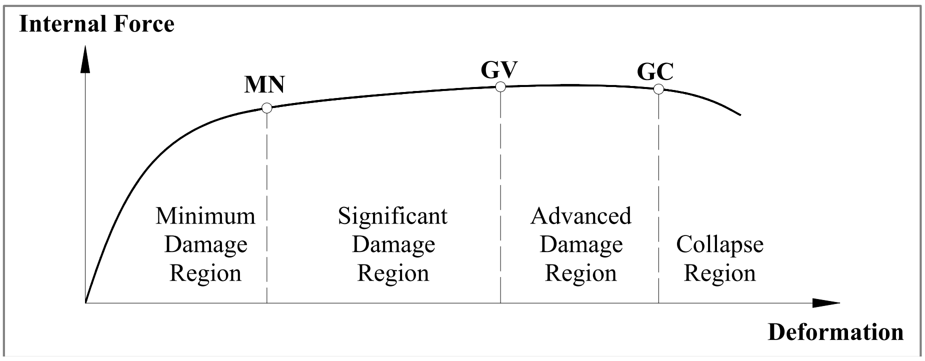

Figure 2.17: Damage levels in sections and elements.

- Strain limits for Minimum Damage performance level (MN)

$$\begin{aligned}(\varepsilon_{cu})_{MN} &= 0.0035 \\ (\varepsilon_S)_{MN} &= 0.010\end{aligned} \tag{2.60}$$

- Strain limits for safety performance level (GV)

$$\begin{aligned}(\varepsilon_{cg})_{GV} &= 0.0135 \\ (\varepsilon_S)_{GV} &= 0.040\end{aligned} \tag{2.61}$$

- Strain limits for collapse performance level (GC)

$$\begin{aligned}(\varepsilon_{cg})_{GC} &= 0.018 \\ (\varepsilon_S)_{GC} &= 0.060\end{aligned} \tag{2.62}$$

Where:

- (ε_{cu}) = Compression strain in extreme concrete fiber.
- (ε_{cg}) = Compression strain in extreme confined concrete fiber.
- (ε_s) = Strain in the extreme layer of longitudinal tension reinforcement.
- MN = Minimum Damage.
- GV = Safety.
- GC = Collapse.

$$\frac{V}{b_w d.f_{ctm}} < 0.65 \tag{2.63}$$

The strain limits in equations 2.60, 2.61 and 2.62 are acceptable when the shear force ratio given in equation 2.63 is less than 0.65. For Shear Force ratio bigger than 1.3 the strain limits will be multiplied by 0.50, for other values linear interpolation will be applied.

- V = Design Shear Force from Nonlinear Static Procedure (Pushover).
- b_w = Web width.

- d = Distance from extreme compression fiber to centroid of tension reinforcement.
- f_{ctm} = Tension Strength of concrete.

- Performance level in Buildings

The Performance level in a Building will be established based on the Damage Zone on which its members remain.

- Immediate Occupancy (HK)

At most 10% of the beams on each floor enter to the Significant Damage Zone and all the other elements remain in the Minimum Damage Zone.

- Life Safety (CG)

Less than 30% of the beams on each floor enter to the Advanced Damage Zone. Furthermore, if there are vertical elements in Advanced Damage Zone, they will represent less than 20% of all the shear strength on each floor

- Collapse Prevention (GO)

At most 20% of the beams on each floor enter to the Collapse Zone. Also, the vertical elements in Advanced Damage Zone represent less than 20% of all the shear strength on each floor

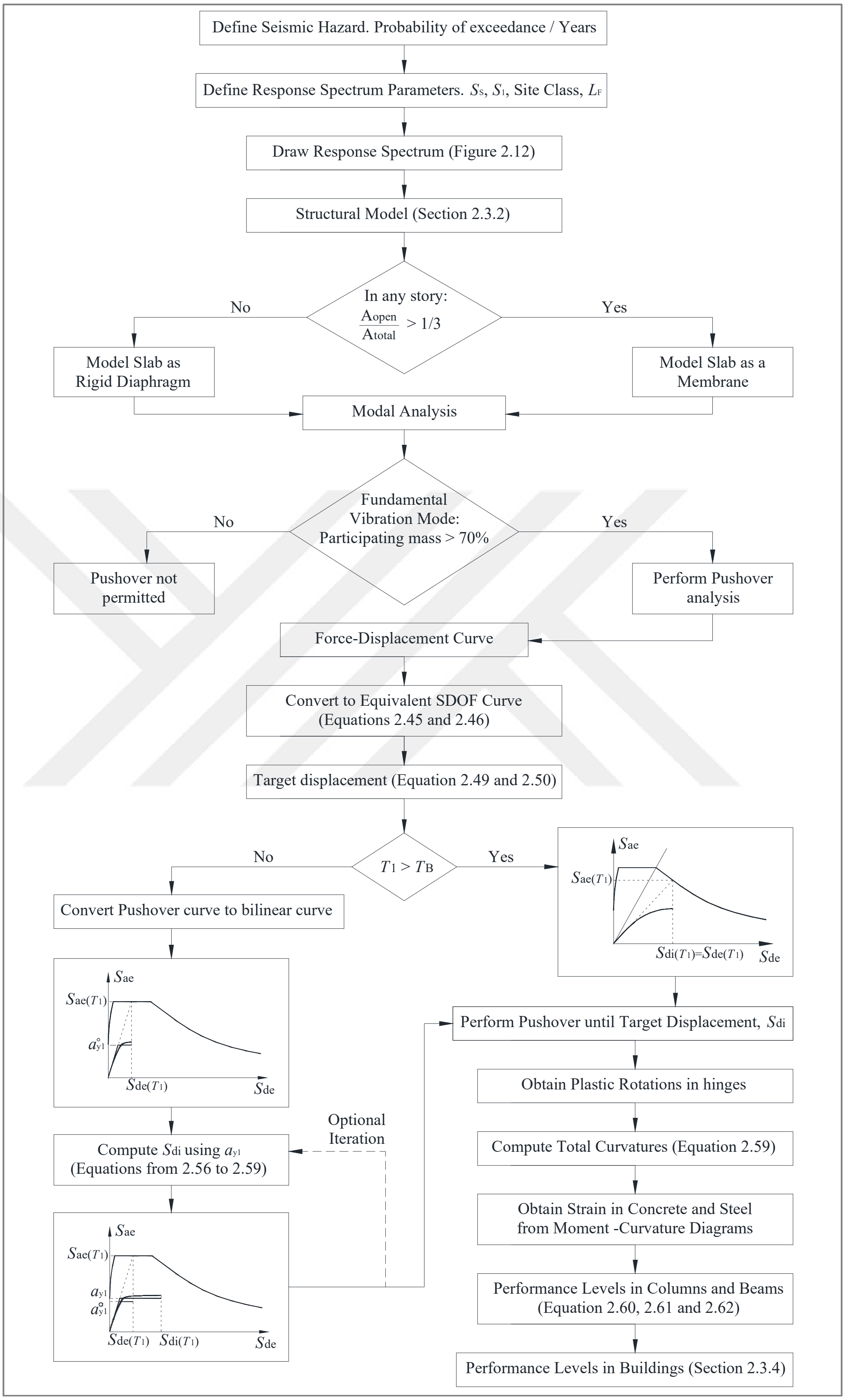

Figure 2.18: Performance Assessment Procedure in TBDY-16.

2.4. Comparison of General Requirements for Nonlinear Performance Assessment

The general requirements for nonlinear performance assessment in those three standards will be compared in this section. Tables will be presented in order to emphasize the differences existent between them.

2.4.1. Target Building Performace Levels

Each of the standards studied have established three performance levels which are shown in table 2.18. Since those performance levels have similar definitions they can be considered equivalent.

Table 2.18: Target Building Performance Levels.

ASCE-41-13	**Eurocode EN 1998-3**	**TBDY-16**
Immediate occupancy Life Safety Collapse Prevention	Damage Limitation Significant Damage Near Collapse	Immediate Occupation Life Safety Collapse Prevention

Immediate Occupancy (IO) in ASCE-41-13, Damage Limitation (DL) in EN 1998-3 and Immediate Occupation (HK) in TBDY-16; three of them correspond to buildings that are expected to sustain minimal or no damage to their structural elements after a major earthquake. Immediate reoccupancy of the building is possible although it might be necessary to perform some cleanup and restoration of utility service. The risk to Life Safety is very low.

Life Safety (LS) in ASCE-41-13, Significant Damage (SD) in EN 1998-3 and Life Safety (CG) in TBDY-16 are equivalent; in a building in those performance levels there will be few, or no injuries to occupants or any person in the immediate vicinity. Buildings meeting those levels may experience extensive damage. Repairs may be required before reoccupancy and repairs may be economically impractical. The risk to Life Safety is low.

Collapse Prevention (CP) in ASCE-41-13, Near Collapse (DL) in EN 1998-3 and Collapse Prevention (GO) in TBDY-16; three of them correspond to buildings where substantial damage has occurred, significant degradation in the stiffness and strength of the lateral-force-resisting system and large permanent lateral deformation are also expected. However, all significant components of the gravity-load-resisting system continue to carry their gravity loads. The structure might not be practical to repair and is not safe for reoccupancy because an aftershock could cause collapse.

2.4.2. Seismic Hazard

Seismic hazard shall be selected as a probability of exceedance in a specific time period. ASCE-41-13 recommends five different seismic hazards, similarly TBDY-16 allows to use four seismic hazards.

EN 1998-3 presents only two seismic hazards. In order to obtain additional levels of seismic hazard, the seismic action must be multiplied by importance factors. An importance factor equal to 1.0 is associated with 10% / 50years; an importance factor equal to 1.5 is associated with 2% / 50years.

Table 2.19: Seismic Hazards.

ASCE-41-13	**Eurocode EN 1998-3**	**TBDY-16**
2% / 50years		2% / 50years
5% / 50 years	10% / 50 years	10% / 50 years
10% / 50 years		50% / 50 years
20% / 50 years	10% / 10 years	50% / 30 years
50% / 50 years		

2.4.3. Response Spectrum

Response spectrums shall be defined using the parameters shown in table 2.20. Those include ground motion parameters obtained from contour maps and the characteristic of the soils where building is located.

Table 2.20: Parameters for Response Spectrum.

ASCE-41-13	Eurocode EN 1998-3	TBDY-16
S_S, S_1, Site Class	a_g, Ground type	S_S, S_1, Site Class, L_F

ASCE-41-13 and TBDY-16 define their spectrums using S_S and S_1, which are the spectral response acceleration parameter for 0.2s and 1.0s respectively. EN 1998-3 uses the ground acceleration parameter, a_g.

In order to consider the characteristics of different soils, ASCE-41-13 and TBDY-16 defined 5 site classes, those are, solid rock, moderately solid rock, very dense sand, dense and soft clay. EN 1998-3 uses 4 ground types, rock, very dense sand, dense sand and soft clay. The characteristics of those type of soils are detailed in tables 2.5, 2.10 and 2.15.

TBDY-16 included one additional factor to consider the proximity to a seismic fault, L_F, this factor shall be taken into account for distances less than 25 km and it can increase the spectrum values until a 20% .

Figures 2.19 and 2.20 show two examples of response spectrum, in order to compare the three standards used. The parameters used were as following, S_s=1.06, S_1=0.39, a_g=0.4, L_F=25km and moderately solid rock and dense sand as soil type. One of the reasons for the differences observed are the site coefficients; F_a and F_v in ASCE-41-13 and F_S and F_1 in TBDY-16. Those coefficients were higher in ASCE-41-13 for rock soil, contrarily they were higher in TBDY-16 for sand soil.

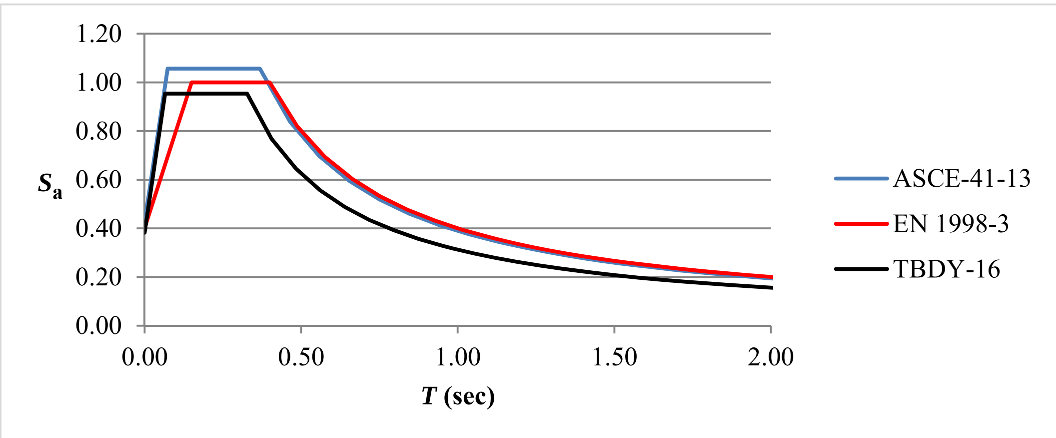

Figure 2.19: Response Spectrum Comparison (S_S=1.06, S_1=0.39, a_g=0.4, Soil: Rock).

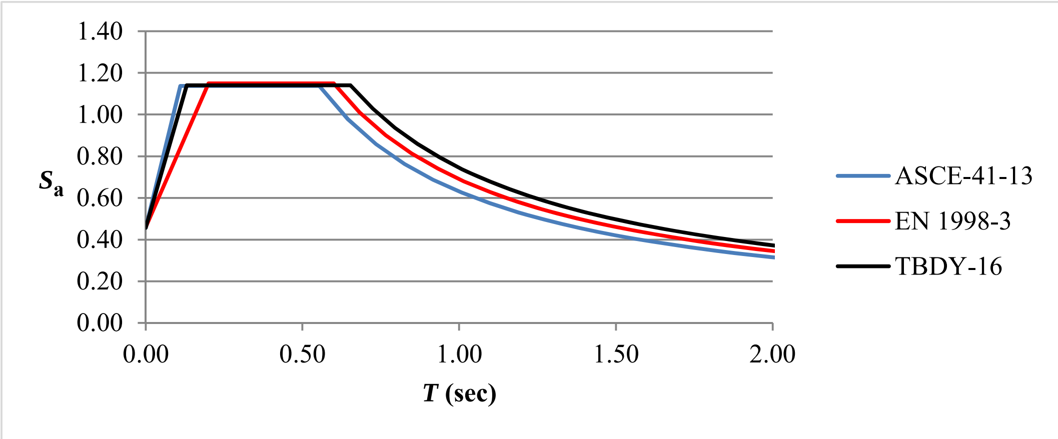

Figure 2.20: Response Spectrum Comparison (S_S=1.06, S_1=0.39, a_g=0.4, Soil: Sand).

2.4.4. Structural Model

This sections shows some of the requirements for structural models for nonlinear performance assessment in the three standards studied, their differences will be analyzed.

- Effective Stiffness

Table 2.21 shows the effective cracked rigidities in elements that shall be considered in structural models for nonlinear performance assessment.

In EN 1998-3 flexural inertias shall be calculated for each member considering yielding moment, M_y, and chord rotation at yield, θ_y. In TBDY-16 flexural inertias shall be constant as the values shown in table 2.21. In ASCE-41-13 the flexural inertia for columns shall be between 0.3 and 0.7 depending on the axial load in them. In buildings designed to resist earthquake forces the axial load in columns is expected to be low, therefore, in those cases ASCE-41-13 could have lower inertias in columns, which result in more flexible structures.

The shear stiffness in slabs will be lower in TBDY-16, this will cause a bigger effect of non-rigid diaphragm in the deformed structures.

Table 2.21: Effective Stiffness values.

ASCE-41-13	Eurocode EN 1998-3	TBDY-16
Flexural Stiffness:		
Beams: $0.3I_g$ Columns: $(0.3 – 0.7)I_g$ Walls: $= 0.5I_g$	$\dfrac{M_y L}{6\theta_y}$	Beams: $0.35I_g$ Colums: $0.7I_g$ Walls: $0.5I_g$
Shear Stiffness:		
Walls: $0.4E_cA_g$ Slabs: $0.4E_cA_g$	Walls: $0.5E_cA_g$ Slabs: $0.5E_cA_g$	Walls: $0.25E_cA_g$ Slabs: $0.25E_cA_g$

- Plastic Hinge length

Using ASCE-41-13, the design engineer does not require to determine a plastic hinge length because the analysis is performed in terms of rotations only.

Plastic hinge length in EN 1998-3 will depend both on properties of the member (h) and the seismic loads (L_V = M/V), therefore it will change as lateral forces increases during pushover analysis.

In TBDY-16, plastic hinge length will be calculated as 0.5 times the flexural depth of the beam or column.

Table 2.22: Plastic hinge length.

ASCE-41-13	Eurocode EN 1998-3	TBDY-16
(Not required)	$L_{pl} = \dfrac{L_V}{30} + 0.20h + 0.11\dfrac{d_{bL} f_y}{\sqrt{f'_c}}$	$L_p = 0.5h$

- Slab model in irregular buildings

According to ASCE-41-13, diaphragms shall be classified as flexible where the maximum horizontal deformation of the diaphragm is more than twice the average drift of the story immediately below the diaphragm.

EN 1998-3 establishes that diaphragm must be taken as rigid, if, when it is modelled with its actual in-plane flexibility, its horizontal displacements nowhere exceeds those resulting from the rigid diaphragm assumption by more than 10%.

According to TBDY-16, slabs shall be modeled as a membrane if the open area in the slab including stairs and elevators exceeds one third of the total area.

Table 2.23: Classification of diaphragms.

ASCE-41-13	Eurocode EN 1998-3	TBDY-16
$\Delta_{dia} > 2\Delta_{avg}$ (See figure 2.3)	$\Delta_{(flexible)} > 1.1\Delta_{(rigid)}$	$\frac{A_{(open)}}{A_{(total)}} > 1/3$

2.4.5. Nonlinear Static (Pushover) Procedure

This sections points out the differences existing in the standard studied regarding the procedure for nonlinear static analysis of structures.

• Nonlinear Static (Pushover) Procedure limitations

In the three standards, in order to apply pushover analysis the condition required is that the higher vibration modes of the structure must be not significant. This condition is verified using different characteristics. In ASCE-41-13 Shear Story resulting from the first mode is compared with the ones resulting from higher modes which cause 90% participating mass. In EN 1998-3 the period of the fundamental period must be low and the building must be regular in elevation. TBDY-16 establish that the participating mass in the fundamental mode must be higher than 70% and the torsional coefficient must be lower than 1.4.

Table 2.24: Nonlinear Static (Pushover) Procedure limitations.

ASCE-41-13	Eurocode EN 1998	TBDY-16
$V_{(\text{n modes, 90\% mass})} \leq 1.3\, V_{(\text{1st mode})}$	$T_1 \leq \begin{cases} 2.0s \\ 4T_c \end{cases}$ Regularity in Elevation	$\eta_{bi} < 1.4$ Participating mass ≥ 70%

• Equivalent SDOF Force-Displacement Curve

Generally in pushover procedure the nonlinear force-displacement relationship shall be converted to an idealized bilinear curve. However, in TDBY-16 this step is necessary only for short periods ($T_1 < T_B$).

The main criteria to develop the bilinear curve in the three standards is that the area below both curves must be equal.

In ASCE-41-13 the first line will begin at the origin and intersect the original curve at a base shear force equal to 60% of the effective yield strength of the structure. In EN 1998-3 the initial slope will be the slope necessary to make equal areas below original curve and bilinear curve. In TBDY-16 the initial slope will be equal to the square of the fundamental angular frequency, $(\omega_1)^2$.

In EN 1998-3 and TBDY-16 the second line will be a horizontal line. In ASCE-41-13 the second line will have the slope necessary to make equal areas below original curve and bilinear curve.

Table 2.25: Idealized Bilinear Force-Displacement curve.

ASCE-41-13	**Eurocode EN 1998-3**	**TBDY-16**
Initial slope: K_e 2nd line: (V_y,Δ_y – V_d,Δ_d)	 2nd line: horizontal	Initial Slope: $(\omega_1)^2$ 2nd line: horizontal
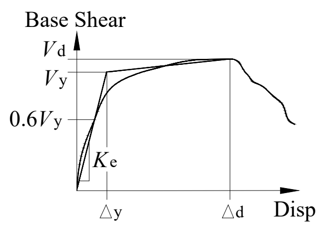	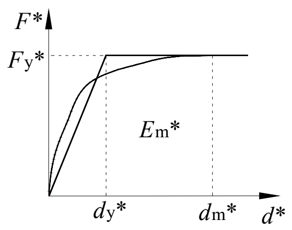	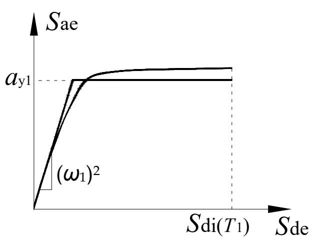

• Target displacement

ASCE-41-13 presents the coefficient method for calculating target displacement which uses the response spectrum acceleration, $S_a(T_e)$, and three main coefficients, C_0,C_1 and C_2. C_0 converts displacement in a multi degree of freedom system (MDOF) to a single degree of freedom system (SDOF), C_1 relates expected maximum inelastic displacement to displacements calculated for linear response, and *C2* represents the effects of pinched hysteresis shape and cyclic stiffness degradation.

Table 2.26: Target displacement.

ASCE-41-13	**Eurocode EN 1998**	**TBDY-16**
Target displacement:		
$\delta_t = C_0 C_1 C_2 S_a \dfrac{T_e^{\,2}}{4\pi^2} g$	d_t^*	$d_{1,\max} = S_{di}(T_1)$ $S_{di}(T_1) = C_R S_{de}(T_1)$
Long period Range:		
$T > 1.0, \quad C_1 = 1.0$	$T_1 > T_C, \quad d_t^* = d_{et}^*$ 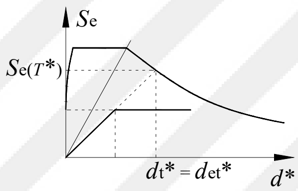	$T_1 > T_B, \quad C_R = 1.0$ 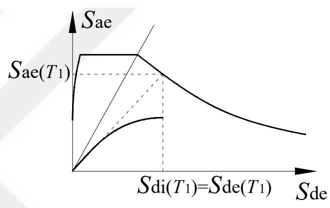
Short period Range:		
$T < 1.0,$ $C_1 = 1 + \dfrac{\mu_{strength} - 1}{a.T_e^{\,2}}$	$T_1 < T_C,$ $d_t^* = \dfrac{d_{et}^*}{q_u}\left(1 + (q_u - 1)\dfrac{T_C}{T^*}\right)$	$T_1 < T_B, \quad R_y = \dfrac{S_{ae}(T_1)}{a_{y1}}$ $\mu(R_y, T_1) = 1 + (R_y - 1)\dfrac{T_B}{T_1}$ $C_R = \dfrac{\mu(R_y, T_1)}{R_y}$

In EN 1998-3 and TBDY-16 the target displacement is determined from the elastic response spectrum and base shear-displacement curve. For periods higher than the upper limit of the constant spectral acceleration branch, inelastic target displacement will be equal to the elastic target displacement, which is obtained from the response spectrum as shown in table 2.26. For lower periods inelastic target displacements will be obtained as elastic target displacements multiplied by an incremental factors.

2.4.6. Acceptance Criteria

ASCE-41-13 establishes performance levels in sections according to plastic rotations in hinges. Plastic rotations are obtained from a structural analysis in the following way, first, the stiffness matrix of the structure is developed, and then forces in joints are multiplied by the inverse of the stiffness matrix of the structure, this gives as results, displacements in joints, rotations in joints and plastic rotations in hinges. This means that plastic rotations can be obtained directly from a structural analysis.

In EN 1998-3 the performance levels are assigned in accordance with the chord rotations in the edge of elements, this rotation shall be an elastic + plastic part.

TBDY-16 establishes performance levels in elements according to strains in concrete and steel reinforcement. Strains can be obtained from Moment-curvature diagrams, using the total curvature calculated according to its plastic rotations, plastic hinge length and yielding curvature.

Table 2.27: Parameters for Acceptance Criteria.

ASCE-41-13	**Eurocode EN 1998**	**TBDY-16**
Plastic Rotations	Chord Rotation (Total Rotations)	Concrete strains Steel strains

3. STUDY CASE

In this chapter, all the procedure described in chapter 2 will be applied to five structures. The methodology used during the analysis will be explained and their results will be analyzed.

3.1. Description of the studied Buildings

This section describes all the characteristics of buildings necessary to carry out a nonlinear performance assessment of buildings.

3.1.1. Geometry

The buildings selected are six-story reinforced concrete buildings, the shape of the buildings is rectangular and the story height is 3.5 m. The slabs in all the stories have open areas in their centers, this open area will be between 20% and 60% of the total area, therefore 5 buildings were selected, each of them with 20%, 30%, 40%, 50% and 60% open area approximately. The details of total areas and open areas are shown in table 3.1.

The slabs were designed as one way ribbed slabs, with a minimum thickness equal to l/24. All the details of the structures are shown in figures from 3.1 to 3.14.

l = Span length of one-way ribbed slab.

Table 3.1: Open Areas in studied Structures.

Structure	Total Area (m2)	Open Area (m2)	Open Area (%)
1	1911.0	375.0	19.6
2	2000.0	600.0	30.0
3	3000.0	1200.0	40.0
4	3111.0	1575.0	50.6
5	3726.0	2200.0	59.0

3.1.2. Material

The concrete has a strength of 25 MPa and the reinforcement steel has a yielding stress equal to 420 MPa.

3.1.3. Loading

The buildings were designed for residential use, therefore the dead and live loads are 2.5 kN/m^2 and 2.0kN/m^2 in floors and 2.0 kN/m^2 and 1.0kN/m^2 in roof respectively

The seismic loads were calculated using the following parameters, 1.06 as the short period response acceleration parameter, 0.39 as the spectral response acceleration parameter at 1-s period, rock ground type and importance factor equal to 1.0.

Since the seismicity is considerably high, the buildings necessarily were designed as a system with high ductility, such as special moment frames, consequently the seismic response modification coefficient, R, was taken as 8.0 and the overstrength factor, Ω, equal to 2.5.

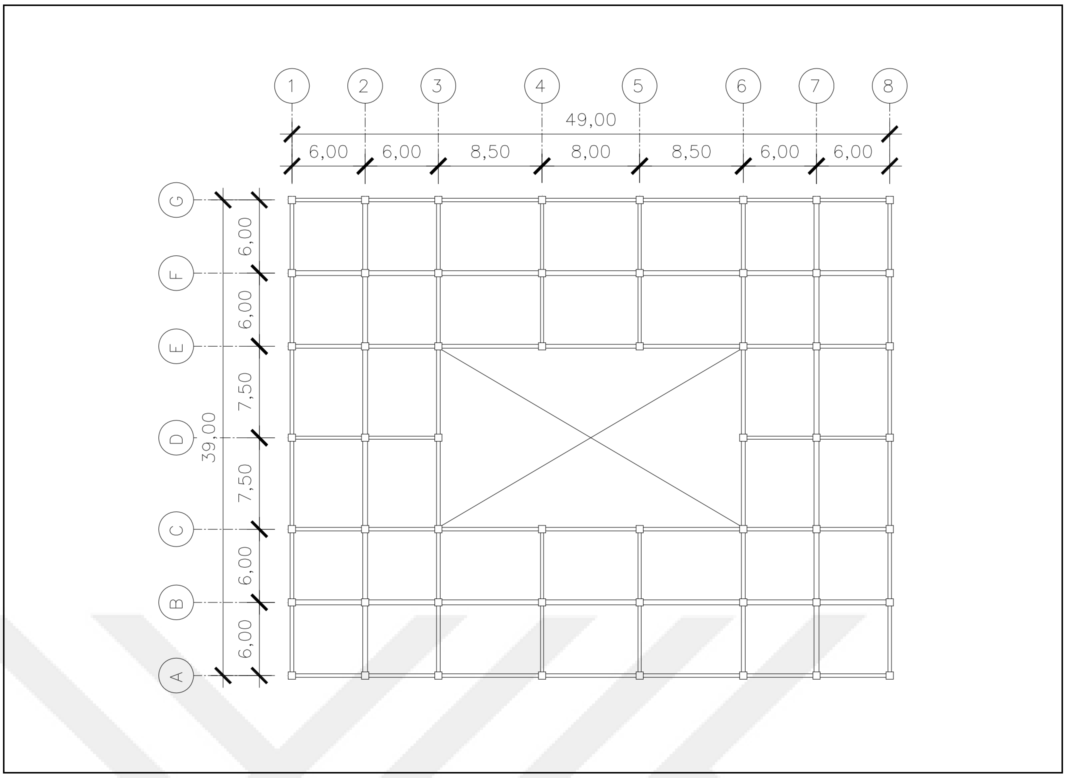

Figure 3.1: Typical floor plan for 6 story Structure 1 (20%).

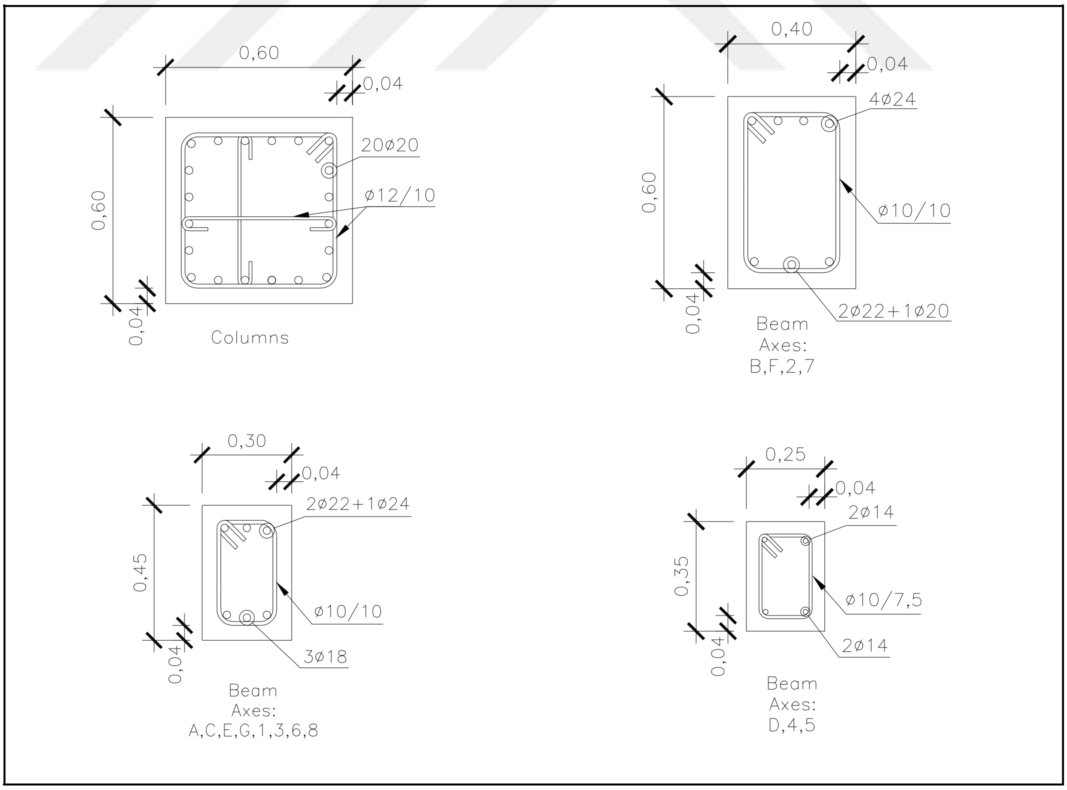

Figure 3.2: Section of the Elements in Structure 1 (20%).

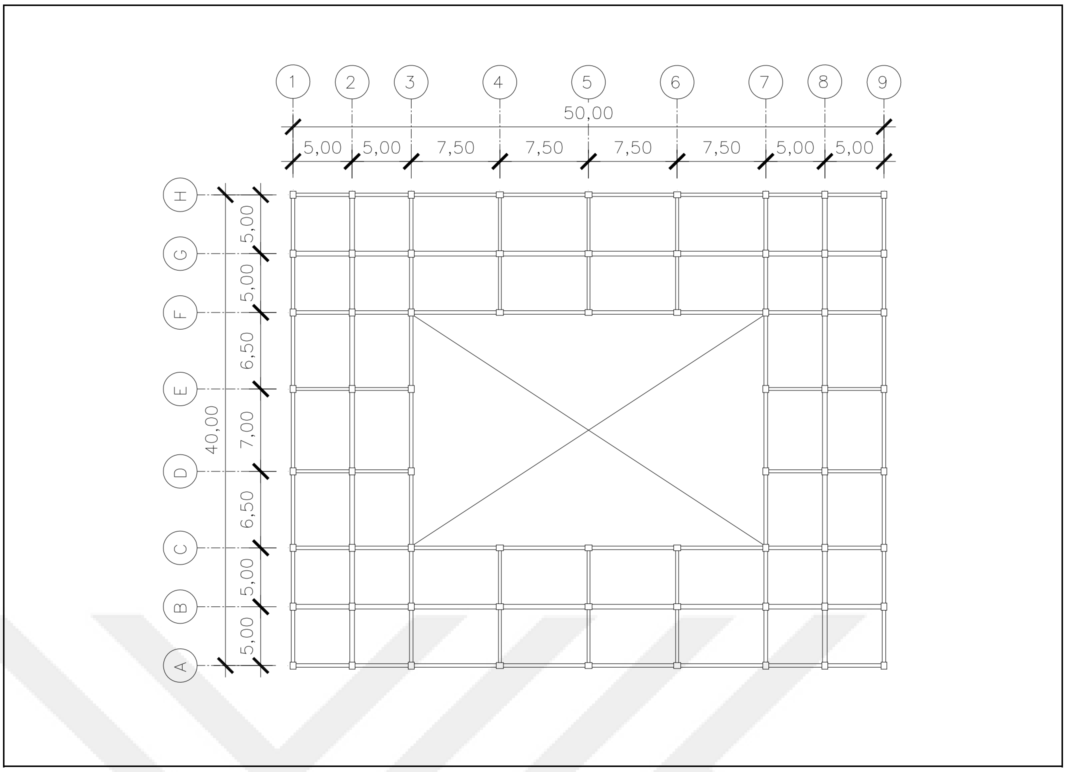

Figure 3.3: Typical floor plan for 6 story Structure 2 (30%).

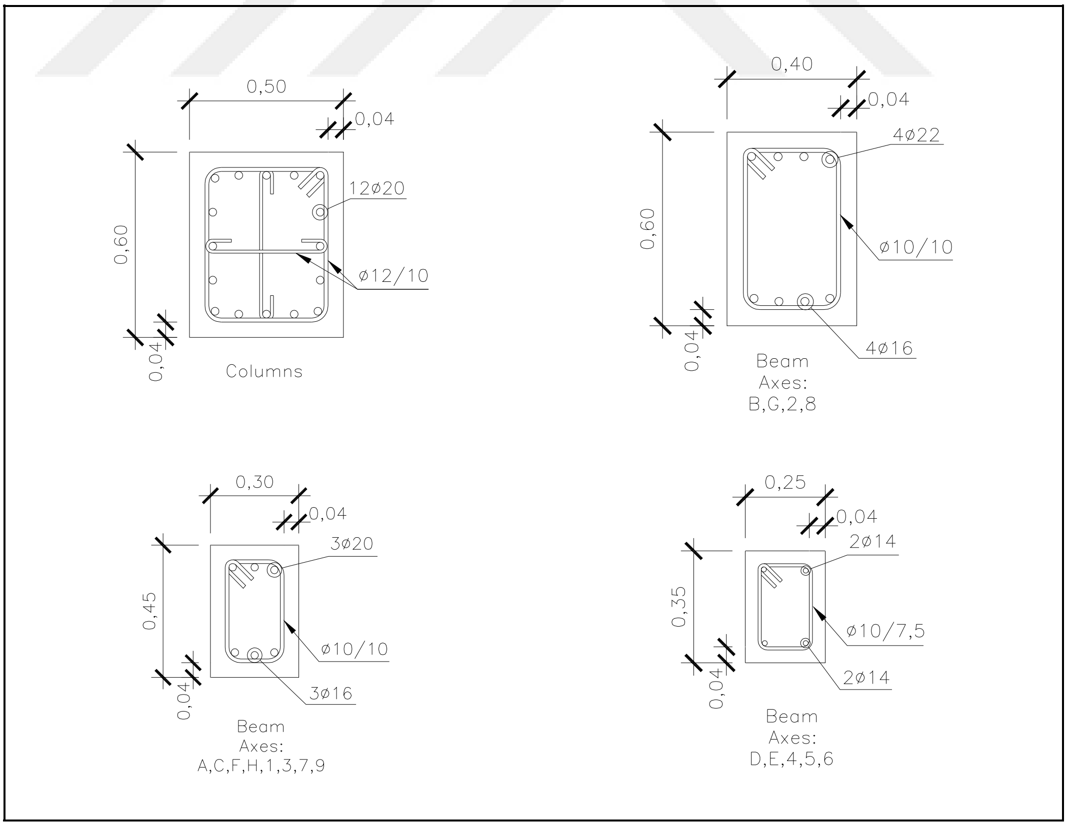

Figure 3.4: Section of the Elements in Structure 2 (30%).

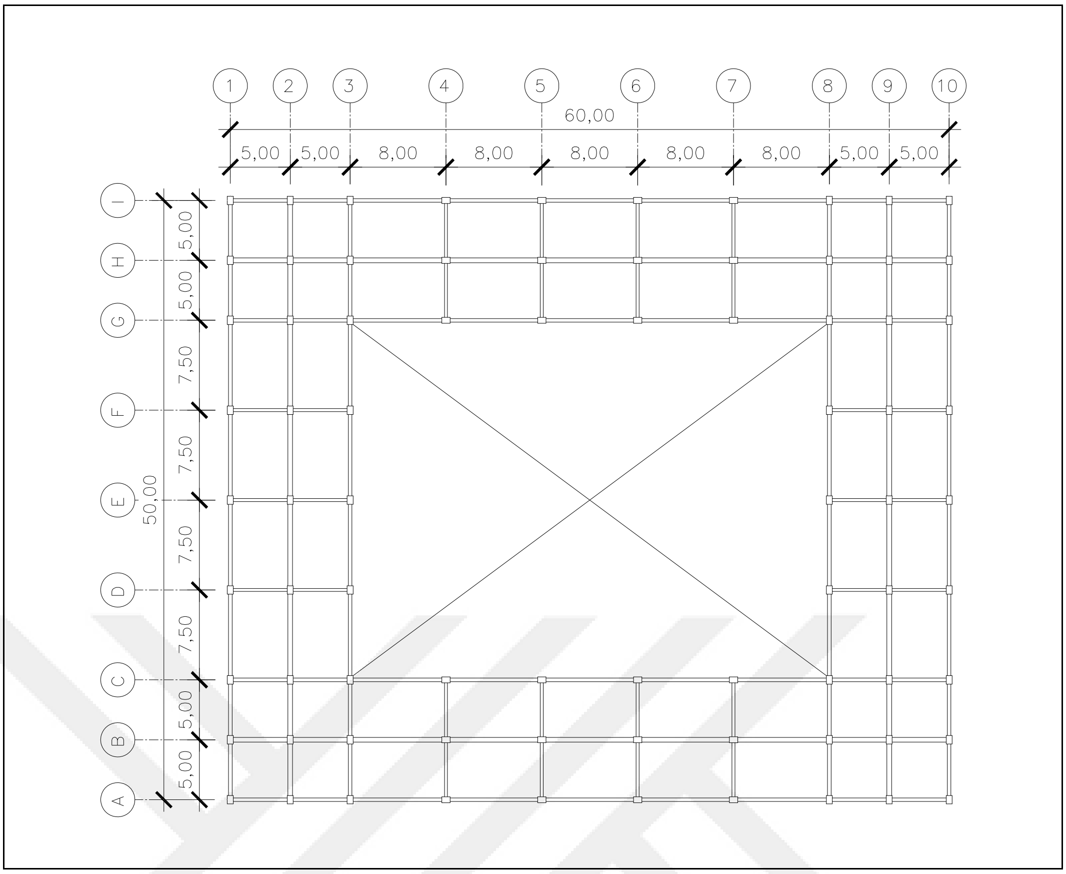

Figure 3.5: Typical floor plan for 6 story Structure 3 (40%).

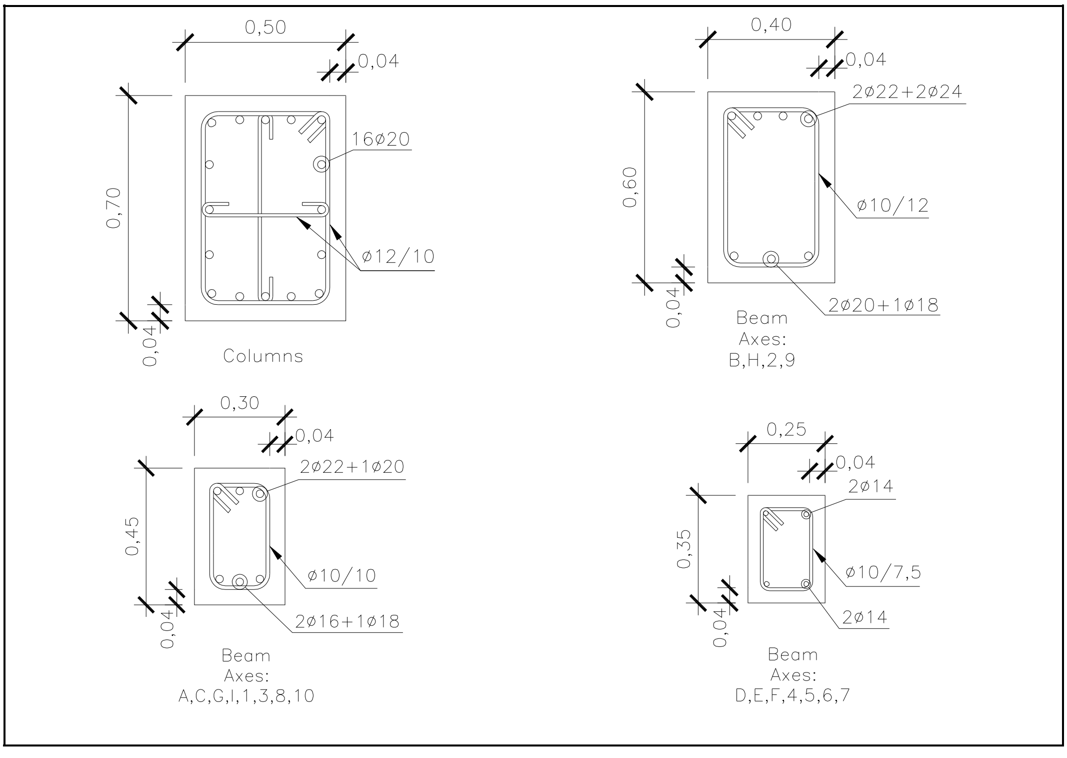

Figure 3.6: Section of the Elements in Structure 3 (40%).

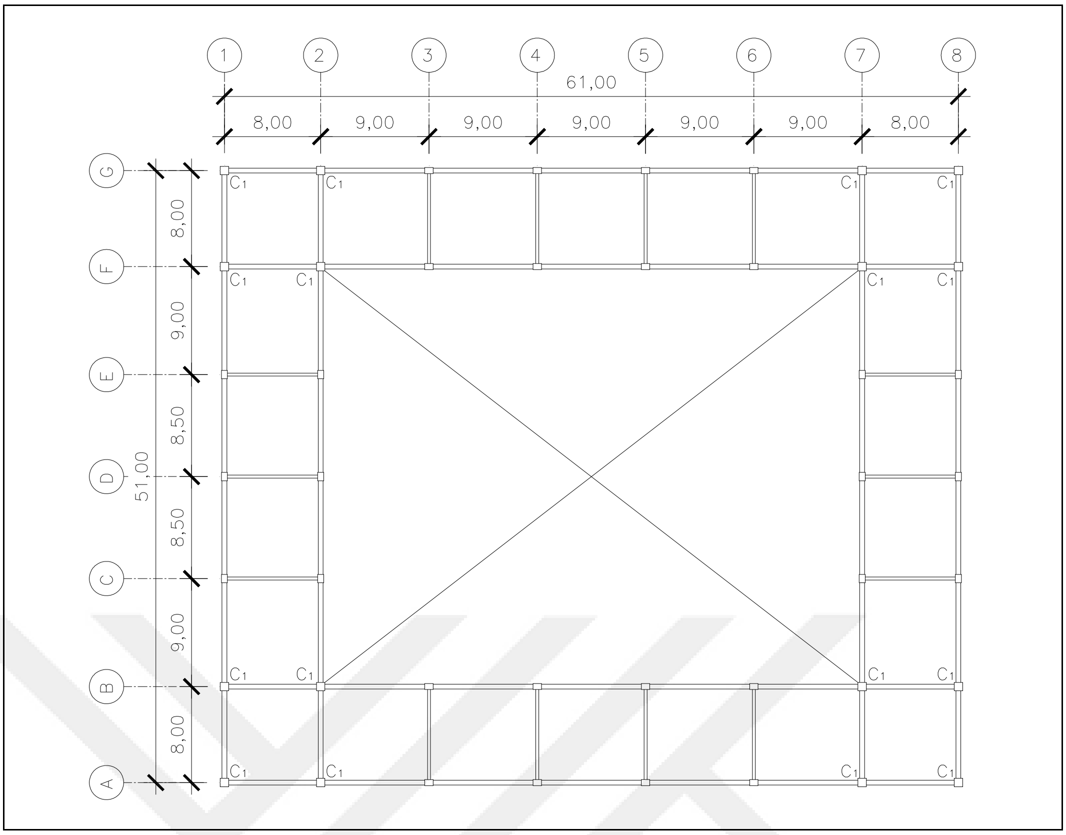

Figure 3.7: Typical floor plan for 6 story Structure 4 (50%).

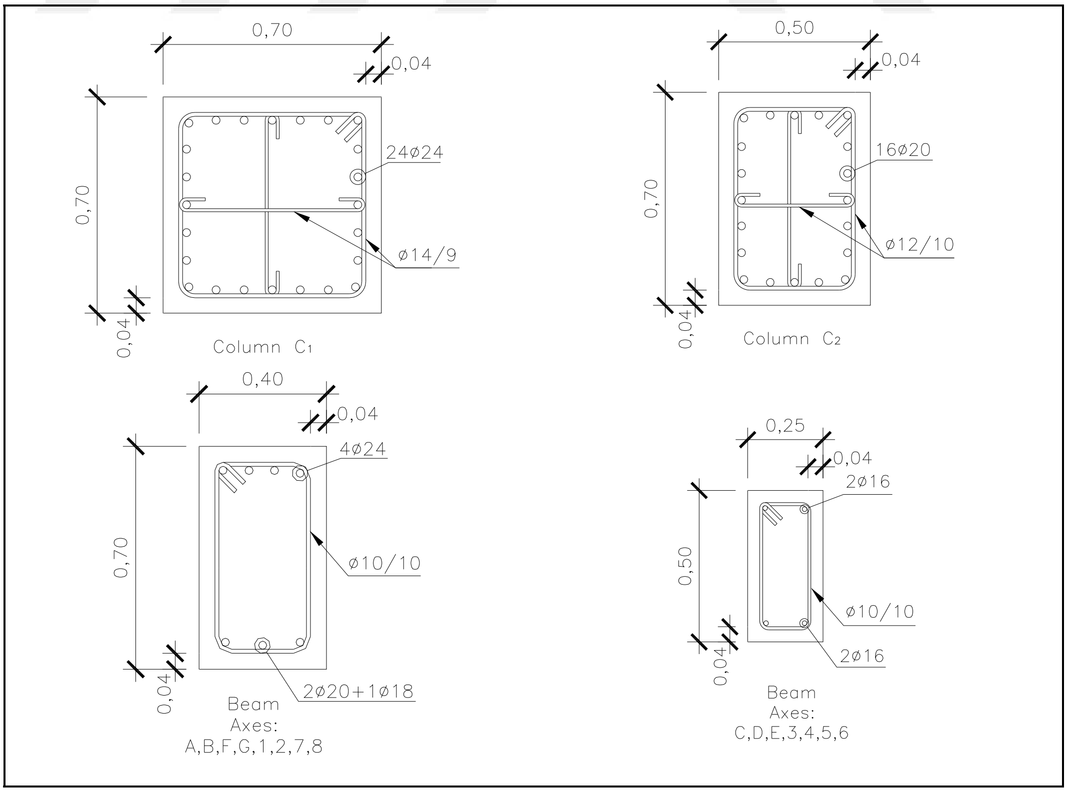

Figure 3.8: Section of the Elements in Structure 4 (50%).

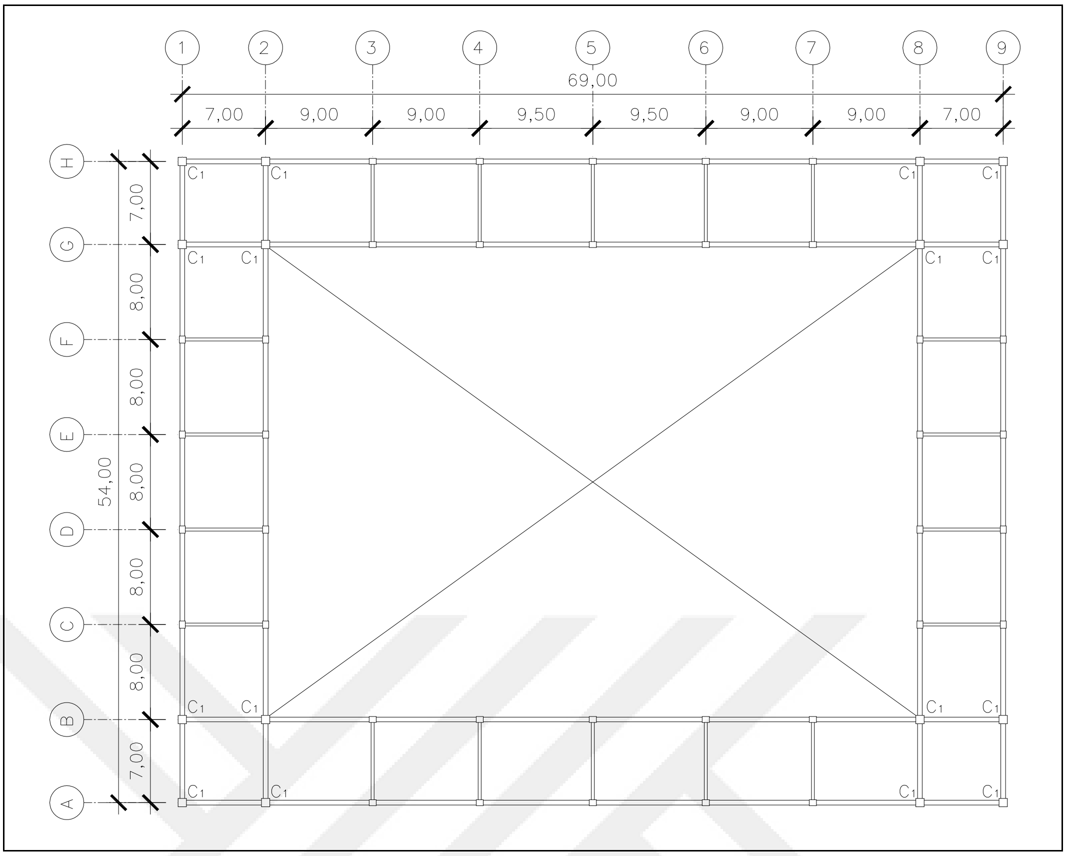

Figure 3.9: Typical floor plan for 6 story Structure 5 (60%).

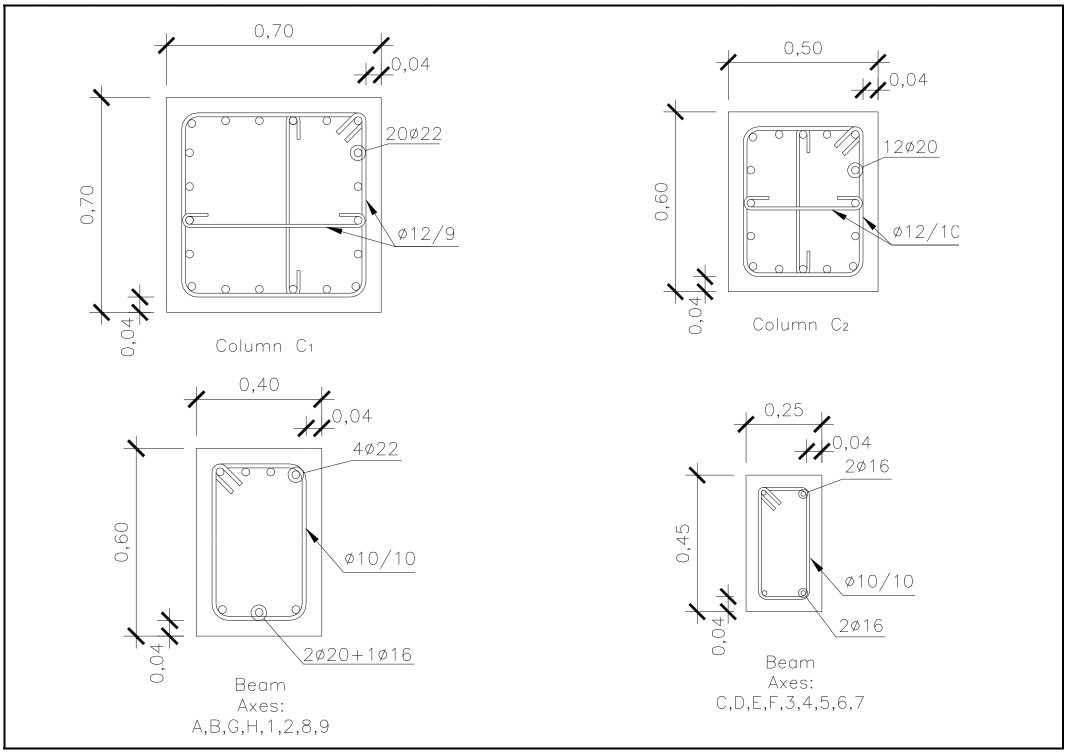

Figure 3.10: Section of the Elements in Structure 5 (60%).

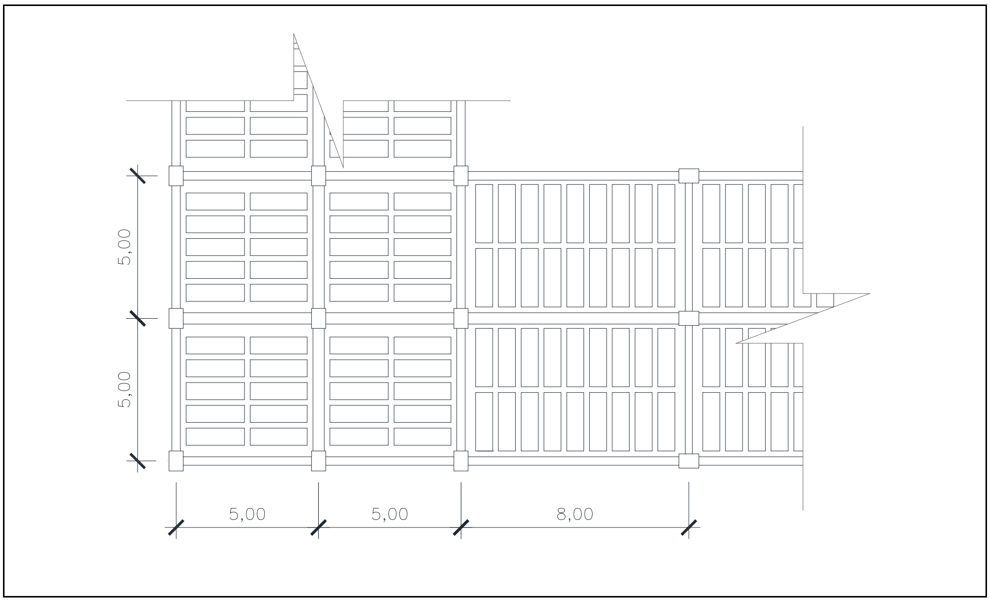

Figure 3.11: Typical Slab Plan.

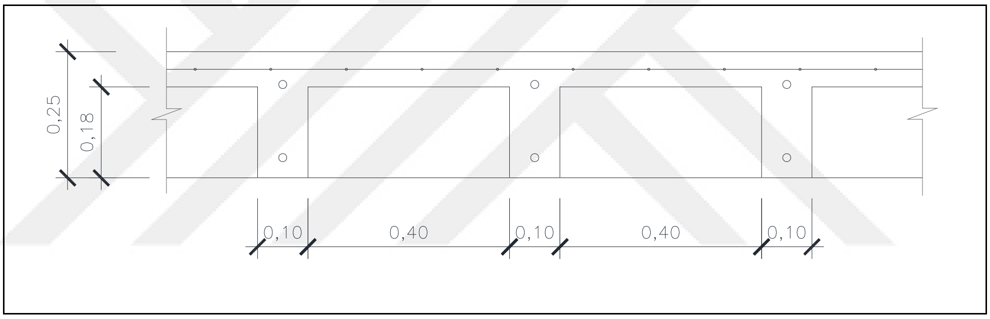

Figure 3.12: Slab section in Structure 1, Structure 2 and Structure 3.

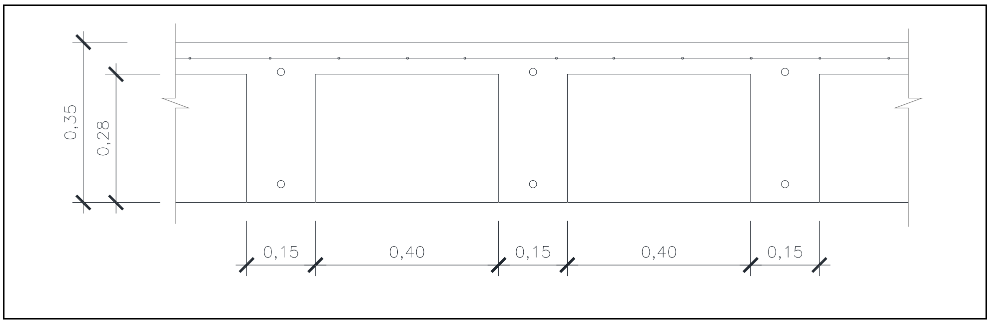

Figure 3.13: Slab section in Structure 4 and Structure 5.

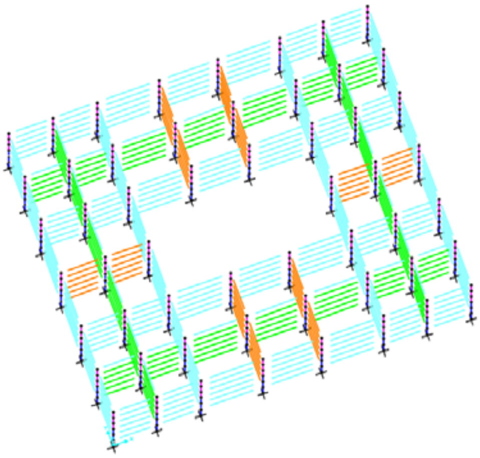

Structure 1 (20% open area)

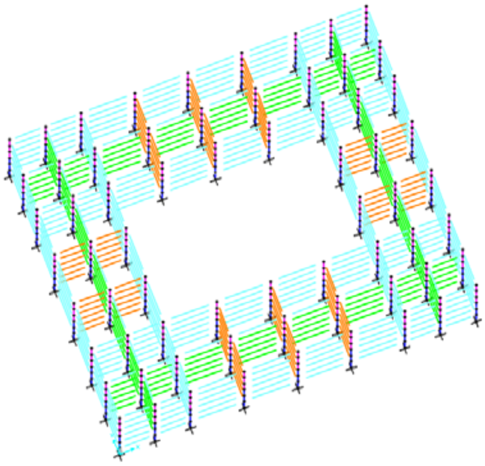

Structure 2 (30% open area)

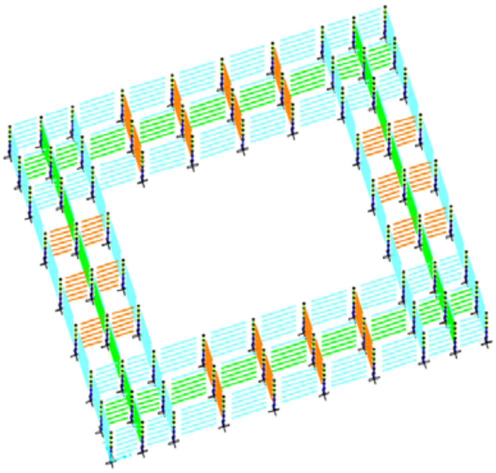

Structure 3 (40% open area)

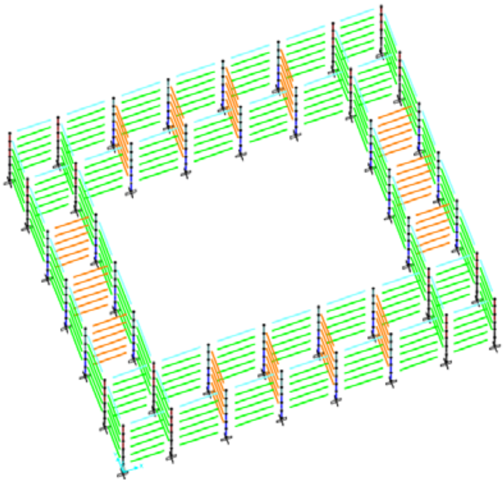

Structure 4 (50% open area)

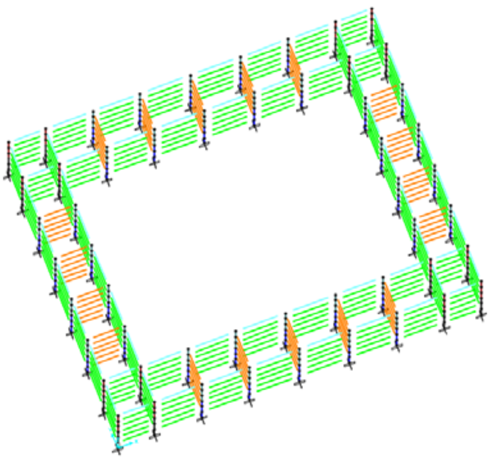

Structure 5 (60% open area)

Figure 3.14: Three dimensional SAP models.

3.2. Analysis Methodology

This section shows the procedure applied for nonlinear performance assessment of the five structures described in section 3.1.

3.2.1. Seismic Hazard

Seismic hazard was chosen as 2% probability of exceedance in 50years. This hazard is also known as the Maximum Considered Earthquake.

3.2.2. Response Spectrum

The parameters for response spectrum were obtained for the following coordinates, 30.6 latitude and 39.8 longitude, that corresponds to Eskisehir province in Turkey. The following parameters were obtained from 2%/50years maps, 1.06 as the short-period response acceleration parameter, S_S; and 0.39 as the response acceleration parameter at a 1-s period, S_1; those parameters are used both in ASCE-41-13 and TBDY-16. For response spectrum in EN 1998-3, ground acceleration, a_g, will be assumed as 0.40 in order to obtain 3 spectrum approximately equal.

Type of soil was considered as rock, this will be a Site Class B in ASCE-41-13, Ground Type A in EN 1998-3 and Site Class ZB in TBDY-16.

Critical damping must be considered as 5%, therefore β factor will be 0.05 and ξ will be 5% in ASCE-41-13 and EN 1998-3 respectively. The orthogonal distance to nearest fault, L_F, used in TBDY-16, was assumed as 25 km.

The result of the three spectrum are shown in figure 3.15.

The lower and upper limit of the constant acceleration branch are 0.07 and 0.37 in ASCE-41-13, 0.15 and 0.4 in EN 1998-3, 0.06 and 0.33 in TBDY-16.

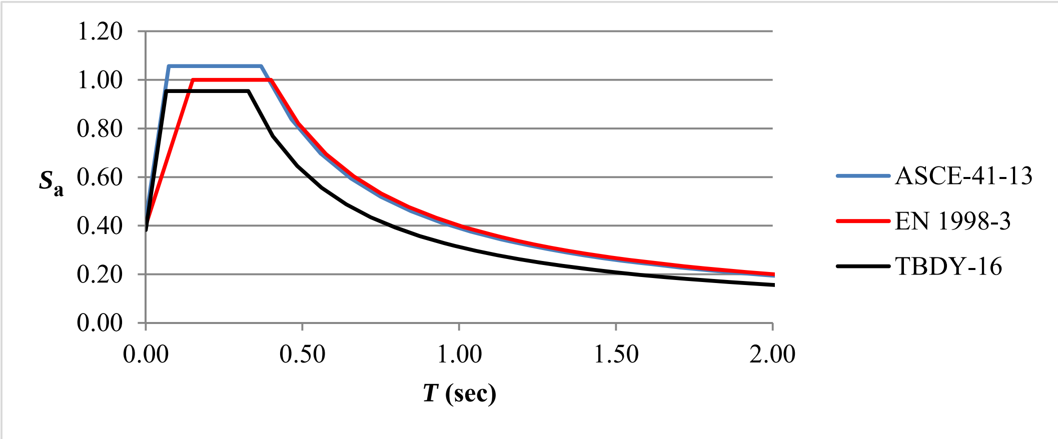

Figure 3.15: Response Spectrums.

3.2.3. Structural Model

This sections shows the criteria and values used in the structural models created in SAP2000 for the five structures.

- Damping

For nonlinear static analysis the structural models do not consider the damping. 5% critical damping was used only to develop response spectrums.

- Gravity loads

The gravity loads mentiond in section 3.1.3 were assigned to the slabs using the command "Assign Area Uniform Loads to Frames", and selecting the option to distribute loads in one way as required for one way ribbed slab models. Figure 3.16 shows one example of the distribution of the loads in slabs.

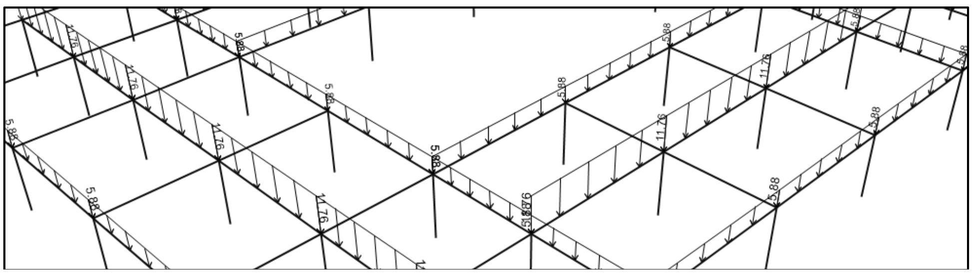

Figure 3.16: Load distribution in slabs.

- Effective Stiffness

For ASCE-41-13, the effective stiffness values were assigned according to table 2.6, the columns showed low axial loads, therefore their effective stiffness values were between 0.3*EcIg* and 0.4*EcIg*.

For EN 1998-3 the effective inertias were calculated according to equation 2.18, for columns the average of the values found was 0.5; for beams, values between 0.15 and 0.25 were assigned.

Values shown in Table 2.17 were assigned to models corresponding to TBDY-16.

- Joint Model

Rigid ends were assigned in beams and columns, with a length equal to half of the height of the member which they are connected to.

- Hinge Model

Hinge were assigned in both edges in beams and columns. Moment hinges were used in beams and interacting Axial Load-Moment hinges were used in columns.

- Slab model in irregular buildings

The slabs were modeled as membranes in order to consider their flexibility. Their thickness is 5cm and the effective inertia factors shown in table 2.6, section 2.2.4 and table 2.17 were assigned as property modifiers in SAP2000.

3.2.4. Modal Analysis

In order to perform a pushover analysis, one of the main requirements is to obtain the period of vibration of the structures among other modal characteristics. This section show the results obtained from modal analysis.

• ASCE-41-13

In order to check the acceptability of nonlinear static procedure in ASCE-41-13, the first step is to make a modal analysis with enough modes to reach 90% of participating mass, it was found that ten modes are enough for all the structures. As an example Figure 3.17 shows this verification in structure 3; with ten modes, participating mass is 95% in “x” direction and 94% in “y” direction.

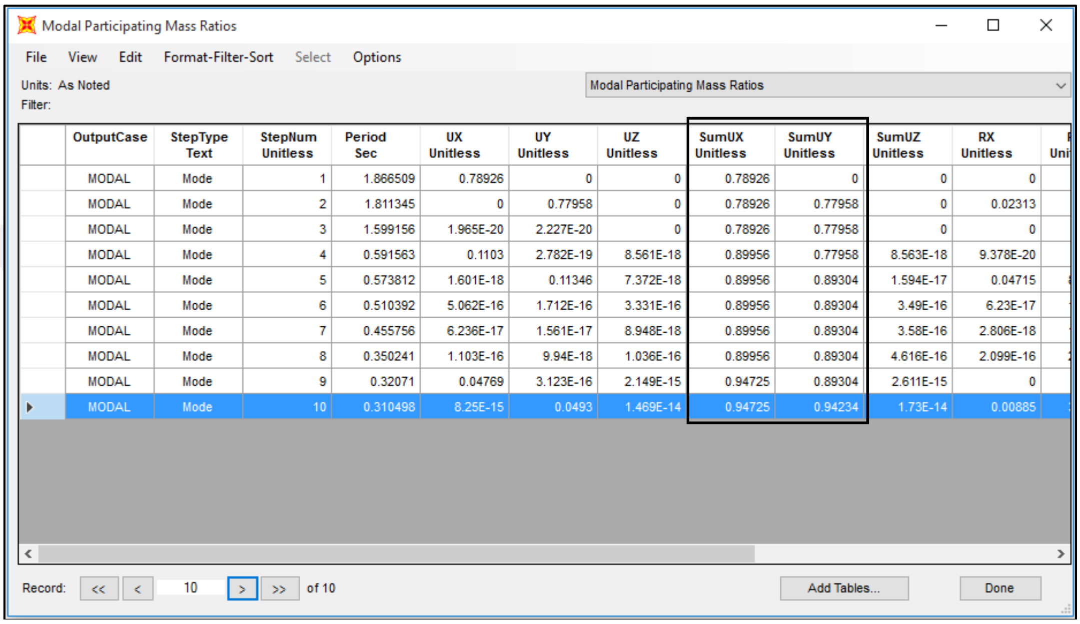

OutputCase	StepType Text	StepNum Unitless	Period Sec	UX Unitless	UY Unitless	UZ Unitless	SumUX Unitless	SumUY Unitless	SumUZ Unitless	RX Unitless
MODAL	Mode	1	1.866509	0.78926	0	0	0.78926	0	0	0
MODAL	Mode	2	1.811345	0	0.77958	0	0.78926	0.77958	0	0.02313
MODAL	Mode	3	1.599156	1.965E-20	2.227E-20	0	0.78926	0.77958	0	0
MODAL	Mode	4	0.591563	0.1103	2.782E-19	8.561E-18	0.89956	0.77958	8.563E-18	9.378E-20
MODAL	Mode	5	0.573812	1.601E-18	0.11346	7.372E-18	0.89956	0.89304	1.594E-17	0.04715
MODAL	Mode	6	0.510392	5.062E-16	1.712E-16	3.331E-16	0.89956	0.89304	3.49E-16	6.23E-17
MODAL	Mode	7	0.455756	6.236E-17	1.561E-17	8.948E-18	0.89956	0.89304	3.58E-16	2.806E-18
MODAL	Mode	8	0.350241	1.103E-16	9.94E-18	1.036E-16	0.89956	0.89304	4.616E-16	2.099E-16
MODAL	Mode	9	0.32071	0.04769	3.123E-16	2.149E-15	0.94725	0.89304	2.611E-15	0
MODAL	Mode	10	0.310498	8.25E-15	0.0493	1.469E-14	0.94725	0.94234	1.73E-14	0.00885

Figure 3.17: Modal participating mass ratios, Structure 3.

Second step is to compare shear stories resulting from first mode with shear resulting from 10 modes. “Draw / Section cut” command in SAP 2000 was used to obtain total shear per story. Figures 3.18 and 3.19 show this verification for structure 3 in direction x.

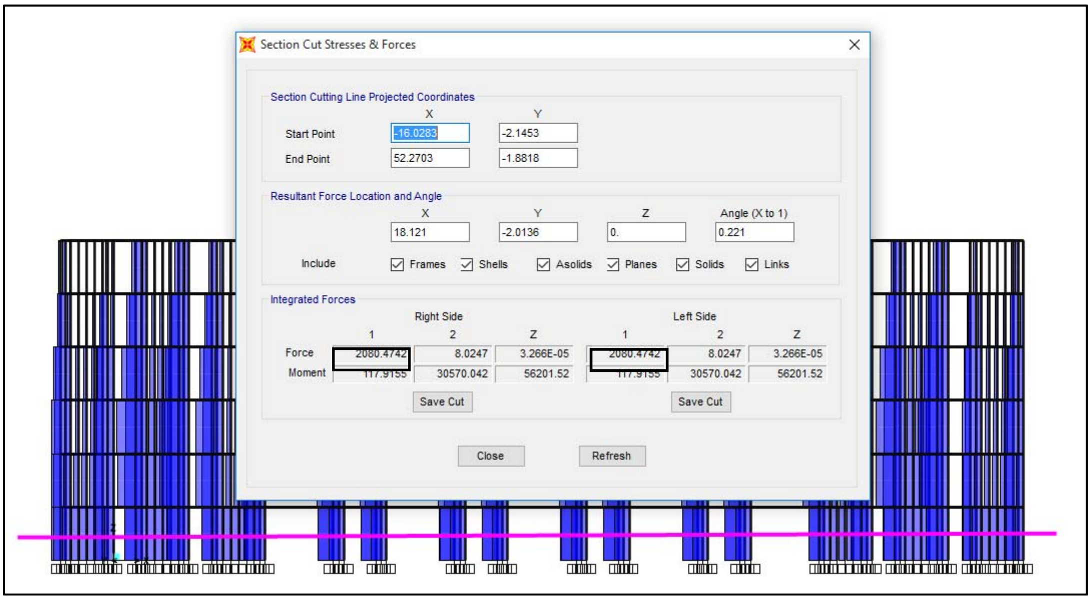

Figure 3.18: Shear story resulting from first mode, Structure 3, direction x.

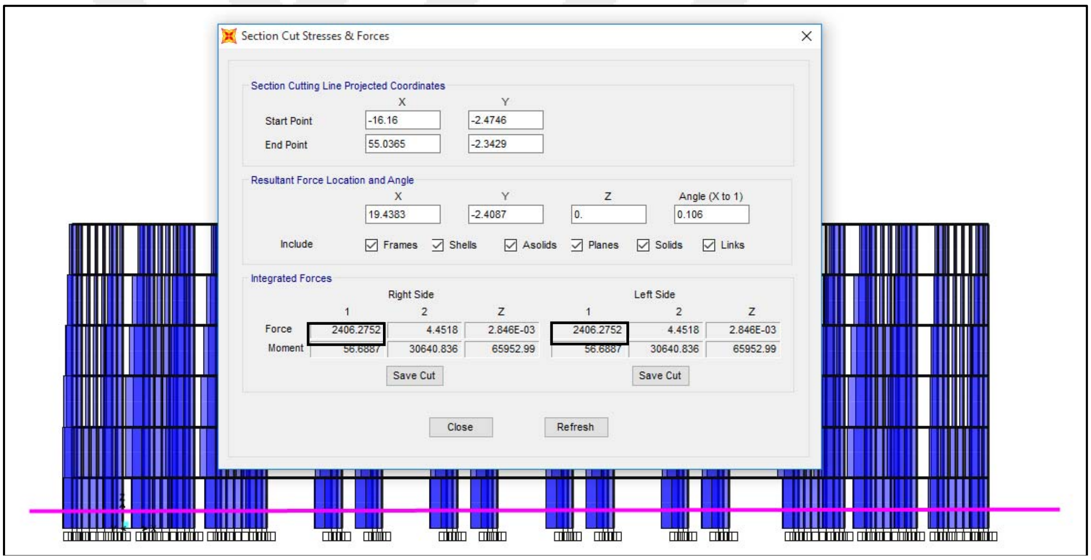

Figure 3.19: Shear story resulting from ten modes, Structure 3, direction x.

Shear obtained in first story considering only first mode was 2080.5kN, the same shear considering ten modes was 2406.3kN; this shows a ratio equal to 1.15, which is less than the maximum allowed 1.30. Similarly was analyzed in all the stories and all the structures and it was found that they are adequate for pushover analysis. The modal characteristic of the structures are shown in tables from 3.2 to 3.6.

Table 3.2: Modal Characteristics, Structure 1, ASCE-41-13.

Mode	Period (sec)	Modal participating mass ratio		
		Translational		Rotational
		x	y	z
1	1.75	0	0.78	0
2	1.71	0.79	0	0
3	1.54	0	0	0.79

Table 3.3: Modal Characteristics, Structure 2, ASCE-41-13.

Mode	Period (sec)	Modal participating mass ratio		
		Translational		Rotational
		x	y	z
1	1.82	0.80	0	0
2	1.80	0	0.79	0
3	1.58	0	0	0.795

Table 3.4: Modal Characteristics, Structure 3, ASCE-41-13.

Mode	Period (sec)	Modal participating mass ratio		
		Translational		Rotational
		x	y	z
1	1.87	0.79	0	0
2	1.81	0	0.78	0
3	1.60	0	0	0.79

Table 3.5: Modal Characteristics, Structure 4, ASCE-41-13.

Mode	Period (sec)	Modal participating mass ratio		
		Translational		Rotational
		x	y	z
1	1.84	0	0.78	0
2	1.76	0.78	0	0
3	1.55	0	0	0.78

Table 3.6: Modal Characteristics, Structure 5, ASCE-41-13.

Mode	Period (sec)	Modal participating mass ratio		
		Translational		Rotational
		x	y	z
1	1.70	0	0.80	0
2	1.69	0.80	0	0
3	1.46	0	0	0.80

• Eurocode EN 1998-3

For all the structures analyzed in accordance with EN 1998-3, the fundamental periods found are smaller than 2.0 second, those results fulfill the requirements to apply pushover method in direction x and y. The third mode in all the structures is a rotational mode around the vertical axis, the periods and modal participating ratios are shown in tables from 3.7 to 3.11.

Table 3.7: Modal Characteristics, Structure 1, EN 1998-3.

Mode	Period (sec)	Modal participating mass ratio		
		Translational		Rotational
		x	y	z
1	1.78	0	0.77	0
2	1.73	0.77	0	0
3	1.54	0	0	0.78

Table 3.8: Modal Characteristics, Structure 2, EN 1998-3.

Mode	Period (sec)	Modal participating mass ratio		
		Translational		Rotational
		x	y	z
1	1.80	0.78	0	0
2	1.80	0	0.77	0
3	1.56	0	0	0.78

Table 3.9: Modal Characteristics, Structure 3, EN 1998-3.

Mode	Period (sec)	Modal participating mass ratio		
		Translational		Rotational
		x	y	z
1	1.86	0.77	0	0
2	1.82	0	0.76	0
3	1.58	0	0	0.77

Table 3.10: Modal Characteristics, Structure 4, EN 1998-3.

Mode	Period (sec)	Modal participating mass ratio		
		Translational		Rotational
		x	y	z
1	1.87	0	0.77	0
2	1.78	0.77	0	0
3	1.55	0	0	0.78

Table 3.11: Modal Characteristics, Structure 5, EN 1998-3.

Mode	Period (sec)	Modal participating mass ratio		
		Translational		Rotational
		x	y	z
1	1.75	0	0.78	0
2	1.73	0.78	0	0
3	1.47	0	0	0.78

- Turkish Seismic Code TBDY-16

The modal participating mass ratios of the fundamental vibration modes, in direction x and y, are above 0.70, consequently, pushover can be applied in accordance with TBDY-16. The periods and modal participating ratios of the five studied structures are shown in tables from 3.12 to 3.16.

Table 3.12: Modal Characteristics, Structure 1, TBDY-16.

Mode	Period (sec)	Modal participating mass ratio		
		Translational		Rotational
		x	y	z
1	1.50	0	0.77	0
2	1.47	0.77	0	0
3	1.32	0	0	0.78

Table 3.13: Modal Characteristics, Structure 2, TBDY-16.

Mode	Period (sec)	Modal participating mass ratio		
		Translational		Rotational
		x	y	z
1	1.52	0.78	0	0
2	1.52	0	0.77	0
3	1.33	0	0	0.78

Table 3.14: Modal Characteristics, Structure 3, TBDY-16.

Mode	Period (sec)	Modal participating mass ratio		
		Translational		Rotational
		x	y	z
1	1.57	0.77	0	0
2	1.53	0	0.76	0
3	1.35	0	0	0.77

Table 3.15: Modal Characteristics, Structure 4, TBDY-16.

Mode	Period (sec)	Modal participating mass ratio		
		Translational		Rotational
		x	y	z
1	1.58	0	0.77	0
2	1.50	0.77	0	0
3	1.33	0	0	0.78

Table 3.16: Modal Characteristics, Structure 5, TBDY-16.

Mode	Period (sec)	Modal participating mass ratio		
		Translational		Rotational
		x	y	z
1	1.47	0	0.78	0
2	1.46	0.78	0	0
3	1.26	0	0	0.78

• Modal Shapes

Pushover method will be applied in x and y direction, this means, the models will be subjected to increasing lateral loads representing inertia forces in an earthquake. Those lateral loads will be applied using a vertical distribution proportional to the shape of the fundamental modes in the direction under consideration, those modes are shown in tables 3.17, 3.18 and 3.19.

Table 3.17: Normalized Modal Shapes, ASCE-41-13.

		Structure 1		Structure 2		Structure 3		Structure 4		Structure 5	
Mode		1	2	1	2	1	2	1	2	1	2
Direction		y	x	x	y	x	y	y	x	y	x
Period (sec)		1.75	1.71	1.82	1.80	1.87	1.81	1.84	1.76	1.7	1.69
Story	6	1.00	1.00	1.00	1.00	1.00	1.00	1.00	1.00	1.00	1.00
	5	0.91	0.91	0.92	0.92	0.92	0.91	0.90	0.90	0.91	0.91
	4	0.76	0.77	0.79	0.77	0.78	0.76	0.75	0.76	0.77	0.77
	3	0.55	0.55	0.59	0.56	0.58	0.56	0.55	0.55	0.57	0.57
	2	0.34	0.34	0.36	0.34	0.35	0.33	0.33	0.33	0.35	0.35
	1	0.13	0.13	0.13	0.12	0.12	0.11	0.12	0.12	0.14	0.13

Table 3.18: Normalized Modal Shapes, EN 1998-3.

		Structure 1		Structure 2		Structure 3		Structure 4		Structure 5	
Mode		1	2	1	2	1	2	1	2	1	2
Direction		y	x	x	y	x	y	y	x	y	x
Period (sec)		1.78	1.73	1.80	1.80	1.86	1.82	1.87	1.78	1.75	1.73
Story	6	1.00	1.00	1.00	1.00	1.00	1.00	1.00	1.00	1.00	1.00
	5	0.90	0.90	0.91	0.90	0.89	0.88	0.88	0.88	0.89	0.88
	4	0.74	0.74	0.76	0.75	0.74	0.72	0.73	0.73	0.74	0.74
	3	0.53	0.53	0.56	0.54	0.54	0.51	0.52	0.53	0.54	0.54
	2	0.31	0.31	0.33	0.31	0.31	0.29	0.31	0.31	0.32	0.32
	1	0.11	0.11	0.12	0.11	0.10	0.10	0.10	0.11	0.12	0.12

Table 3.19: Normalized Modal Shapes, TBDY-16.

		Structure 1		Structure 2		Structure 3		Structure 4		Structure 5	
Mode		1	2	1	2	1	2	1	2	1	2
Direction		y	x	x	y	x	y	y	x	y	x
Period (sec)		1.50	1.47	1.52	1.52	1.57	1.53	1.58	1.50	1.47	1.46
Story	6	1.00	1.00	1.00	1.00	1.00	1.00	1.00	1.00	1.00	1.00
	5	0.90	0.90	0.91	0.90	0.90	0.89	0.88	0.89	0.89	0.89
	4	0.74	0.75	0.76	0.75	0.75	0.73	0.73	0.74	0.74	0.74
	3	0.53	0.54	0.56	0.55	0.54	0.52	0.53	0.53	0.55	0.54
	2	0.32	0.32	0.33	0.32	0.32	0.30	0.31	0.31	0.33	0.32
	1	0.11	0.11	0.12	0.11	0.11	0.10	0.11	0.11	0.12	0.11

3.2.5. Flexibility in Slabs

Analyzing the modal shapes obtained, it is seen a very rigid behavior in slabs, their deformed shapes are almost equal to those obtained assuming rigid diaphragms. Several models and several properties of slabs were analyzed and it was found that the main parameter assumed in the model that affects the flexibility of the slabs is the shear stiffness (F12). In the models developed in this research, effective shear stiffness was considered as 0.4, 0.5 and 0.25 of the uncracked stiffness, according to ASCE-41-13, EN 1998-3 and TBDY-16 respectively.

However, the behavior obtained assuming different values of F12 will be also investigated. Several values of F12 will be assumed and the flexibility will be measured. The parameter chosen to assess the flexibility was the relationship between deformation of diaphragms, Δ_{dia}, and the average story drift of the story immediately below, $\Delta_{avg.}$ (See figure 2.3). According to ASCE-41-13, diaphragms shall be classified as flexible when this parameter is bigger than 2.0. Tables from 3.20 to 3.24 show the results obtained. The deformations shown were obtained from modal shapes, therefore they are unitless.

Table 3.20: Flexibility on slabs, Structure 1.

F12	Δ_{dia}	Δ_{avg}	$\Delta_{dia} / \Delta_{avg}$
0.4	0.04	1.62	0.02
0.05	0.21	1.62	0.13
0.01	1.04	1.61	0.65

Table 3.21: Flexibility on slabs, Structure 2.

F12	Δ_{dia}	Δ_{avg}	$\Delta_{dia} / \Delta_{avg}$
0.4	0.05	1.45	0.03
0.05	0.26	1.45	0.18
0.01	1.18	1.46	0.81

Table 3.22: Flexibility on slabs, Structure 3.

F12	Δ_{dia}	Δ_{avg}	$\Delta_{dia} / \Delta_{avg}$
0.4	0.10	1.40	0.07
0.05	0.49	1.40	0.35
0.01	2.28	1.45	1.58

The results show that the flexibility is higher in slabs with bigger open areas (Structure 5), and that this flexibility is sensitive to the shear stiffness of their slabs. The most adequate value of F12 should be obtained through a calibration process.

Table 3.23: Flexibility on slabs, Structure 4.

F12	Δ_{dia}	Δ_{avg}	$\Delta_{dia} / \Delta_{avg}$
0.4	0.16	1.74	0.09
0.05	0.74	1.69	0.44
0.01	3.84	1.67	2.30

Table 3.24: Flexibility on slabs, Structure 5.

F12	Δ_{dia}	Δ_{avg}	$\Delta_{dia} / \Delta_{avg}$
0.4	0.20	1.65	0.12
0.05	0.97	1.57	0.62
0.01	4.78	1.56	3.06

3.2.6. Force-Displacement curves:

Pushover analysis was applied selecting the center of mass in the roof level as the control node, the relation between base shear force and lateral displacement of the control node was generated until a maximum displacement assumed as 40cm. The curves were extracted from SAP2000 as shown in figure 3.20.

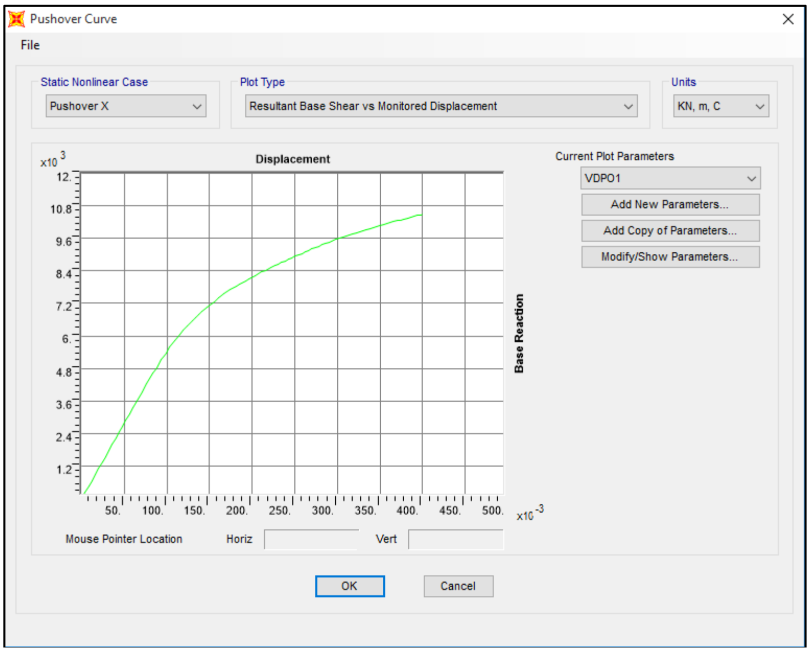

Figure 3.20: Pushover curve from SAP2000, Structure 1, direction x, ASCE-41-13.

Curves from the three standards were plotted together in order to make comparisons, those are shown in figures from 3.21 to 3.30.

In the pushover curves, it is seen a bigger stiffness in models correspondent to TBDY-16. This is caused by higher effective inertia factors assigned to beams and columns in TBDY-16.

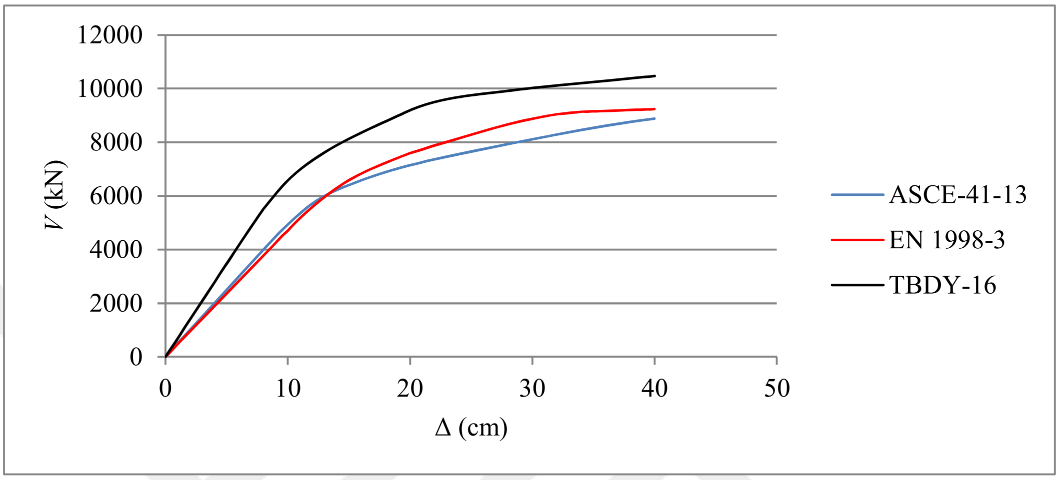

Figure 3.21: Pushover curve, Structure 1, Mode 1 (y direction).

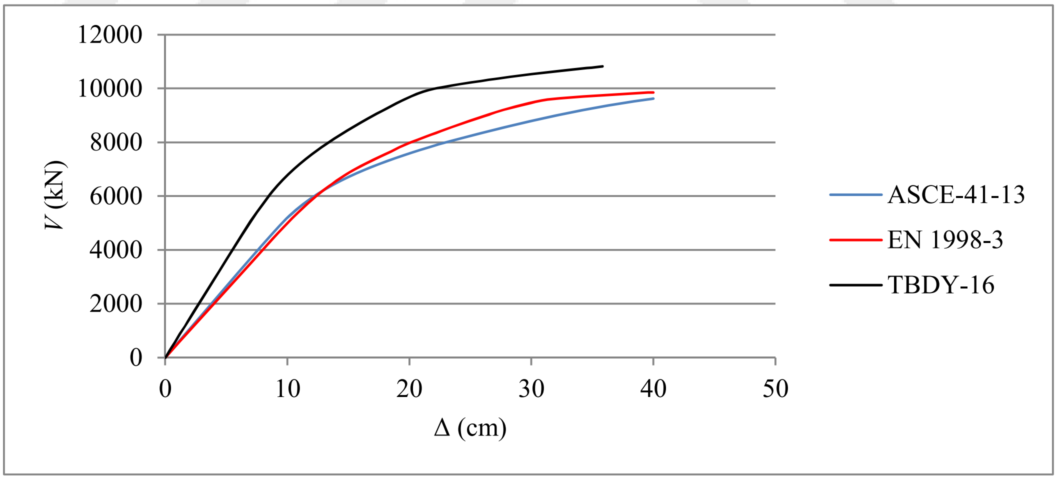

Figure 3.22: Pushover curve, Structure 1, Mode 2 (x direction).

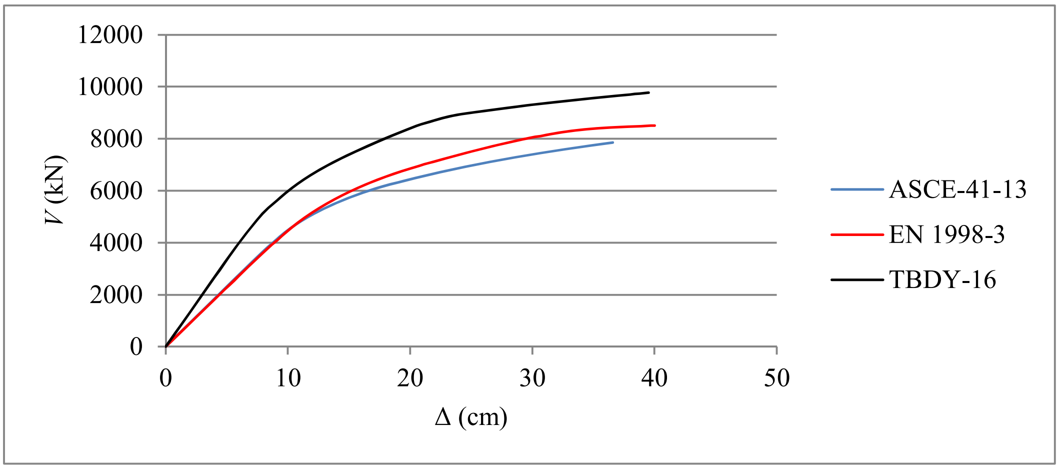

Figure 3.23: Pushover curve, Structure 2, Mode 1 (x direction).

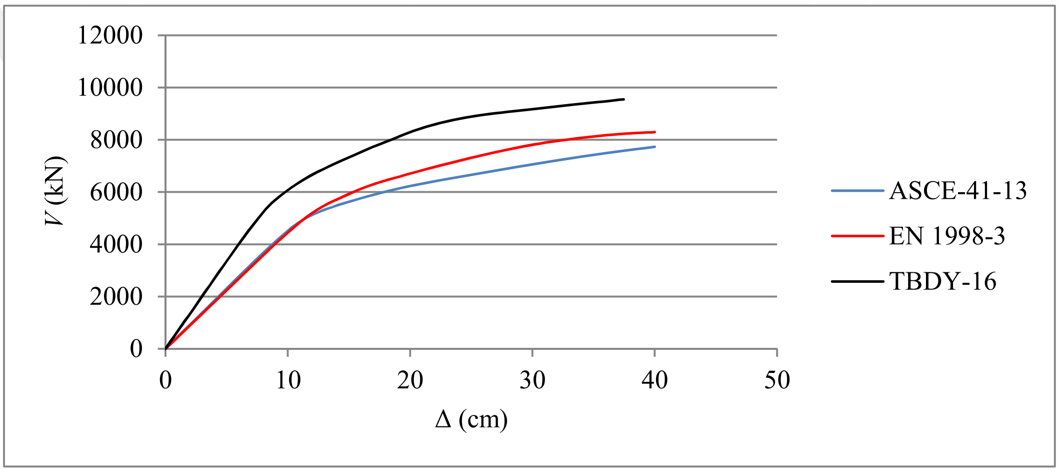

Figure 3.24: Pushover curve, Structure 2, Mode 2 (y direction).

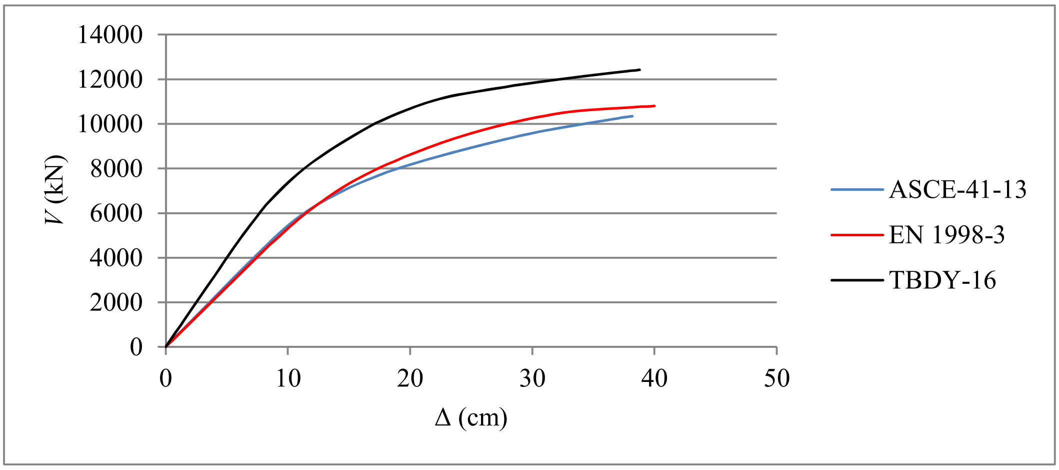

Figure 3.25: Pushover curve, Structure 3, Mode 1 (x direction).

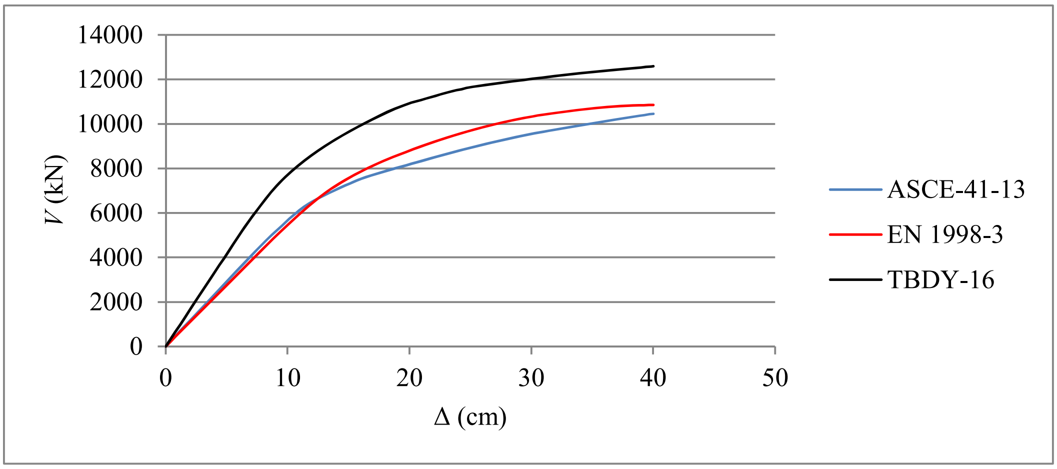

Figure 3.26: Pushover curve, Structure 3, Mode 2 (y direction).

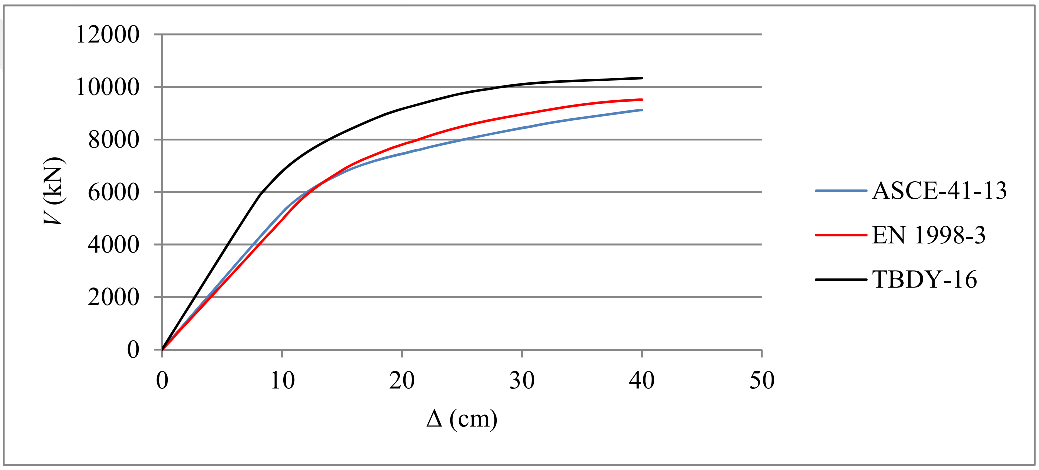

Figure 3.27: Pushover curve, Structure 4, Mode 1 (y direction).

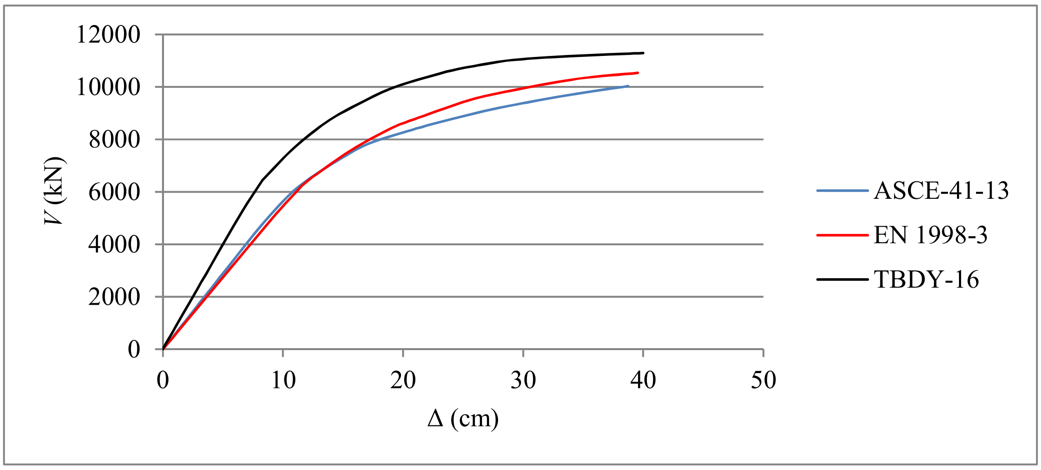

Figure 3.28: Pushover curve, Structure 4, Mode 2 (x direction).

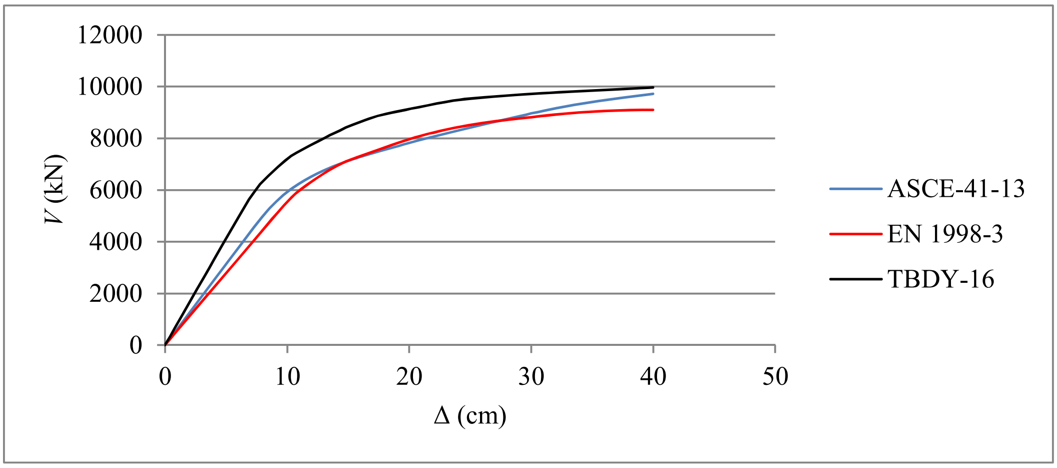

Figure 3.29: Pushover curve, Structure 5, Mode 1 (y direction).

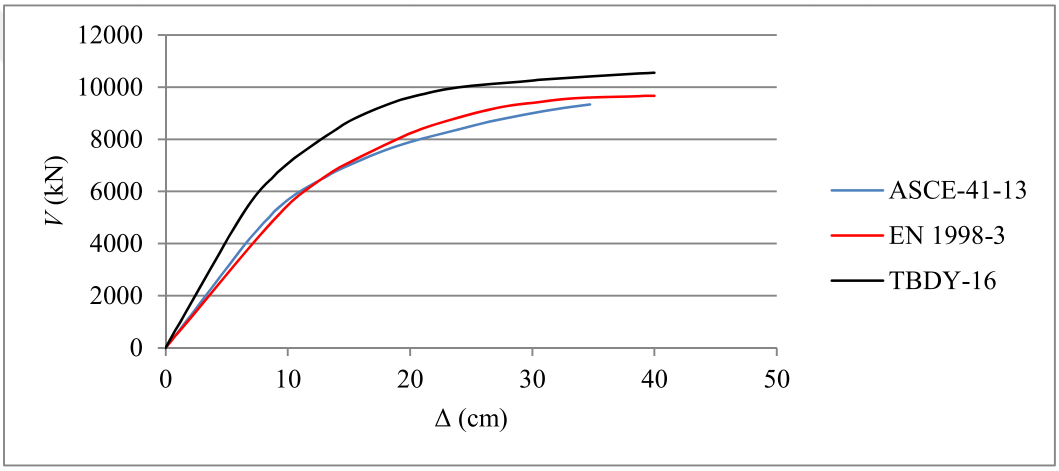

Figure 3.30: Pushover curve, Structure 5, Mode 2 (x direction).

3.2.7. Target displacements

Pushover analysis will be performed until target displacements calculated in this section.

- ASCE-41-13

Target displacements were calculated as described in section 2.1.3 for the five structures in direction “x” and “y”. This calculation will be shown in detail for structure 3 in direction “x”.

- Idealized bilinear Force-Displacement curve

The Force-displacement curves shown in figures from 3.21 to 3.30, will be converted in a bilinear curves. The first segment will begin at the origin and intersect the original curve at a base shear force equal to 60% of the effective yield strength of the structure. The second line will have a positive slope such that the areas below both curves are equal. The last point of the idealized curve will be the lesser of the target displacement or displacement corresponding to the maximum base shear. Since target displacements have not been calculated yet, the last point of the bilinear curve will be assumed firstly as 40cm. The second point of the bilinear curve (V_y, Δ_y) will be obtained making iterations until the areas are equal, excel software is used in this procedure. Figure 3.31 shows the bilinear curve obtained for structure 3 in direction "x".

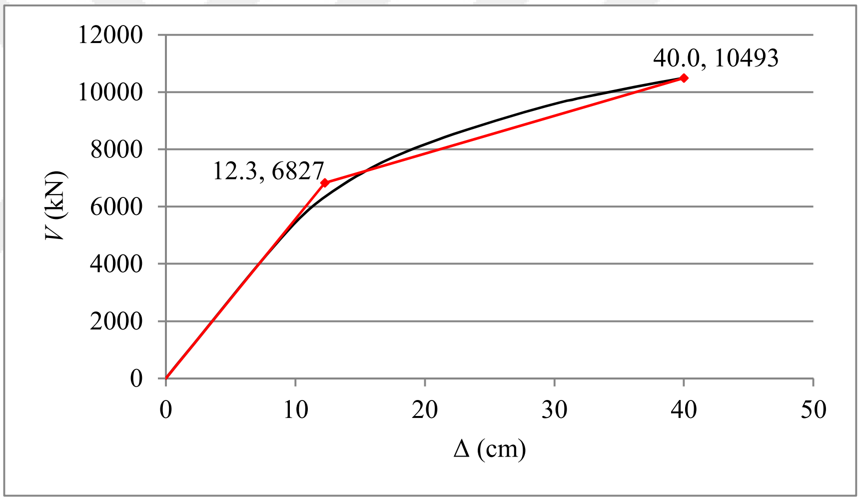

Figure 3.31: Bilinear Pushover curve, Structure 3, direction x, first iteration.

- Target displacement computation

The elastic lateral stiffness of the building, K_i, and the effective stiffness of the building, K_e, are obtained as the initial slope of the original curve and the bilinear curve respectively. For structure 3, direction x, they will be equal to 557.2 kN/cm and 556.1 kN/cm respectively. Elastic fundamental period, T_i, was obtained from modal analysis and is shown in table 3.14. Next step is to calculate the effective fundamental period, T_e, using equation 2.9, its result was 1.87 seconds.

The response acceleration at the effective fundamental period, $S_a(T_e)$, is obtained from the elastic response spectrum shown in figure 3.15, this was equal to 0.208.

Coefficient C_0 is equivalent to mode mass participation factor multiplied by the ordinate of the mode shape at the control node. Modal shapes were normalized so the ordinate in the control node (top of the building) is equal to 1.0, participation factors are given by equation 2.21; for Structure 3, direction x, it is equal to 1.315. Since the effective period is greater than 0.7 seconds, coefficients C_1 and C_2 will be equal to 1.0.

Finally, the target displacement, δ_t, is calculated using equation 2.7, the result found was 23.81 cm.

A second iteration will be made using 23.81cm as the last point of the bilinear curve. The new target displacement, δ_t, obtained is equal to 23.80cm which is close enough and there is no need to make more iterations. Target displacement computations for all the studied structures are summarized in tables 3.25 and 3.26.

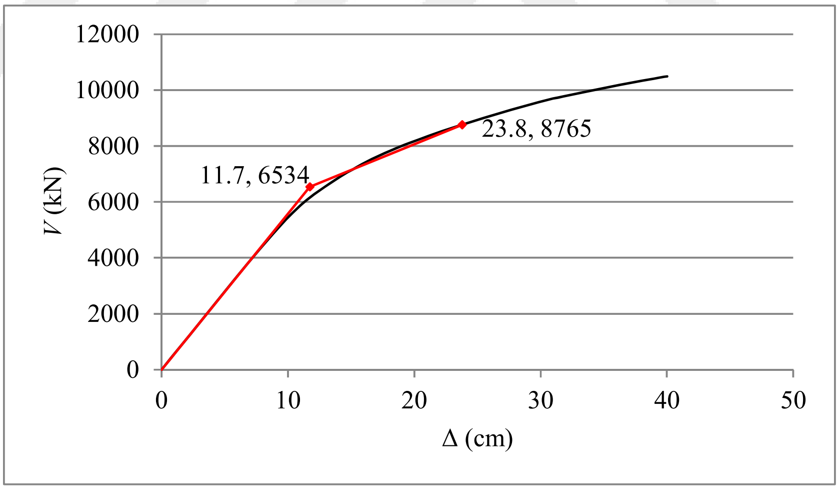

Figure 3.32: Bilinear Pushover curve, Structure 3, direction x, second iteration.

Table 3.25: Target displacement computation, ASCE-41-13, direction x.

	Structure 1	Structure 2	Structure 3	Structure 4	Structure 5
$C_0 = \Gamma$	1.333	1.310	1.315	1.344	1.338
C_1	1.0	1.0	1.0	1.0	1.0
C_2	1.0	1.0	1.0	1.0	1.0
K_i (kN/cm)	526.9	462.2	557.2	579.0	613.6
K_e (kN/cm)	527.4	461.8	556.6	577.9	611.5
T_i (sec)	1.71	1.82	1.87	1.76	1.69
T_e (sec)	1.71	1.82	1.87	1.76	1.69
S_a (T_e)	0.228	0.214	0.208	0.221	0.230
δt (cm) =	22.0	23.1	23.8	22.9	21.9

Table 3.26: Target displacement computation, ASCE-41-13, direction y.

	Structure 1	Structure 2	Structure 3	Structure 4	Structure 5
$C_0 = \Gamma$	1.333	1.310	1.315	1.344	1.338
C_1	1.0	1.0	1.0	1.0	1.0
C_2	1.0	1.0	1.0	1.0	1.0
K_i (kN/cm)	526.9	462.2	557.2	579.0	613.6
K_e (kN/cm)	527.4	461.8	556.6	577.9	611.5
T_i (sec)	1.71	1.82	1.87	1.76	1.69
T_e (sec)	1.71	1.82	1.87	1.76	1.69
S_a (T_e)	0.228	0.214	0.208	0.221	0.230
δt (cm) =	22.6	23.0	23.2	23.9	22.0

• EN 1998-3

Target displacements were calculated as described in section 2.2.5 for the five structures in direction “x” and “y”. This calculation will be shown in detail for structure 1 in direction “x”.

- Idealized bilinear Force-Displacement curve

The force displacement curves shown in figures from 3.21 to 3.30 will be converted in an equivalent SDOF curve using equations 3.11 and 3.12.

This relationship will be replaced with an idealized bilinear curve to define the yield force, F_y*. The initial slope of the idealized curve is determined in such a way that the areas under both curves are equal. The second line will be a horizontal line with an ordinate equal to F_y*.

For structure 1 and direction x, F_y* will be assumed initially -as the maximum base shear in the curve, 7303 kN, its corresponding displacement d_m*, is 29.7cm (see figure 7.33).

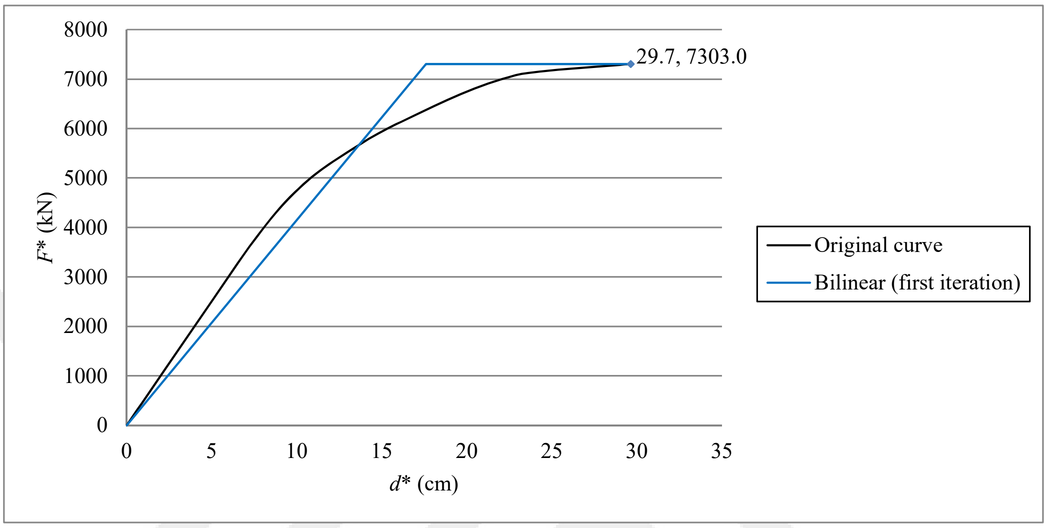

Figure 7.33: Bilinear Pushover curve, Structure 1, direction x, first iteration.

- Target displacement computation

The mass of the equivalent SDOF system, m*, is calculated using equation 2.26, the result obtained is 3892 kN.s^2/m. The period of the system is calculated in accordante with equation 2.25, its result is 1.92 seconds.

Since the period is in the medium and long period range (T_1 > T_C), target displacement is determined from the elastic response spectrum and the idealized force-displacement curve. This calculation is shown in figure 3.34.

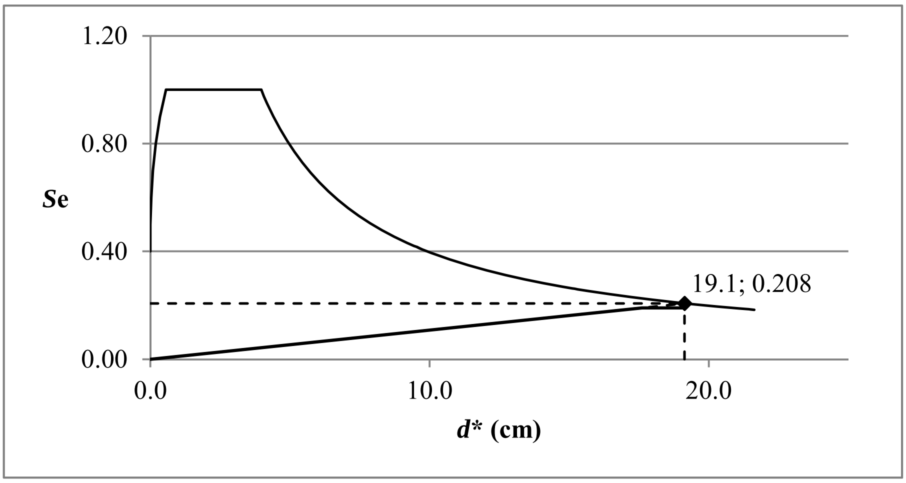

Figure 3.34: Target displacement computation, Structure 1, direction x, first iteration.

The target displacement obtained, d_t*, is equal to 19.1 cm. Since the target displacement is considerably different from d_m*, iterations must be done using a bilinear curve whose maximum displacement will be equal to the previously calculated target displacement, d_t*.

Figure 3.35, 3.36 and 3.37 show second and third iteration, which results are very similar, therefore, no more iterations are needed.

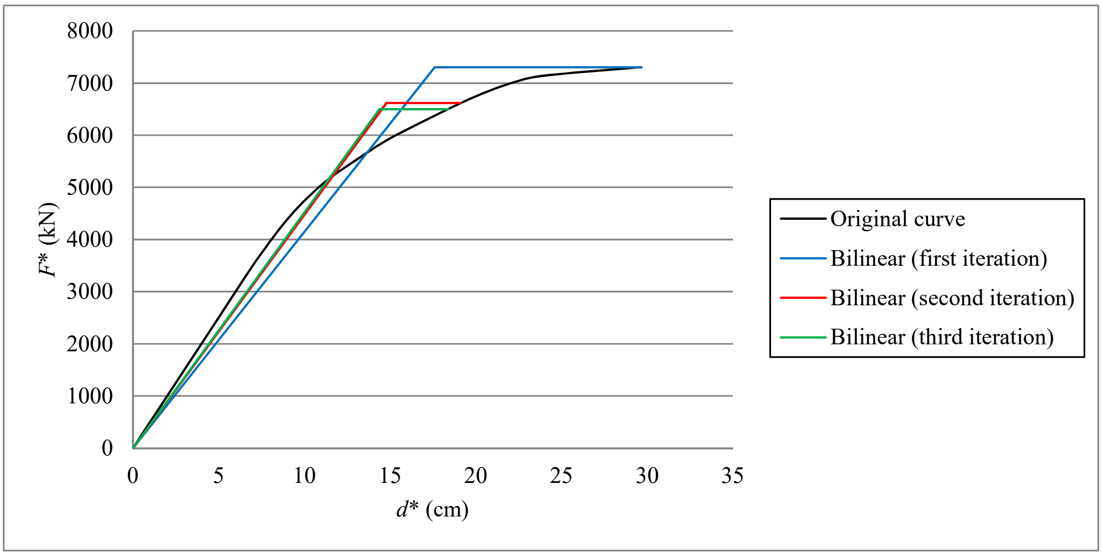

Figure 3.35: Bilinear Pushover curve, Structure 1, direction x, first, second and third iteration.

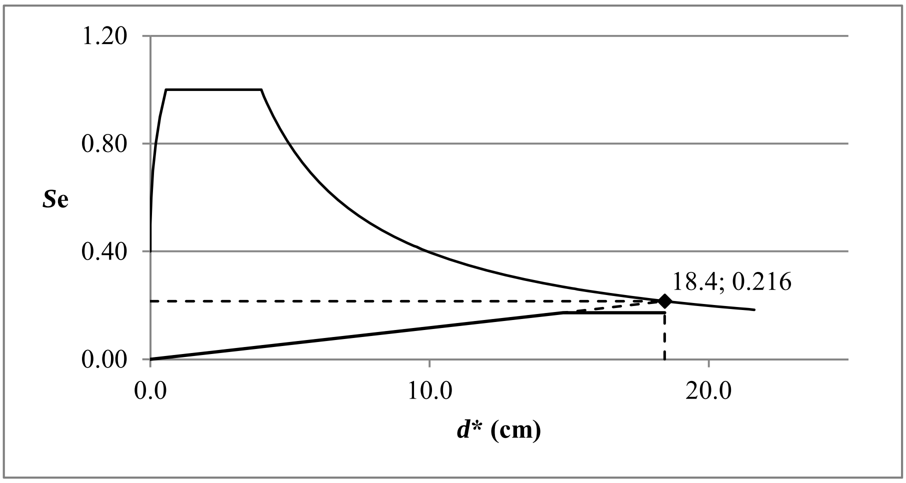

Figure 3.36: Target displacement computation, Structure 1, direction x, second iteration.

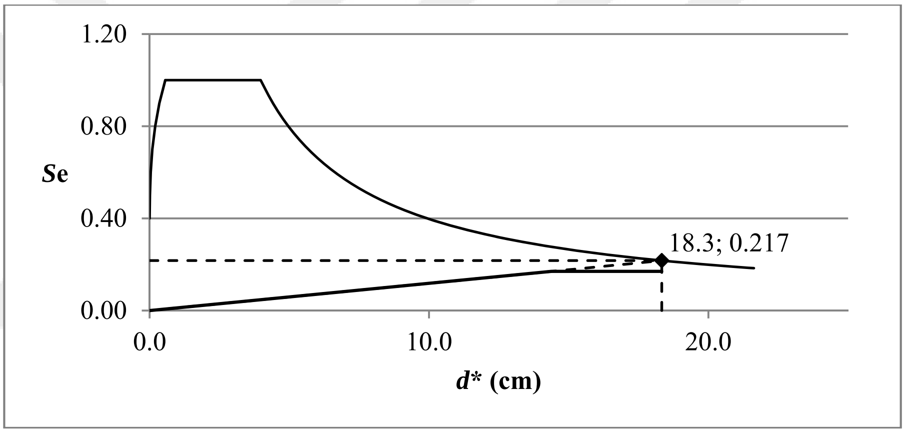

Figure 3.37: Target displacement computation, Structure 1, direction x, third iteration.

The definitive target displacement in the SDOF system is 18.3cm. In order to obtain the target displacement in the control node of the MDOF this displacement must be multiplied by the participation factor, Γ, which is given by equation 2.21 and is equal to 1.349, then the target displacement is equal to 24.7 cm.

All target displacement computations are shown in figures from 3.38 to 3.47 and in tables from 3.27 and 3.28.

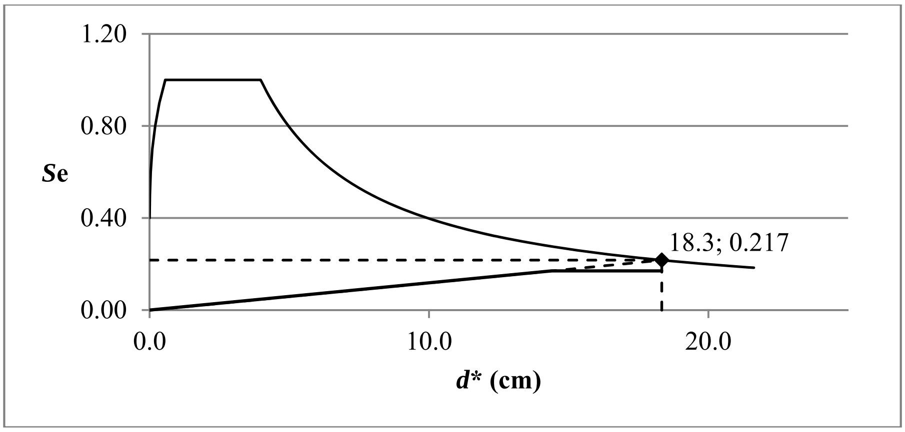

Figure 3.38: Target displacement computation, EN 1998-3, Structure 1, direction x.

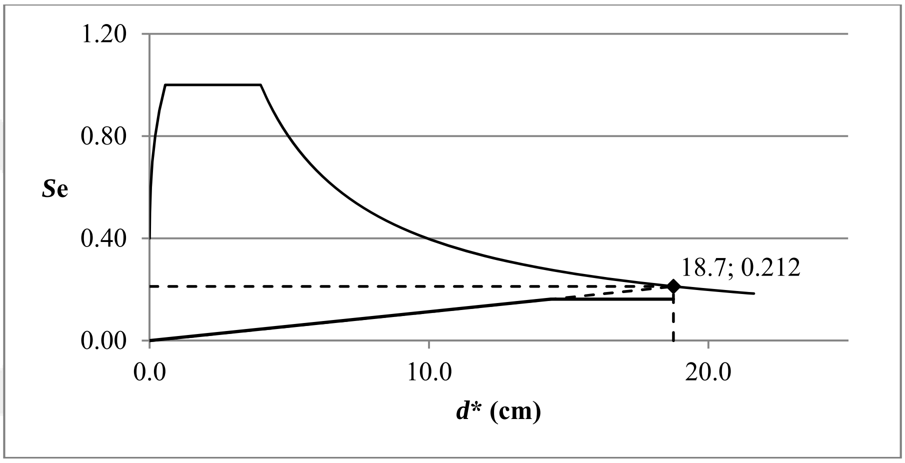

Figure 3.39: Target displacement computation, EN 1998-3, Structure 1, direction y.

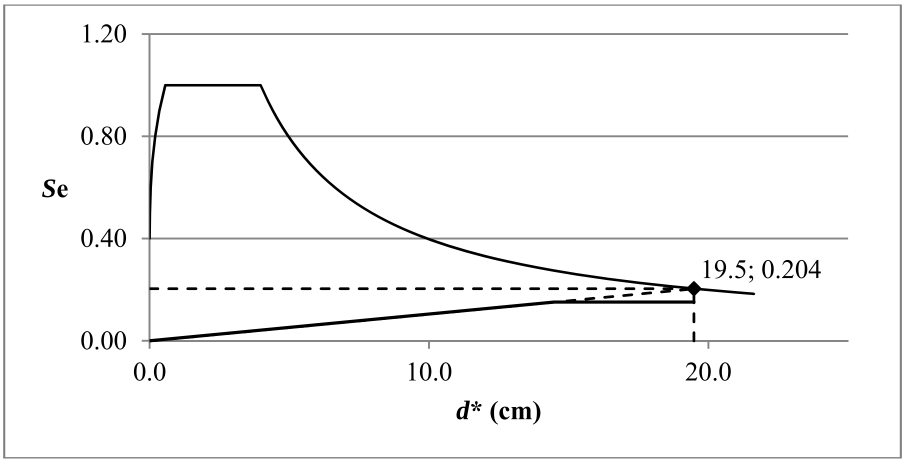

Figure 3.40: Target displacement computation, EN 1998-3, Structure 2, direction x.

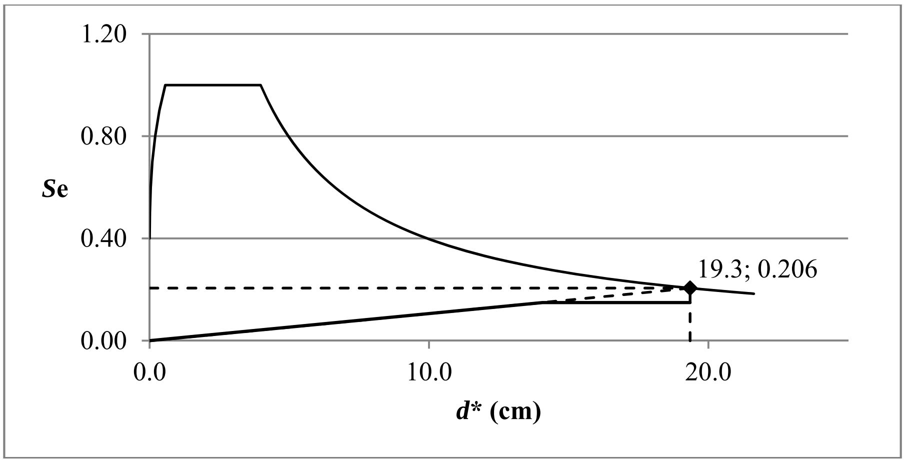

Figure 3.41: Target displacement computation, EN 1998-3, Structure 2, direction y.

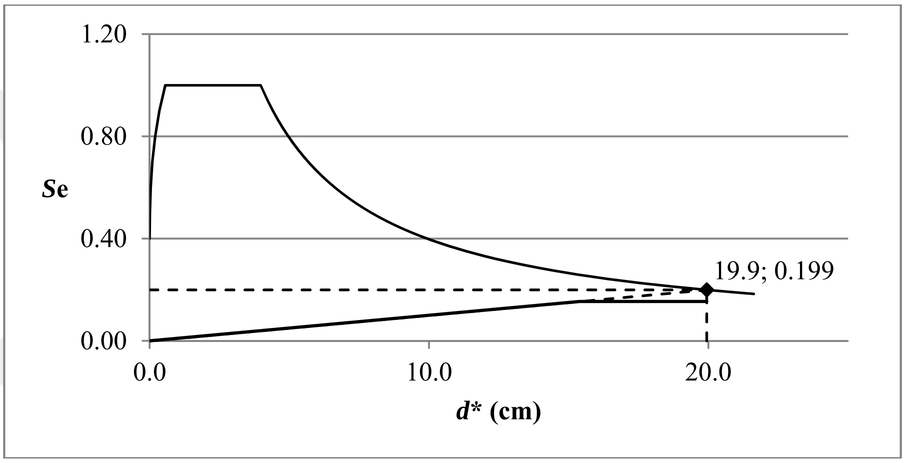

Figure 3.42: Target displacement computation, EN 1998-3, Structure 3, direction x.

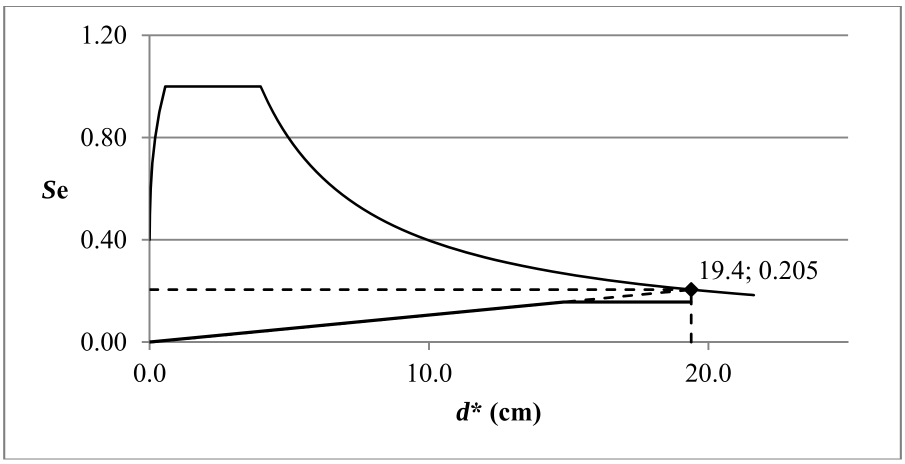

Figure 3.43: Target displacement computation, EN 1998-3, Structure 3, direction y.

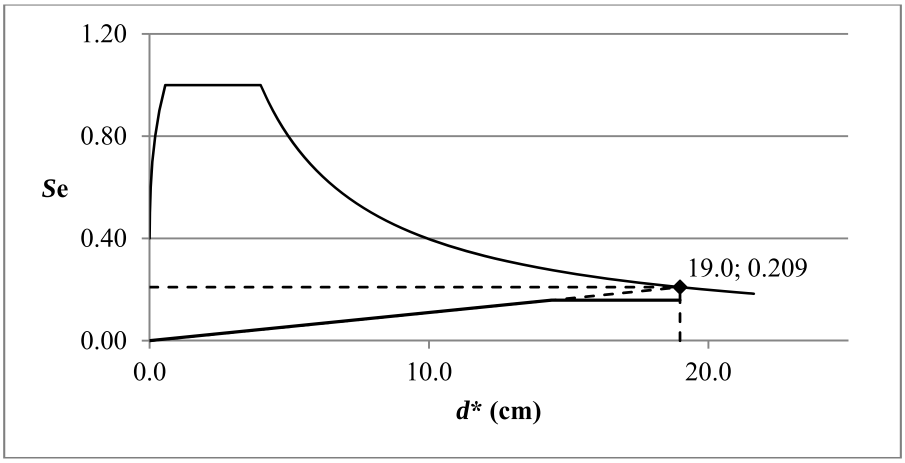

Figure 3.44: Target displacement computation, EN 1998-3, Structure 4, direction x.

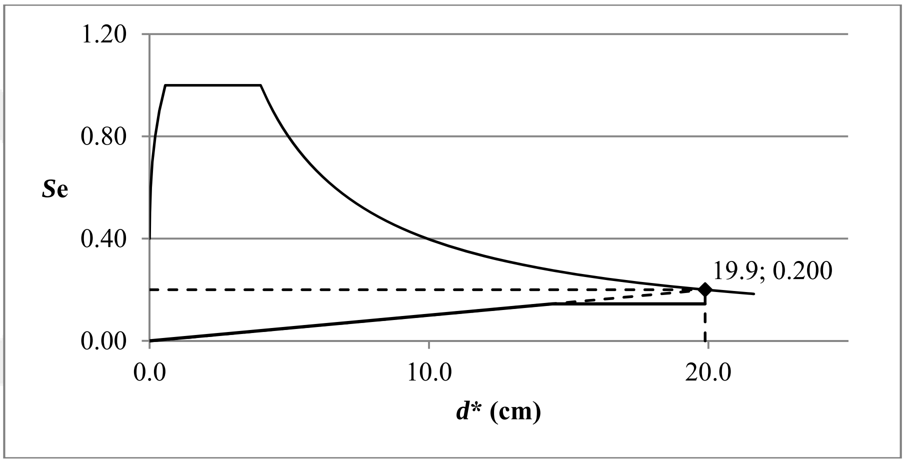

Figure 3.45: Target displacement computation, EN 1998-3, Structure 4, direction y.

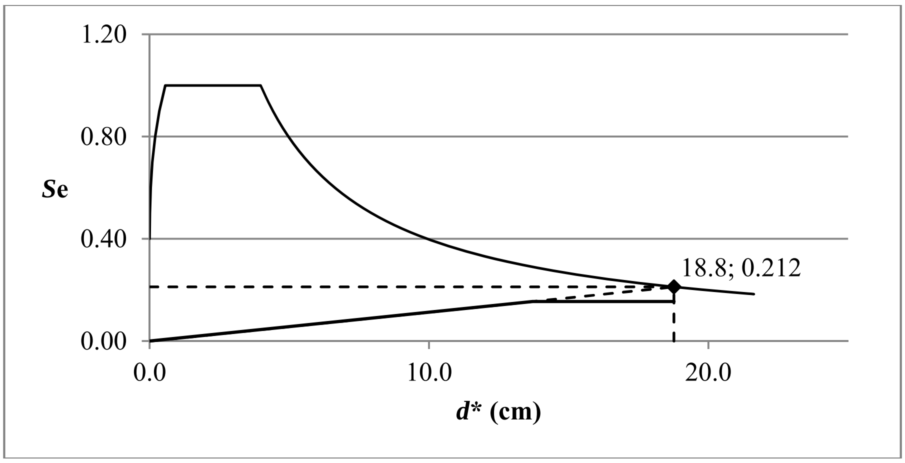

Figure 3.46: Target displacement computation, EN 1998-3, Structure 5, direction x.

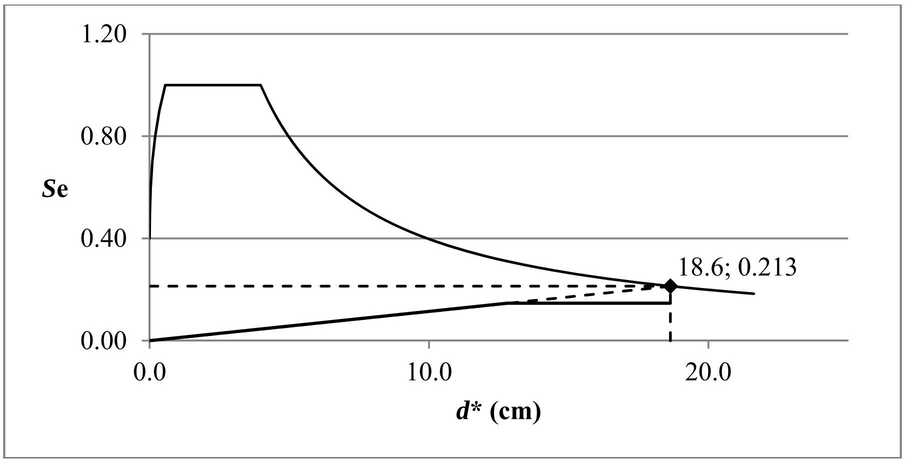

Figure 3.47: Target displacement computation, EN 1998-3, Structure 5, direction y.

Table 3.27: Target displacement computation, EN 1998-3, direction x (summary).

	Structure 1	Structure 2	Structure 3	Structure 4	Structure 5
d_{et}* (cm)	18.3	19.5	19.9	19.0	18.8
Γ	1.349	1.330	1.344	1.365	1.365
d_n (cm)	24.7	25.9	26.7	25.9	25.6

Table 3.28: Target displacement computation, EN 1998-3, direction y (summary).

	Structure 1	Structure 2	Structure 3	Structure 4	Structure 5
d_{et}* (cm)	18.7	19.3	19.4	19.9	18.6
Γ	1.352	1.339	1.356	1.367	1.364
d_n (cm)	25.3	25.9	26.3	27.2	25.4

- TBDY-16

Since all the periods are higher than the upper limit of the constant acceleration branch of the spectrum ($T_1 > T_B$), the spectral displacement ratio, C_R, will be equal to 1.0 and the inelastic response spectrum displacement, $S_{di}(T_1)$, will be equal to the elastic response spectrum displacement, $S_{de}(T_1)$, which is obtained as shown in figures from 3.48 to 3.57.

The target displacements obtained, $S_{de}(T_1)$, correspond to the equivalent SDOF system, those must be multiplied by the modal participating factor to convert them to displacements in the control node, u_N. Modal participating factor are given by equation 2.47. This computation is summarized in tables 3.29 and 3.30.

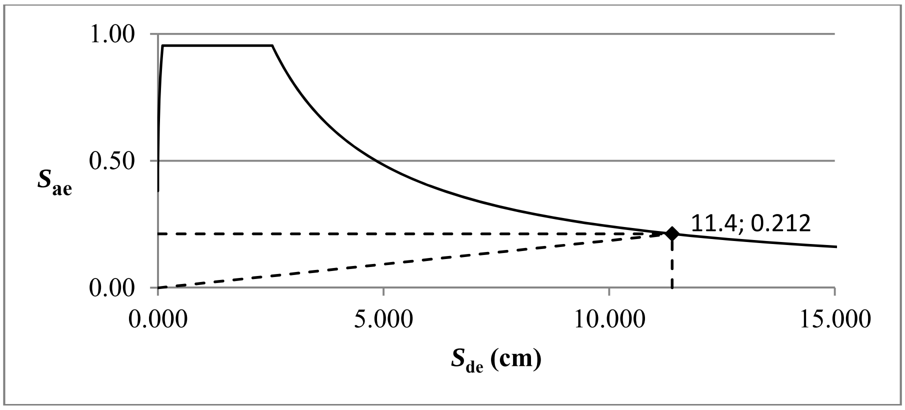

Figure 3.48: Target displacement computation, TBDY-16, Structure 1, direction x.

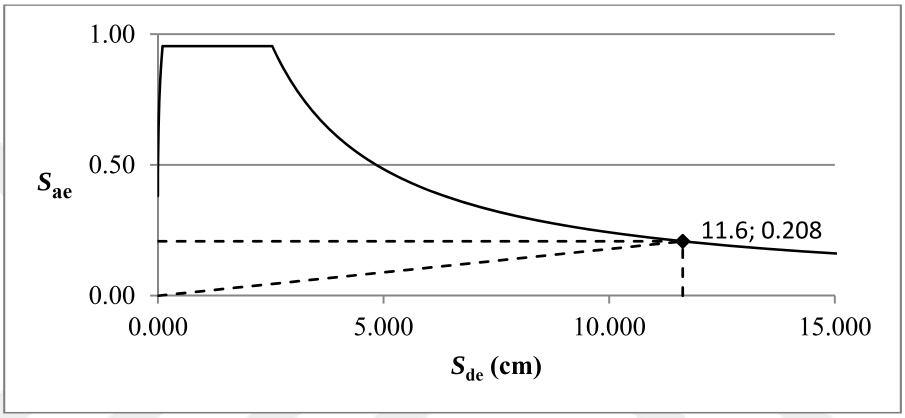

Figure 3.49: Target displacement computation, TBDY-16, Structure 1, direction y.

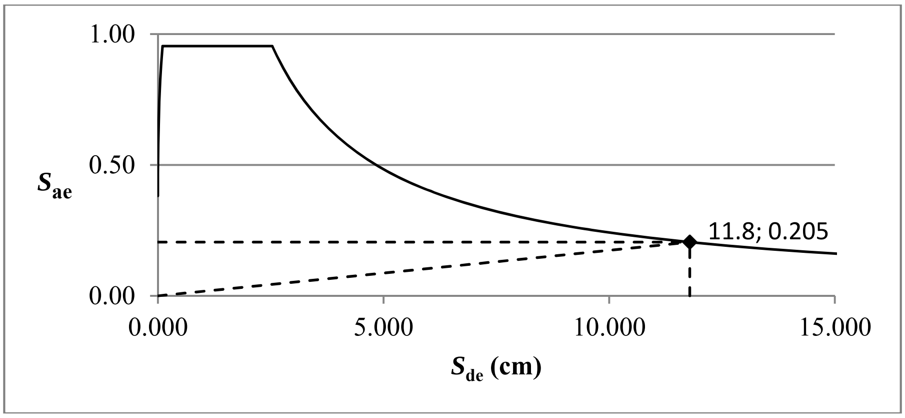

Figure 3.50: Target displacement computation, TBDY-16, Structure 2, direction x.

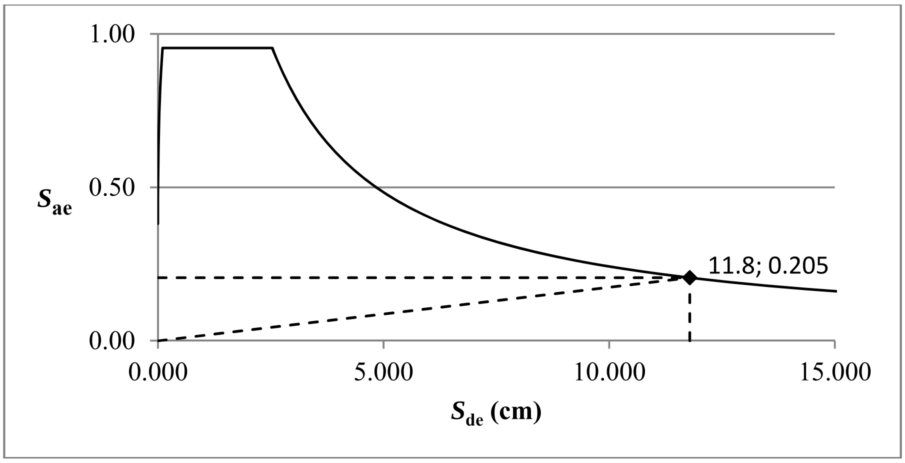

Figure 3.51: Target displacement computation, TBDY-16, Structure 2, direction y.

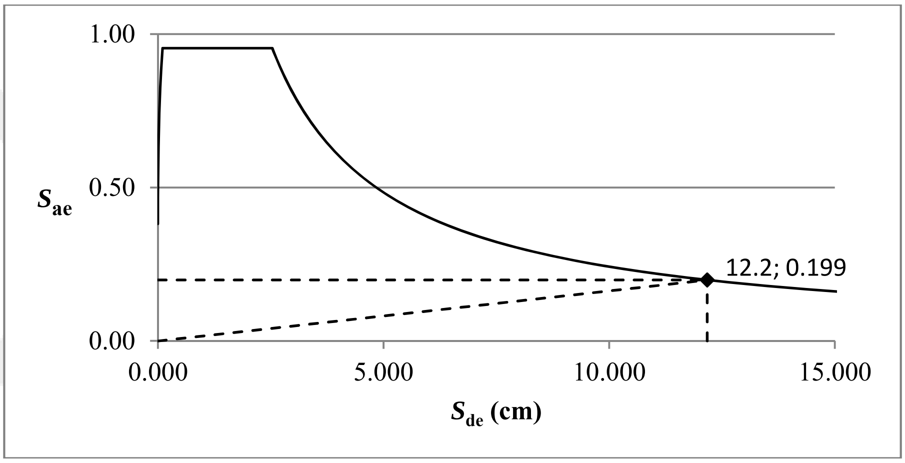

Figure 3.52: Target displacement computation, TBDY-16, Structure 3, direction x.

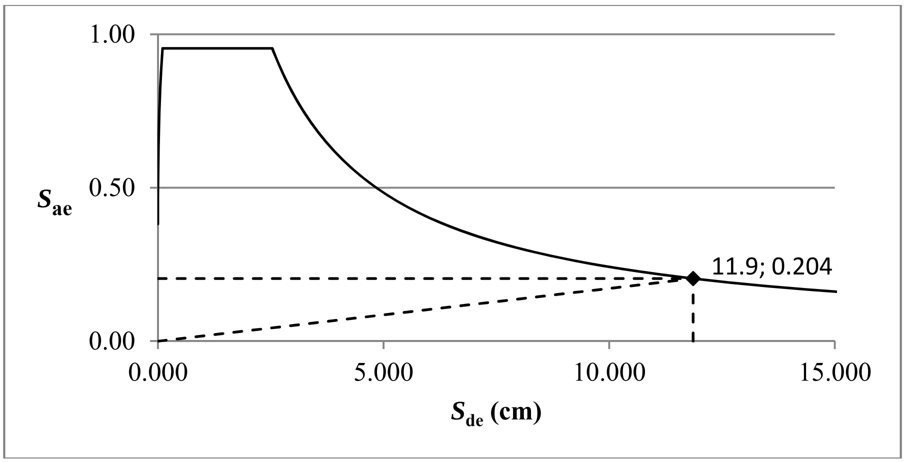

Figure 3.53: Target displacement computation, TBDY-16, Structure 3, direction y.

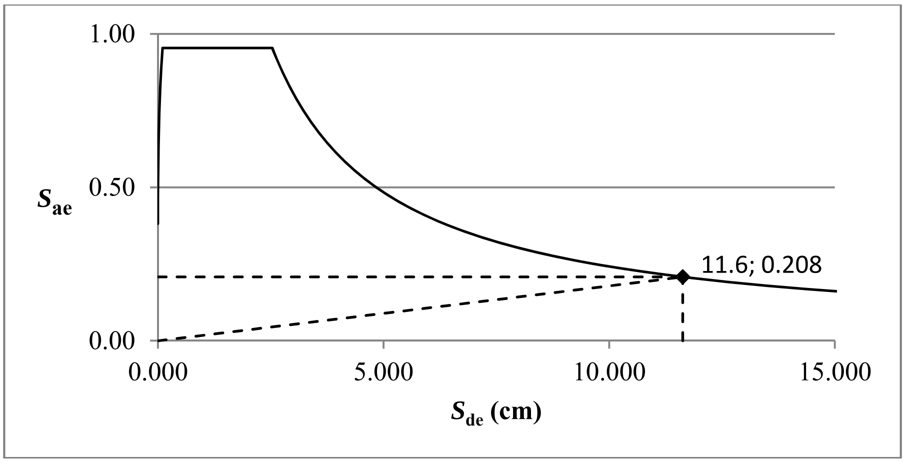

Figure 3.54: Target displacement computation, TBDY-16, Structure 4, direction x.

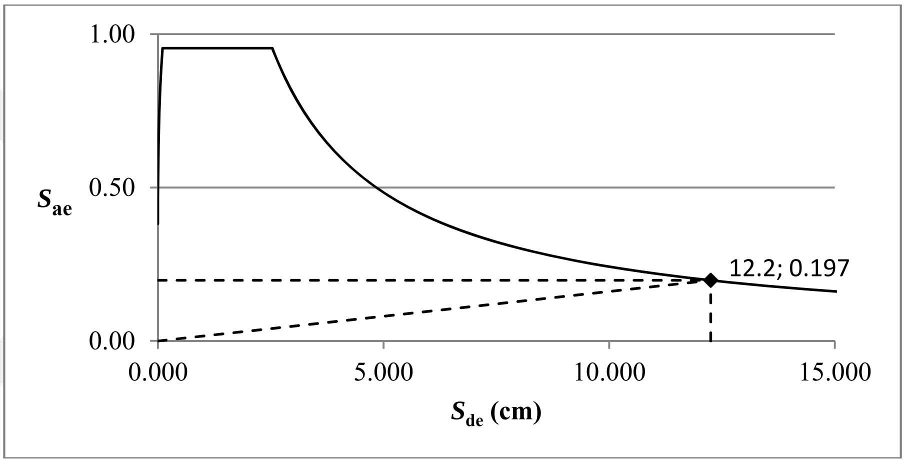

Figure 3.55: Target displacement computation, TBDY-16, Structure 4, direction y.

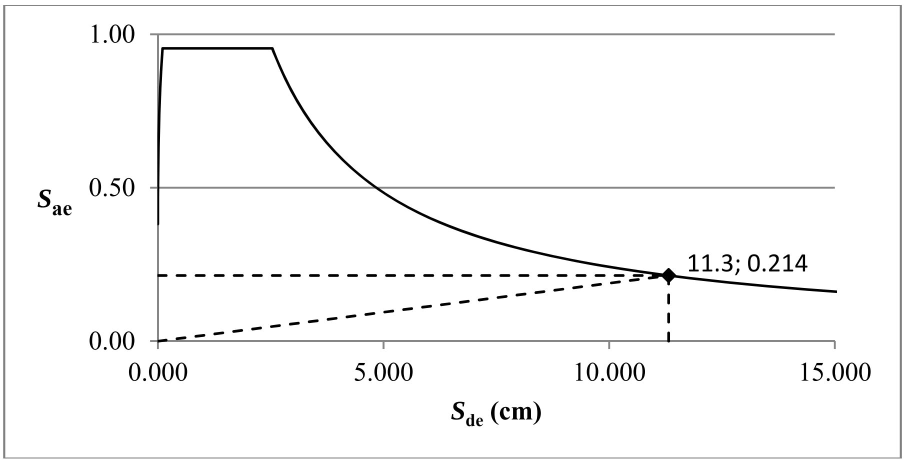

Figure 3.56: Target displacement computation, TBDY-16, Structure 5, direction x.

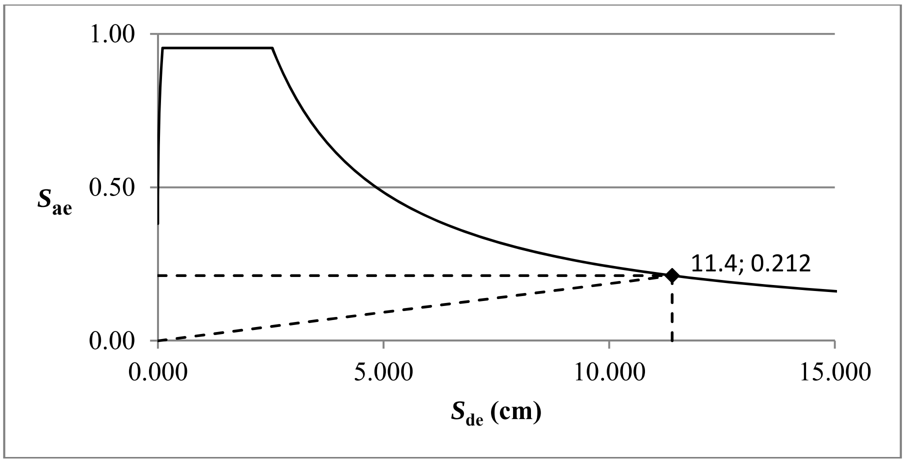

Figure 3.57: Target displacement computation, TBDY-16, Structure 5, direction y.

Table 3.29: Target displacement computation, TBDY-16, direction x (summary).

	Structure 1	Structure 2	Structure 3	Structure 4	Structure 5
S_{di} (cm)	11.4	11.8	12.2	11.6	11.3
Γ	1.346	1.326	1.339	1.360	1.354
u_N (cm)	15.3	15.6	16.3	15.8	15.3

Table 3.30: Target displacement computation, TBDY-16, direction y (summary).

	Structure 1	Structure 2	Structure 3	Structure 4	Structure 5
S_{di} (cm)	11.6	11.8	11.9	12.2	11.4
Γ	1.348	1.334	1.350	1.361	1.359
u_N (cm)	15.7	15.7	16.0	16.7	15.5

The target displacements obtained for the three codes are compared in tables 3.31 and 3.32.

For x direction, in all the structures, the maximum target displacement was found in Structure 3 (40% open area). Those are, 23.8cm for ASCE-41-13, 26.7cm for Eurocode, and 16.3cm for TBDY-16.

For y direction, the maximum target displacements were obtained in Structure 4 (50% open area). Those are, 23.9cm for ASCE-41-13, 27.2cm for Eurocode, and 16.7cm for TBDY-16.

Table 3.31: Target displacement, x direction (cm).

Structure	ASCE-41-13	EN 1998-3	TBDY-16
1	22.0	24.7	15.3
2	23.1	25.9	15.6
3	23.8	26.7	16.3
4	22.9	25.9	15.8
5	21.9	25.6	15.3

Table 3.32: Target displacement, y direction (cm).

Structure	ASCE-41-13	EN 1998-3	TBDY-16
1	22.6	25.3	15.7
2	23.0	25.9	15.7
3	23.2	26.3	16.0
4	23.9	27.2	16.7
5	22.0	25.4	15.5

3.2.8. Pushover until target displacements

Pushover procedure will be applied until target displacements shown in tables 3.31 and 3.32. The deformed shapes of the structures are shown in the figures in Appendix A. Those figures also indicate the elements which experienced plastic rotations in hinges after applying lateral increasing loads. It is observed that the beams are the weak elements and they suffer damages first than columns. Furthermore, the structures remain stable, because not mechanism is formed.

- Drifts

The drifts obtained after applying pushover until target displacements are shown in figures from 3.58 to 3.67. In all the structures, for x and y direction, maximum drifts were found in the third story. Structure 4 (50% open are) shows the biggest drifts, those are, 0.0173 for ASCE-41-13, 0.0186 for Eurocode, and 0.0115 for TBDY-16.

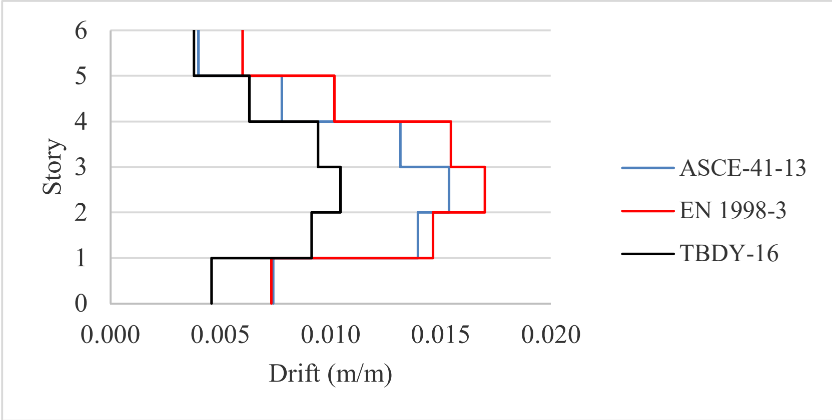

Figure 3.58: Drift (Δ/h), Structure 1, x direction.

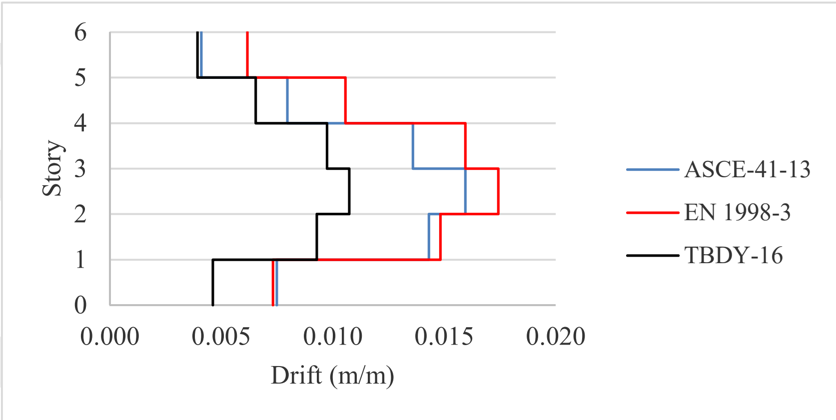

Figure 3.59: Drift (Δ/h), Structure 1, y direction.

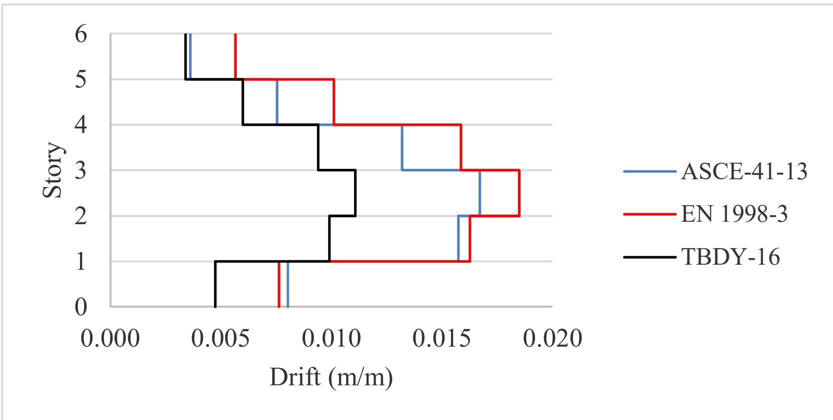

Figure 3.60: Drift (Δ/h), Structure 2, x direction.

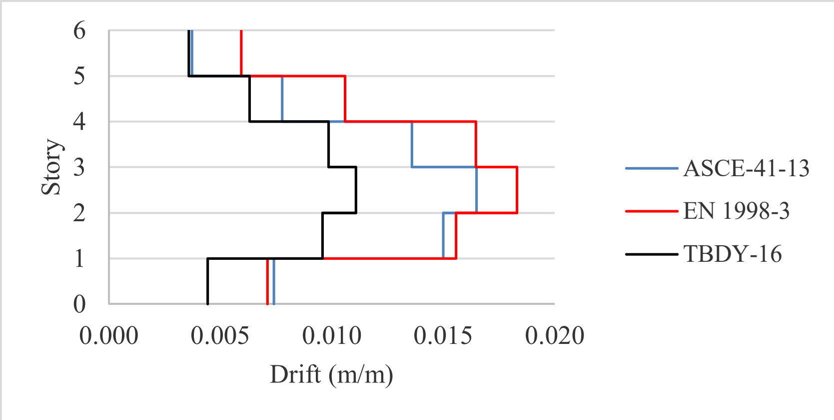

Figure 3.61: Drift (Δ/h), Structure 2, y direction.

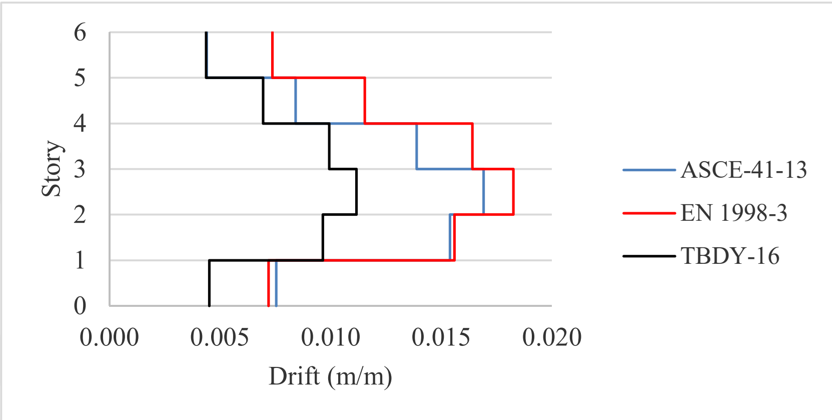

Figure 3.62: Drift (Δ/h), Structure 3, x direction.

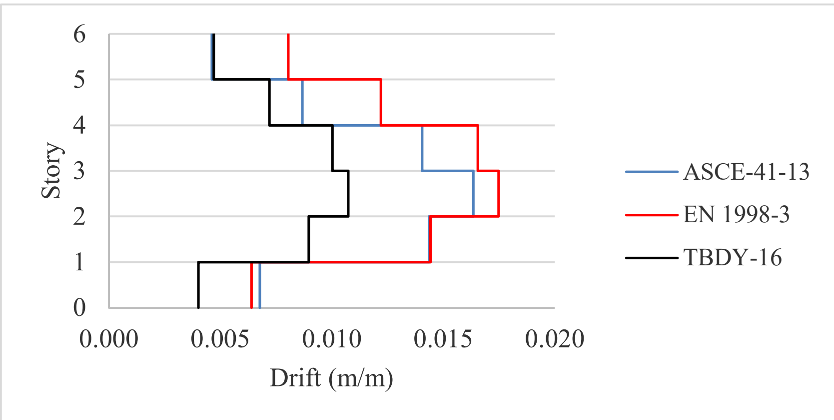

Figure 3.63: Drift (Δ/h), Structure 3, y direction.

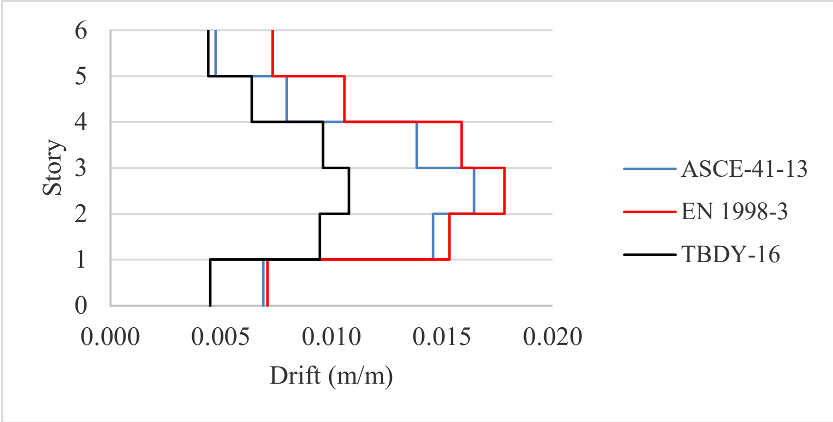

Figure 3.64: Drift (Δ/h), Structure 4, x direction.

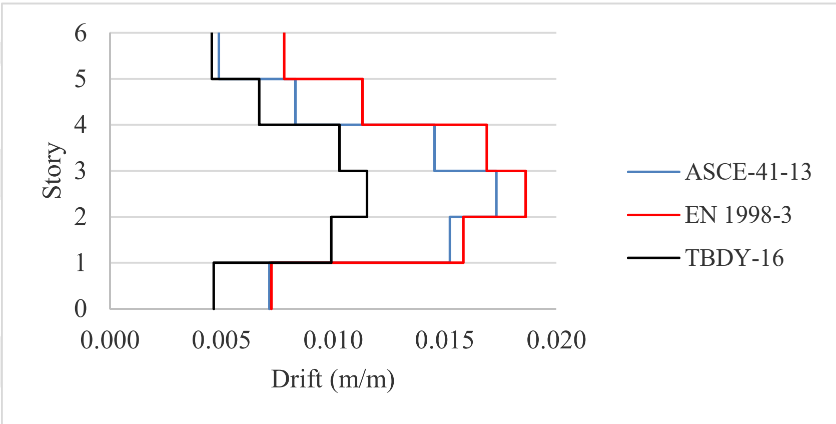

Figure 3.65: Drift (Δ/h), Structure 4, y direction.

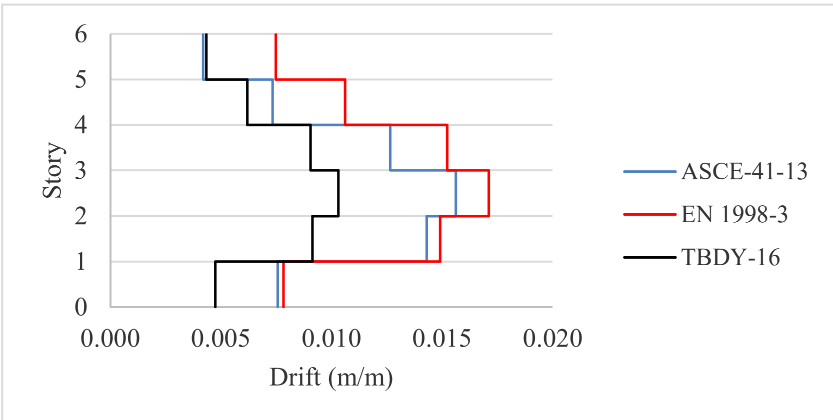

Figure 3.66: Drift (Δ/h), Structure 5, x direction.

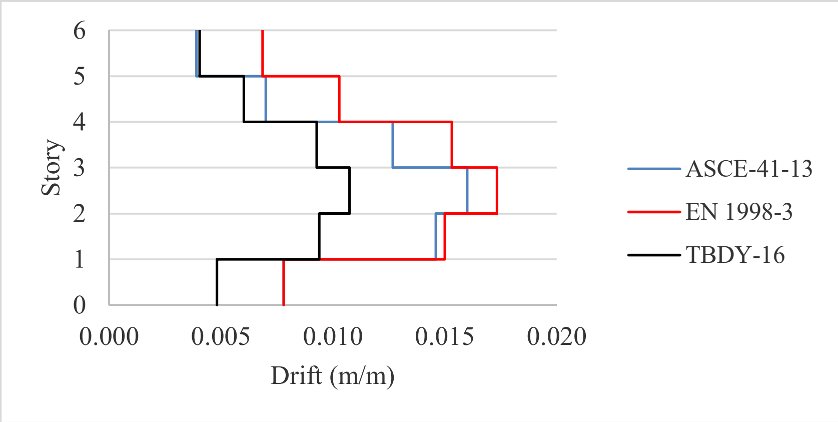

Figure 3.67: Drift (Δ/h), Structure 5, y direction.

3.2.9. Performance Levels

Performance levels will be established to each element in all the structures, based in their deformations after being subjected pushover loads.

- ASCE-41-13

Performance levels shall be established according to maximum plastic rotation values indicated in tables 2.7 and 2.8.

All the plastic rotations in columns were equal to zero, only plastic rotations in beams will be analyzed.

Performance level computation will be shown for one beam, for this purpose, Frame B in Structure 3 (See figure A1.9) will be analyzed with pushover in direction x. The beam selected will be the beam with the maximum plastic rotation.

In this Frame all the beams has 40x60cm section (see figure 3.6). Table 3.33 shows the maximum plastic rotation in beams per story.

Maximum plastic rotation is found in story 2, specifically in element number 443, which is a 5m long beam between axes 1 and 2. (see figures 3.68 and 3.5)

The plastic rotations are 0.0151 rad and -0.0068 rad in “I-end” and “J-end” respectively, as shown in figure 3.70 (positive rotation indicates tension in bottom and compression in top of the beam). “I-end” will be analyzed.

Table 3.33: Maximum plastic rotation in beams, Structure 3, Frame B, ASCE-41-13.

Story	Maximum Plastic Rotation (rad)
6	0.0
5	0.0009
4	0.0089
3	0.0140
2	0.0151
1	0.0102

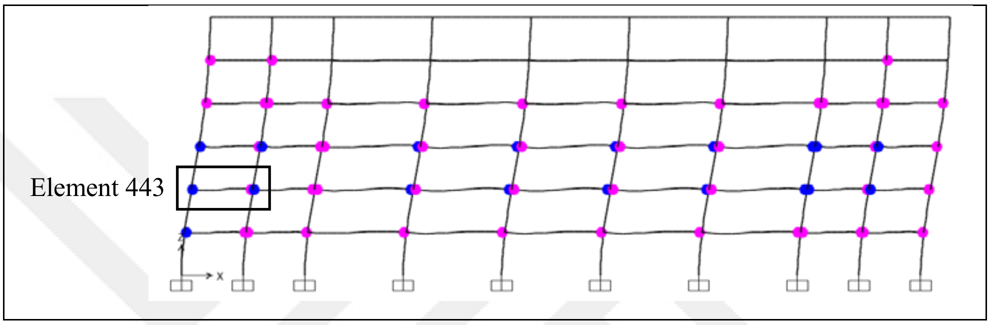

Figure 3.68: Deformed shape, Structure 3, Frame B.

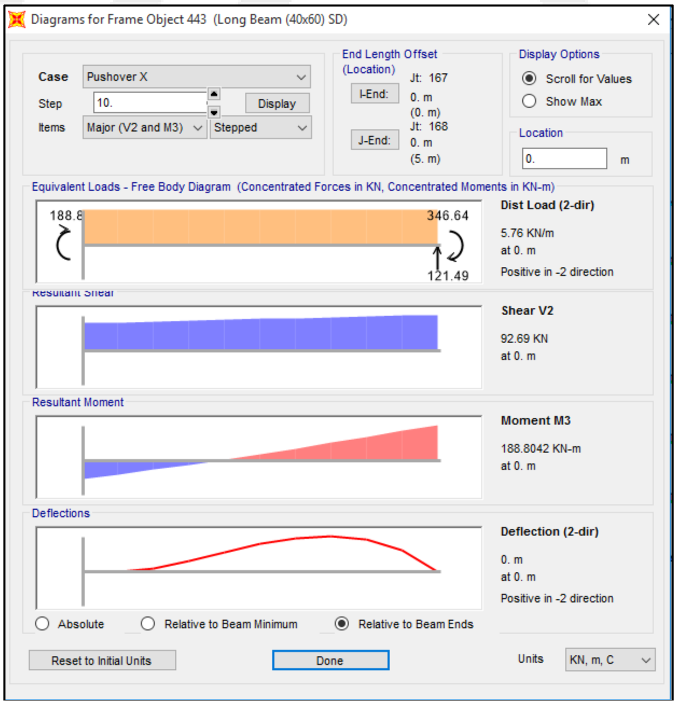

Figure 3.69 Deformed shape and internal forces in element 443.

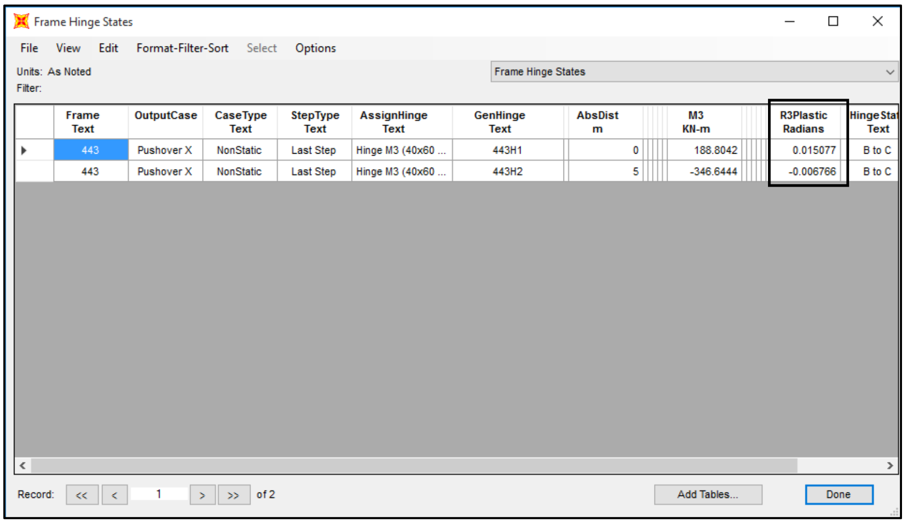

Figure 3.70: Plastic rotations in element 443.

The maximum plastic rotation for different performance levels shall be obtained according to longitudinal reinforcement, transverse reinforcement and shear force from table 2.7.

The studied beam has 883 mm^2 in tension reinforcement (bottom), and 1665 mm^2 in compression reinforcement (top), this corresponds to 0.0040 and 0.0076 ratio of tension and compression reinforcement respectively. Therefore, the result of the equation in first column in table 2.7 will be smaller than zero.

The spacing of hoops in the edges of the beams is 120mm, this is considered conforming since it is smaller than one third of the distance from extreme compression fiber to centroid of tension reinforcement, *d*.

The Maximum shear in “I-end” is 92.7 kN as shown in figure 3.69, the result of the equation in third column in table 2.7 is 0.08, which is smaller than 0.25.

According to the three conditions described, the maximum plastic rotations for Immediate Occupancy (IO), Life Safety (LS) and Collapse Prevention (CP) are 0.010, 0.025 and 0.05 respectively.

The performance level in the studied beam (element number 443) is Life Safety. Maximum rotations per story shown in table 3.33 indicates that there are beams in Life Safety (LS) performance level in stories between first and third. In stories between fourth and sixth all beams remain in Immediate Occupancy (IO) performance level. Tables from 3.35 to 3.44 show the amount of elements on each performance level for the five structures.

• EN 1998-3

Performance levels in columns and beams shall be established according to total chord rotation limits given in equation 2.31, 2.32 and 2.33.

Most of the columns remained elastic after applying pushover loads until target displacements, the maximum chord rotation found in columns was 0.0003 rad, this value is always smaller than the limit rotation for Damage Limitation performance level (equation 2.33); therefore, it can be assured that all the columns remain in Damage Limitation (DL).

Performance level computation will be shown in detail for one beam. The beam selected was element 448 in Frame B in Structure 3, which is an 8.0m long beam in second story and located between axes 6 and 7 (see figures 3.5 and A.9). This beam has a 40x60 section (see figure 3.6).

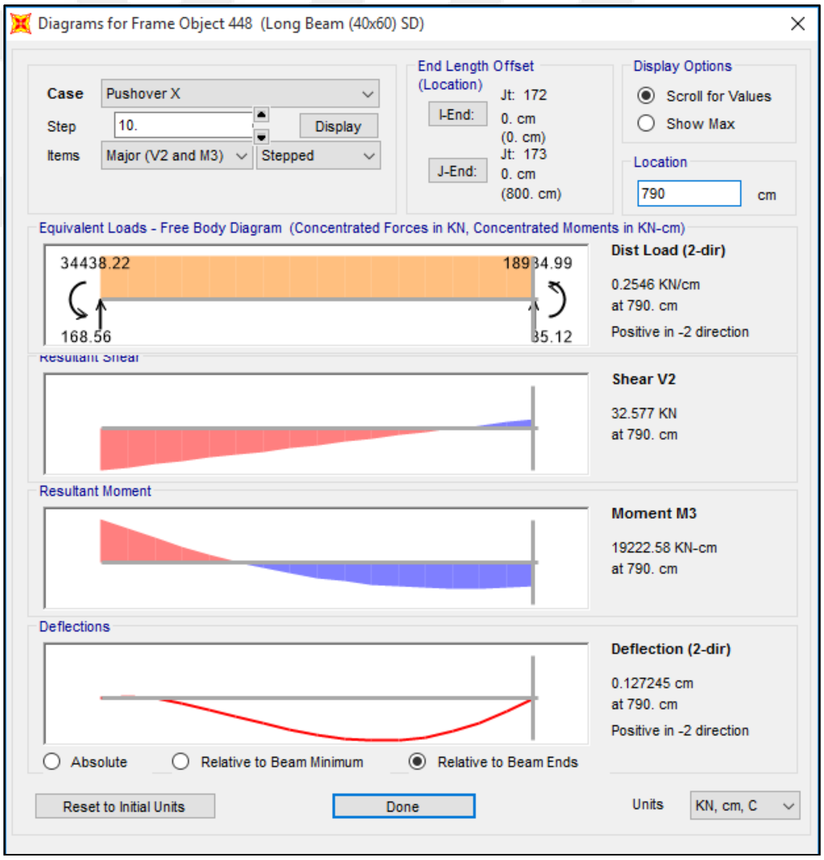

Figure 3.71: Deformed shape and internal forces in element 448.

Figure 3.71 shows the deformed shape of the beam, it is seen a bigger chord rotation in “J-end”. This chord rotation can be calculated as the slope of the tangent line to the deformed shape shown in the figure. This slope is estimated as 0.127 cm divided by 10 cm, as a result the chord rotation is 0.0127 rad (positive rotation indicates tension in bottom and compression in top of the beam).

The maximum chord rotations for different performance levels shall be obtained in accordance with equations 2.31, 2.32 and 2.33.

Yield curvature, ϕ_y, will be obtained from moment-curvature diagram, this graphic was extracted from "Section Designer" in SAP2000. Figure 3.72 shows this curve and an equivalent bilinear curve in order to find the effective yielding curvature.

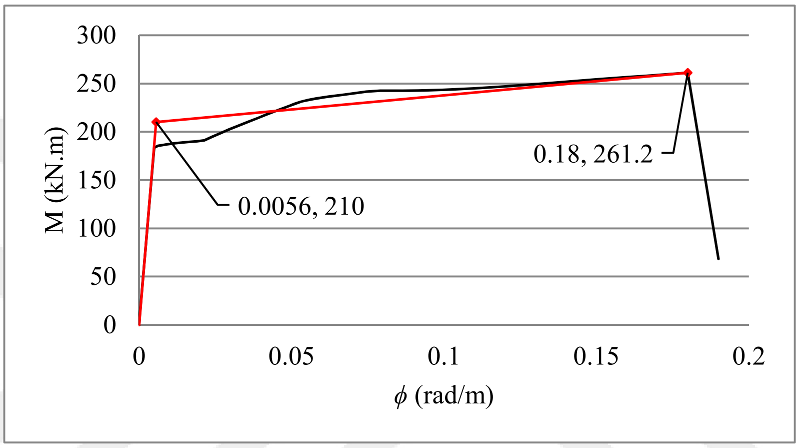

Figure 3.72 Moment-curvature diagram in 40x60cm section beam.

The theoretical formula of θ_y (equation 2.33) is too sensitive to the value assumed by shear span L_v; therefore, it is neccesary to consider L_v = L/2 instead of its correct definition [Mpampatsikos et al., 2008]. For this beam, L_v will be assumed as 4.0m. The distance from extreme compression fiber to centroid of tension and compression reinforcement, d and d', are 550 mm and 50mm respectively. The mean diameter of tension reinforcement, d_{bL}, is 20mm.

The limit chord rotation for Damage Limitation performance level, θ_y, is calculated using equation 2.33, the result found was 0.0103 rad.

The beam studied has a chord rotation equal to 0.0127 rad, this means that this beam will be in Significant Damage (SD) or Near Collapse (NC) performance level, the limit rotation for those two performance levels will be calculated hereafter.

Plastic hinge length, L_{pl}, is computed as given by equation 2.35, its result was 0.44m. Ultimate curvature, ϕ_u, is obtained from the moment-curvature diagram (see figure 3.72), this will be taken as 0.18 rad/m.

Finally, using equations 2.31 and 2.32, limit chord rotation for Significant Damage (SD) and Near Collapse (NC), θ_{SD} and θ_{um}, are 0.0435 and 0.058 rad respectively. Therefore, studied beam is expected to be in Significant Damage (SD) performance level. Performance levels for all the beams are shown in tables from 3.35 to 3.44.

- TBDY-16

Performance levels in columns and beams shall be established according to strain limits indicated in equation 2.60, 2.61 and 2.62. In order to obtain strains, the first step is to obtain plastic rotation in hinges from structural analysis, second step is to calculate curvature in sections as given by equation 2.59, in last step strains in concrete and steel can be obtained from moment-curvature diagrams.

Only four columns showed plastic rotations, the maximum value found was 1.2x10-5 rad, this value can be neglected and only plastic rotations in beams will be analyzed. Performance level computation will be shown in detail for 1 beam, Frame B in Structure 3 (See figure A1.9) will be analyzed with pushover loads in direction x. The beam selected will be the beam with the maximum plastic rotation.

In this Frame all the beams has 40x60cm section (see figure 3.6). Table 3.34 shows the maximum plastic rotation in beams per story.

Maximum plastic rotation is found in story 3, specifically in element number 659, which is a 5m long beam between axes 9 and 10 (see figures 3.5 and A.9).

Table 3.34: Maximum plastic rotation in beams, Structure 3, Frame B, TBDY-16.

Story	Maximum Plastic Rotation (rad)
6	0.0
5	0.0021
4	0.0067
3	0.0093
2	0.0092
1	0.0060

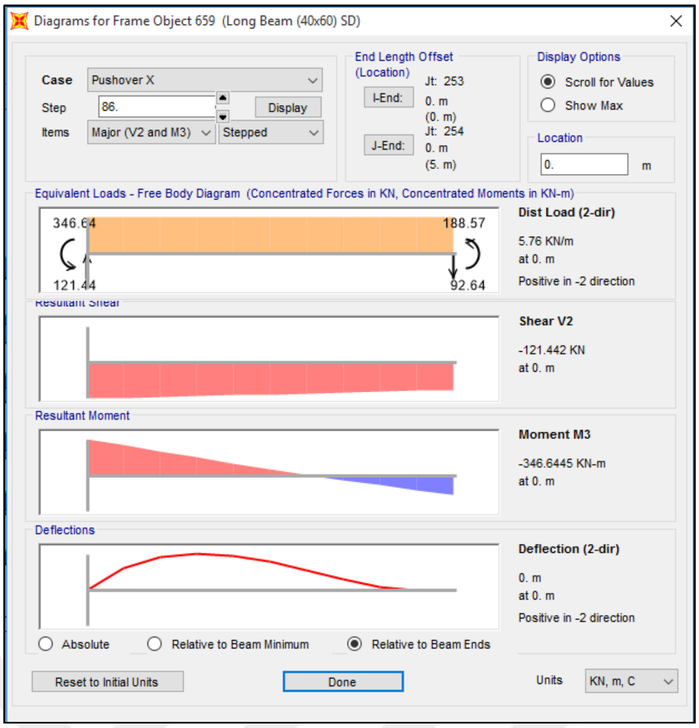

Figure 3.73: Deformed and internal forces in element 659.

The plastic rotations are -0.0027 rad and 0.0093 rad in “I-end” and “J-end” respectively (positive rotation indicates tension in bottom and compression in top of the beam). “J-end” will be analyzed.

Using this plastic rotation, as a second step equation 2.59 will be applied, yielding curvature was obtained in figure 3.72; plastic length will be equal to half of the height of the beam. Finally, the total curvature obtained is 0.037 rad/m.

Moment curvature diagrams were generated using “Section Designer” function in SAP2000, strains in concrete and steel will be obtained from this graphic for a 40x60 section beam with a curvature equal to 0.037 rad/m. The strains obtained are 0.0006 and 0.0175 in concrete and steel respectively (see figure 3.74).

In order to apply limit strains provided in equations 2.61, 2.62 and 2.63, shear ratio from equation 2.63 must be verified.

The Maximum shear in “J-end” is 121.4 kN as shown in figure 3.73, the result of equation 2.63 is 0.11, which is smaller than 0.65. Therefore, the limit strains in equations 2.61, 2.62 and 2.63 are acceptable and the performance level in the studied beam (element number 659) is Life Safety (CG).

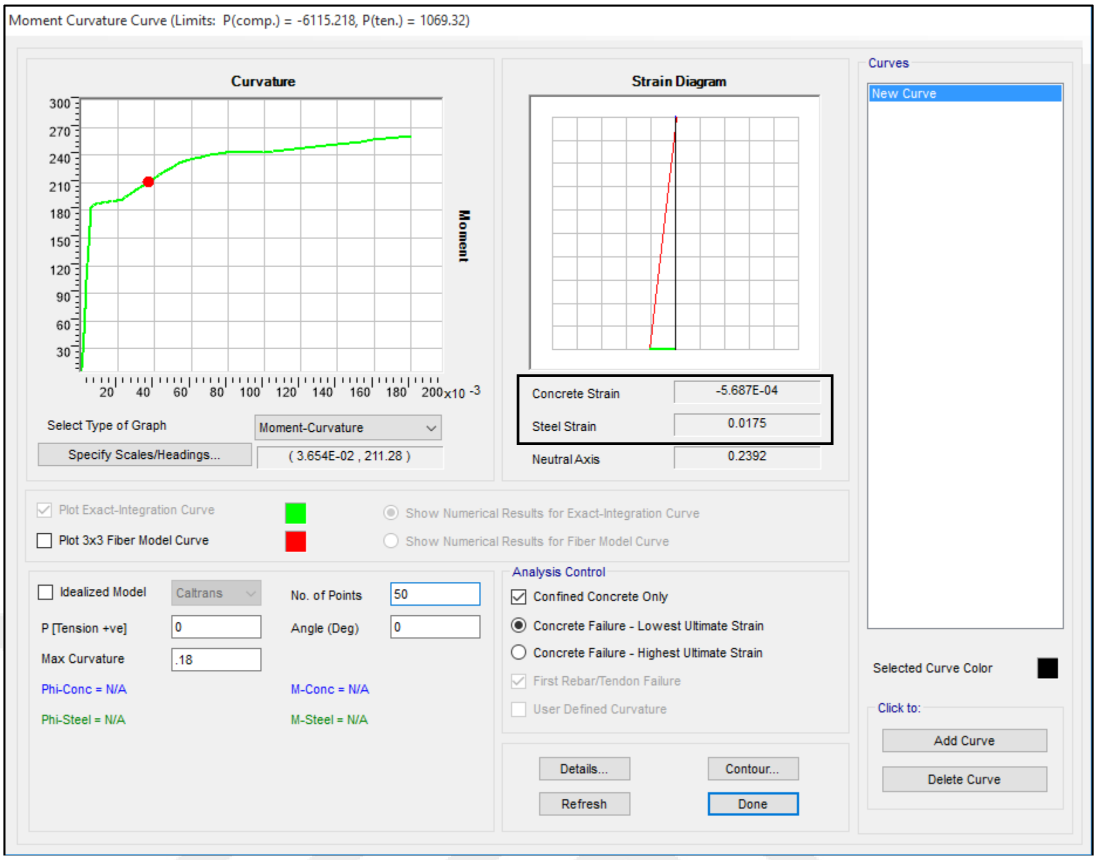

Figure 3.74: Strains in concrete and steel for 0.037rad/m curvature.

For all the buildings, the three codes showed damages in beams in stories from 1 to 4 and in columns in first floor. The damages in columns are very low, consequently the performance levels in all the columns are Immediate Occupancy (IO) for ASCE-41-13, Damage Limitation (DL) for EN 1998-3 and Immediate Occupancy (HK) for TBDY-16. The performance levels for beams are shown in tables from 3.35 to 3.44

Table 3.35: Percentage of Beams by Performance level, Structure 1, x direction.

Story	ASCE-41-13			EN 1998-3			TBDY-16		
	IO	LS	CP	DL	SD	NC	HK	CG	GO
6	100.0	0.0	0.0	100.0	0.0	0.0	100.0	0.0	0.0
5	100.0	0.0	0.0	100.0	0.0	0.0	100.0	0.0	0.0
4	100.0	0.0	0.0	91.3	8.7	0.0	91.3	8.7	0.0
3	0.0	100.0	0.0	47.8	52.2	0.0	0.0	100.0	0.0
2	0.0	100.0	0.0	52.2	47.8	0.0	0.0	100.0	0.0
1	91.3	8.7	0.0	82.6	17.4	0.0	82.6	17.4	0.0

Table 3.36: Percentage of Beams by Performance level, Structure 1, y direction.

Story	ASCE-41-13			EN 1998-3			TBDY-16		
	IO	LS	CP	DL	SD	NC	HK	CG	GO
6	100.0	0.0	0.0	100.0	0.0	0.0	100.0	0.0	0.0
5	100.0	0.0	0.0	100.0	0.0	0.0	100.0	0.0	0.0
4	100.0	0.0	0.0	100.0	0.0	0.0	81.8	18.2	0.0
3	36.4	63.6	0.0	72.7	27.3	0.0	0.0	100.0	0.0
2	36.4	63.6	0.0	72.7	27.3	0.0	0.0	100.0	0.0
1	81.8	18.2	0.0	100.0	0.0	0.0	81.8	18.2	0.0

Table 3.37: Percentage of Beams by Performance level, Structure 2, x direction.

Story	ASCE-41-13			EN 1998-3			TBDY-16		
	IO	LS	CP	DL	SD	NC	HK	CG	GO
6	100.0	0.0	0.0	100.0	0.0	0.0	100.0	0.0	0.0
5	100.0	0.0	0.0	100.0	0.0	0.0	100.0	0.0	0.0
4	100.0	0.0	0.0	93.1	6.9	0.0	71.4	28.6	0.0
3	0.0	100.0	0.0	10.7	89.3	0.0	0.0	100.0	0.0
2	0.0	100.0	0.0	19.6	80.4	0.0	0.0	100.0	0.0
1	92.9	7.1	0.0	85.7	14.3	0.0	71.4	28.6	0.0

Table 3.38: Percentage of Beams by Performance level, Structure 2, y direction.

Story	ASCE-41-13			EN 1998-3			TBDY-16		
	IO	LS	CP	DL	SD	NC	HK	CG	GO
6	100.0	0.0	0.0	100.0	0.0	0.0	100.0	0.0	0.0
5	100.0	0.0	0.0	100.0	0.0	0.0	100.0	0.0	0.0
4	100.0	0.0	0.0	100.0	0.0	0.0	88.9	11.1	0.0
3	48.1	51.9	0.0	55.6	44.4	0.0	0.0	100.0	0.0
2	14.8	85.2	0.0	55.6	44.4	0.0	0.0	100.0	0.0
1	100.0	0.0	0.0	100.0	0.0	0.0	100.0	0.0	0.0

Table 3.39: Percentage of Beams by Performance level, Structure 3, x direction.

Story	ASCE-41-13			EN 1998-3			TBDY-16		
	IO	LS	CP	DL	SD	NC	HK	CG	GO
6	100.0	0.0	0.0	100.0	0.0	0.0	100.0	0.0	0.0
5	100.0	0.0	0.0	100.0	0.0	0.0	100.0	0.0	0.0
4	100.0	0.0	0.0	87.9	12.1	0.0	69.7	30.3	0.0
3	0.0	100.0	0.0	34.8	65.2	0.0	0.0	100.0	0.0
2	0.0	100.0	0.0	30.3	69.7	0.0	0.0	100.0	0.0
1	93.9	6.1	0.0	87.9	12.1	0.0	87.9	12.1	0.0

Table 3.40: Percentage of Beams by Performance level, Structure 3, y direction.

Story	ASCE-41-13			EN 1998-3			TBDY-16		
	IO	LS	CP	DL	SD	NC	HK	CG	GO
6	100.0	0.0	0.0	100.0	0.0	0.0	100.0	0.0	0.0
5	100.0	0.0	0.0	100.0	0.0	0.0	100.0	0.0	0.0
4	100.0	0.0	0.0	100.0	0.0	0.0	68.8	31.3	0.0
3	25.0	75.0	0.0	62.5	37.5	0.0	12.5	87.5	0.0
2	25.0	75.0	0.0	62.5	37.5	0.0	12.5	87.5	0.0
1	100.0	0.0	0.0	100.0	0.0	0.0	100.0	0.0	0.0

Table 3.41: Percentage of Beams by Performance level, Structure 4, x direction.

Story	ASCE-41-13			EN 1998-3			TBDY-16		
	IO	LS	CP	DL	SD	NC	HK	CG	GO
6	100.0	0.0	0.0	100.0	0.0	0.0	100.0	0.0	0.0
5	100.0	0.0	0.0	100.0	0.0	0.0	100.0	0.0	0.0
4	100.0	0.0	0.0	100.0	0.0	0.0	58.8	41.2	0.0
3	0.0	100.0	0.0	0.0	100.0	0.0	0.0	100.0	0.0
2	0.0	100.0	0.0	0.0	100.0	0.0	0.0	100.0	0.0
1	100.0	0.0	0.0	91.2	8.8	0.0	58.8	41.2	0.0

Table 3.42: Percentage of Beams by Performance level, Structure 4, y direction.

Story	ASCE-41-13			EN 1998-3			TBDY-16		
	IO	LS	CP	DL	SD	NC	HK	CG	GO
6	100.0	0.0	0.0	100.0	0.0	0.0	100.0	0.0	0.0
5	100.0	0.0	0.0	100.0	0.0	0.0	100.0	0.0	0.0
4	100.0	0.0	0.0	100.0	0.0	0.0	75.0	25.0	0.0
3	0.0	100.0	0.0	50.0	50.0	0.0	0.0	100.0	0.0
2	0.0	100.0	0.0	50.0	50.0	0.0	0.0	100.0	0.0
1	87.5	12.5	0.0	100.0	0.0	0.0	75.0	25.0	0.0

Table 3.43: Percentage of Beams by Performance level, Structure 5, x direction.

Story	ASCE-41-13			EN 1998-3			TBDY-16		
	IO	LS	CP	DL	SD	NC	HK	CG	GO
6	100.0	0.0	0.0	100.0	0.0	0.0	100.0	0.0	0.0
5	100.0	0.0	0.0	100.0	0.0	0.0	100.0	0.0	0.0
4	100.0	0.0	0.0	100.0	0.0	0.0	60.0	40.0	0.0
3	0.0	100.0	0.0	40.0	60.0	0.0	0.0	100.0	0.0
2	0.0	100.0	0.0	20.0	80.0	0.0	0.0	100.0	0.0
1	70.0	30.0	0.0	100.0	0.0	0.0	60.0	40.0	0.0

Table 3.44: Percentage of Beams by Performance level, Structure 5, y direction.

Story	ASCE-41-13			EN 1998-3			TBDY-16		
	IO	LS	CP	DL	SD	NC	HK	CG	GO
6	100.0	0.0	0.0	100.0	0.0	0.0	100.0	0.0	0.0
5	100.0	0.0	0.0	100.0	0.0	0.0	100.0	0.0	0.0
4	100.0	0.0	0.0	100.0	0.0	0.0	73.7	26.3	0.0
3	0.0	100.0	0.0	73.7	26.3	0.0	0.0	100.0	0.0
2	0.0	100.0	0.0	73.7	26.3	0.0	0.0	100.0	0.0
1	73.7	26.3	0.0	100.0	0.0	0.0	73.7	26.3	0.0

3.3. Analysis Results

The results obtained for response spectrum in the three standards show that different standards could give different response acceleration, which would influence in the performance assessment. For the range of periods in the studied cases (1.46 – 1.87 sec), very similar response acceleration were obtained for ASCE-41-13 and EN 1998-3, but lower values were obtained in TBDY-16. This differences were caused by the differences existing in soil coefficients, F_a, F_v, F_S and F_1.

Effective stiffness assigned according to the three standards were similar in beams. On the other hand, in columns a very important difference exists; the effective stiffness assigned was 0.4 in ASCE-41-13, 0.5 in EN 1998-3 and 0.7 in TBDY-16, this causes very different stiffness in the buildings.

The limitations to apply pushover method were fulfilled by all the structures. This confirms that buildings with a height around 20m or less can be generally adequate for this method.

The vibration periods in the fundamental modes show that the procedure in EN 1998-3 generated the most flexible structures and TDBY-16 the most rigid ones.

The modal shapes also showed that the flexibility in slabs increases considerably for buildings with bigger open areas in them. However, for the five structures studied, using the effective stiffness for slabs stated in standards, the flexibility obtained is still very low. This could be caused by the fact that the modelling technique (membrane) was not the most adequate and this could be corrected reducing the shear stiffness in slabs, F12.

Force-displacement curves showed an important difference in stiffness of buildings, which had already been seen in vibration periods.

In terms of target displacement, comparing the three standards, EN 1998-3 showed the highest values (24.7 – 27.2 cm) and TBDY-16 showed the lowest ones (15.3 – 16.7 cm).

After applying pushover loads until target displacements, deformed shapes showed maximum drifts in third story. Additionally, the biggest damages were obtained in beams in second and third stories, other beams showed lower damages. Columns did not show any damages in models developed in accordance with ASCE-41-13; for EN 1998-3 and TDBY-16, only very low damages were seen in columns in first story.

As expected in buildings designed to resist earthquake loads, beams are the weak elements ant they suffer damages first than the columns, this can be seen in deformed shapes, also it can be stated that structures remain stable because not mechanism is formed.

In terms of performance level, the results according to the three codes are equivalent, however, according to the amount of elements on each performance level, TBDY-16 shows more damage than ASCE-41-13 and EN 1998-3. Therefore, for seismic performance assessment TBDY-16 is the most conservative one.

4. CONCLUSIONS

Six-story reinforced concrete buildings were analyzed using nonlinear static performance assessment method. The structures have discontinuity in diaphragms, which is a horizontal irregularity that consists of open areas in slabs. The main characteristic in this type of buildings is that the common assumption of rigid floor diaphragms is no longer applicable. Those structures had been designed to resist earthquake loads as moment frames with high ductility. Performance levels were assigned to each element in the buildings according to ASCE-41-13, EN 1998-3 and TDBY-16. Performance levels obtained according to different standards were also compared.

The following conclusions can be stated based on the results of the structures analyzed.

- Several parameters have been used for defining Performance levels in buildings subjected to earthquakes, Plastic Rotation in ASCE-41-13, Chord Rotation in EN 1998-3 and Strains in TBDY-16.
- Plastic rotations can be directly obtained from structural analysis. Strains require additional calculations but they provide a better idea of the state of the materials in the structures. Limit states in Eurocode depends both on properties of the member and on the seismic loads (Lv = M/V), consequently the chord rotation capacity may not be defined as a property of the member.
- The target displacement computation is influenced considerably by the estimation of the vibration periods, which at the same time depend on the assumptions of effective inertias in elements. Consequently, one of the main reasons for getting differences in performance assessment using different seismic codes are the estimation of effective inertia in elements.
- Flexible diaphragms is an important consideration for seismic performance assessment of irregular buildings.
- Modelling a slab as membrane is a good method to consider its flexibility, however, according to the models analyzed in this research, in some cases a membrane show results very similar to those obtained using a rigid diaphragm.

- The shear stiffness in a membrane (F12) is the most important parameter that affects its rigidity or flexibility.

- If the shear stiffness in membranes (F12) is reduced, the slabs show their flexible behavior more appropriately, as expected for a building with discontinuity in diaphragms or some other irregularities.

- The performance level result for all the studied buildings can be considered equivalent; Life Safety (LS) in ASCE-41-13, Significant Damage (SD) in EN 1998-3, Life Safety (CG) in TBDY-16. Those performance levels show that buildings with discontinuity in diaphragms, designed with linear methods and subjected to the design earthquake may experience considerable damage, repairs may be required before reoccupancy but structures do not collapse.

- Although the performance levels obtained in the three codes are equivalent, according to the amount of elements on each performance level, TBDY-16 shows more damage than ASCE-41-13 and EN 1998-3. Therefore, for seismic performance assessment TBDY-16 is the most conservative one.

REFERENCES

AFAD, (2016), Türkiye Bina Deprem Yönetmeliği Taslağı, Afet ve Acıl Durum Yönetimi Başkanlığı TBDY-16.

ACI, (2014), Building Code Requirements for Structural Concrete, American Concrete Institute ACI 318-14.

ASCE, (2006), Seismic Rehabilitation Retrofit of Existing Buildings, American Society of Civil Engineers ASCE 41-06.

ASCE, (2013), Seismic Evaluation and Retrofit of Existing Buildings, American Society of Civil Engineers ASCE 41-13.

ASCE, (2010), Minimum Design Loads for Buildings and Other Structures, American Society of Civil Engineers ASCE 7-10.

ATC, (1996), Seismic Evaluation and Retrofit of Concrete Buildings, Applied Technology Council ATC-40.

Basu D., Jain S. (2004), "Seismic Analysis of Asymetric Buildings with Flexible Floor Diaphragms", Journal of Structural Engineering, 2004, 130(8): 1169-1176.

Başak K. (2013), "Perdeli taşıyıcı sistemlerin artımsal itme yöntemi ile deprem performasının değerlendirilmesi", Yüksek Lisans Tezi, Gebze Yüksek Teknoloji Enstitüsü, Fen Bilimleri Enstitüsü.

Bayındırlık ve İskan Bakanlığı (1998), Afet Bölgelerinde Yapılacak Yapılar Hakkında Yönetmelik ABYYHY-98.

Bayındırlık ve İskan Bakanlığı (2007), Deprem Bölgelerinde Yapılacak Binalar Hakkında Yönetmelik DBYBHY-07.

Çevre ve Şehircilik Bakanlığı (2008), Kıyı ve Liman yapılarıi Demiryolları, Hava Meydanları inşaatlarına ilişkin Deprem Teknik Yönetmeliği.

Eurocode, (2005), Design of structures for earthquake resistance – Part3: Assessment and retrofitting of building, European Committee for Standardization EN 1998-3.

FEMA, (1997), NEHRP Guidelines for the Seismic Rehabilitation of Building, Federal Emergency Management Agency FEMA 273.

FEMA, (2000), Prestandard and Commentary for the Seismic Rehabilitation of Building, Federal Emergency Management Agency FEMA 356.

Joel M., Mary D. (2004), "Diaphragm effects in rectangular reinforced concrete buildings", ACI Structural Journal, Sep/Oct2004, 101, 5, p615

Kunnath S., Panahshahi N., Reinhorn A. (1991) “Seismic Response of RC Buildings with Inelastic Floor Diaphragms”, Journal of Structural Engineering, 117, 4, April, 1991.

Özal A. (2008). “Evaluation of deformation capacity criteria of Eurocode 8”. Graduate Program Thesis. Boğaziçi University.

Mpampatsikos V., Nascimbene R., Petrini L. (2008). “A Critical Review of the R.C Frame Existing Building Assessment Procedure According to Eurocode 8 and Italian Seismic Code”, Journal of Earthquake engineering,12(S1):52-82,2008.

Roskelley B. (2010), “An Investigation of the Influence of Diaphragm Flexibility on Building Design through a Comparison of Forced Vibration Testing and Computational Analysis”. Master of Science Thesis. Faculty of California Polytechnic State University.

S. H. Ju, M. C. Lin (1999). “Comparison of Building analyses Assuming Rigid or Flexible Floors”, Journal of Structural Engineering, 125, 1, January.

Yıldız İ., (2015), “Perdeli ve perdesiz betonarme yapıların TDY 2007’ye gore değerlendirilmesi”, Yüksek Lisans Tezi. Aksaray Üniversitesi, Fen Bilimleri Enstitüsü.

BIOGRAPHY

Osleiner Enrique Gonzalez Valdez was born in 1988 in Maracaibo, Venezuela. Between 2005 and 2010 studied Civil Engineering in University of Zulia, Venezuela. In 2015 started his master studies in Gebze Technical University in Earthquake and Structural Engineering.

APPENDICES

Appendix A: Hinge Status

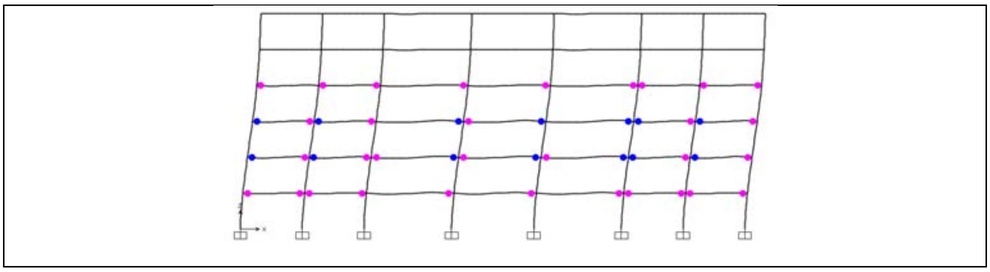

Figure A1.1: Hinge status at performance point, ASCE-41-13, Structure 1, Frame B.

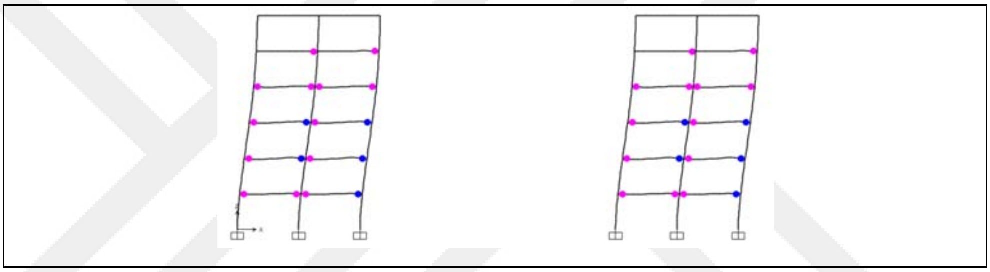

Figure A1.2: Hinge status at performance point, ASCE-41-13 Structure 1, Frame D.

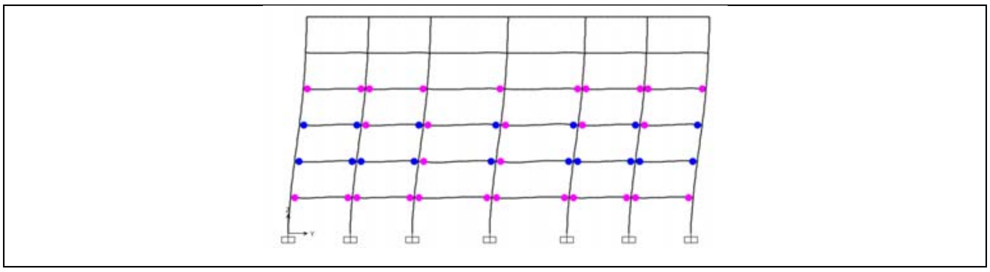

Figure A1.3: Hinge status at performance point, ASCE-41-13, Structure 1, Frame 2.

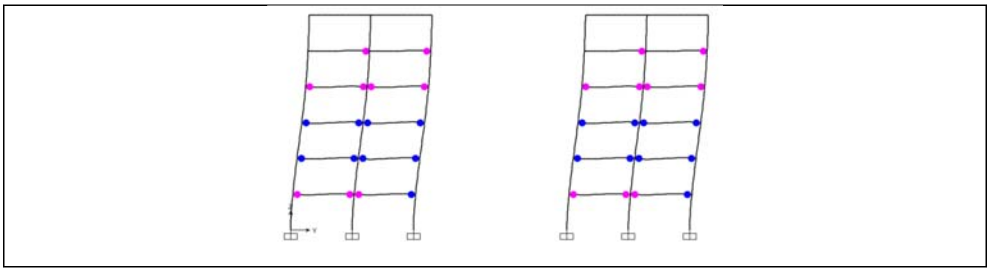

Figure A1.4: Hinge status at performance point, ASCE-41-13, Structure 1, Frame 4.

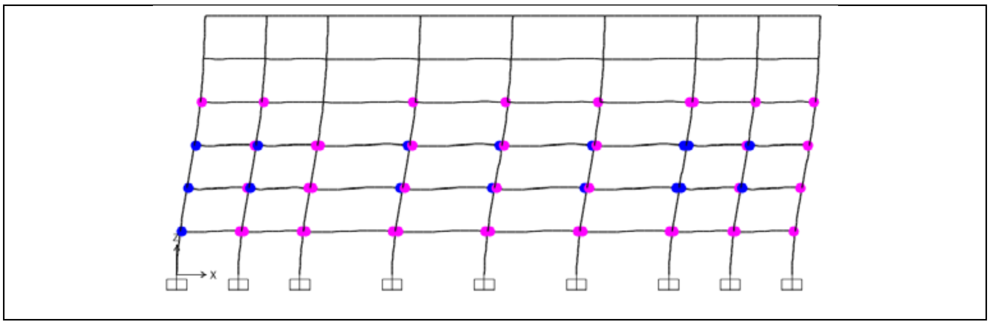

Figure A1.5: Hinge status at performance point, ASCE-41-13, Structure 2, Frame B.

Figure A1.6: Hinge status at performance point, ASCE-41-13, Structure 2, Frame D.

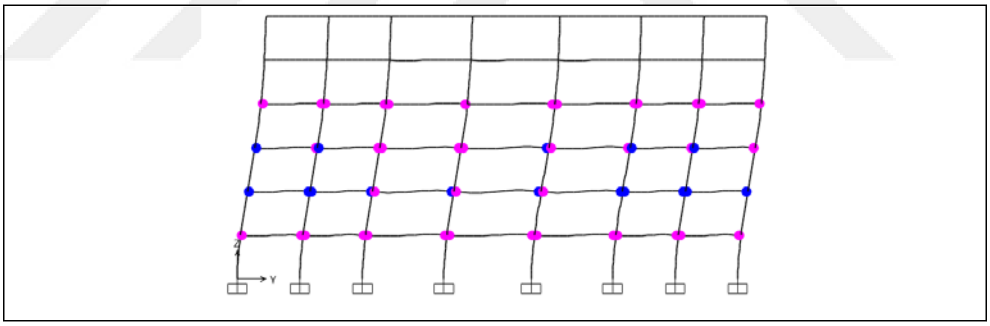

Figure A1.7: Hinge status at performance point, ASCE-41-13, Structure 2, Frame 2.

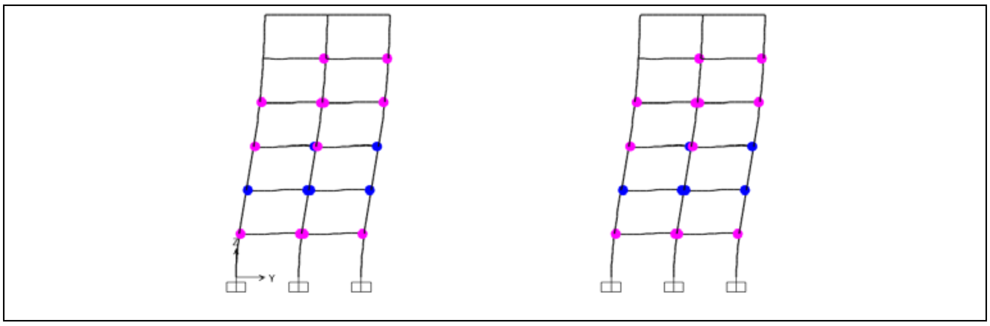

Figure A1.8: Hinge status at performance point, ASCE-41-13, Structure 2, Frame 5.

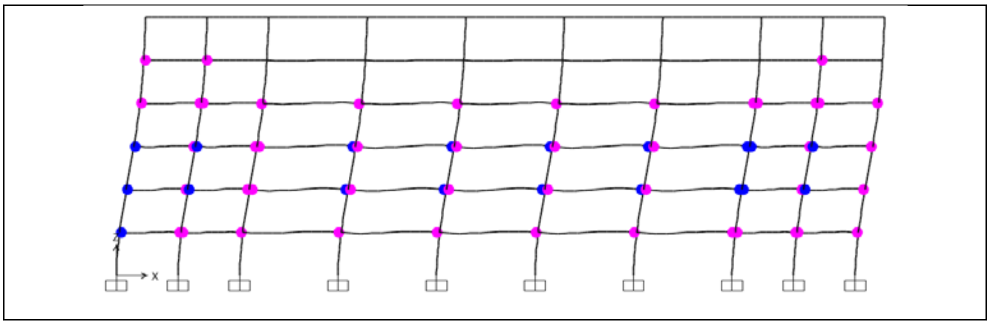

Figure A1.9: Hinge status at performance point, ASCE-41-13, Structure 3, Frame B.

Figure A1.10: Hinge status at performance point, ASCE-41-13, Structure 3, Frame E.

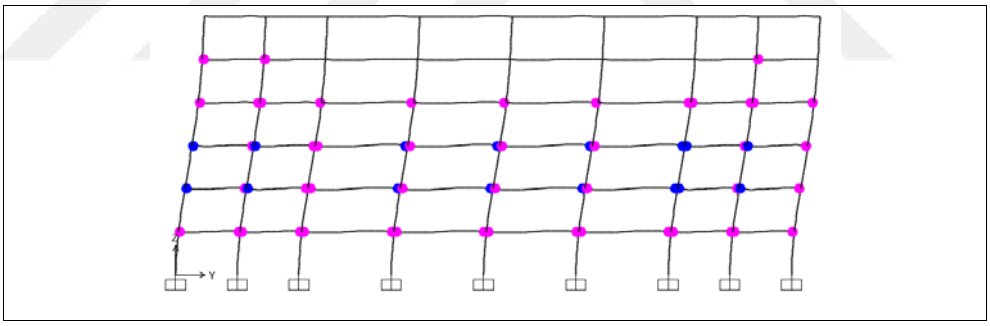

Figure A1.11: Hinge status at performance point, ASCE-41-13, Structure 3, Frame 2.

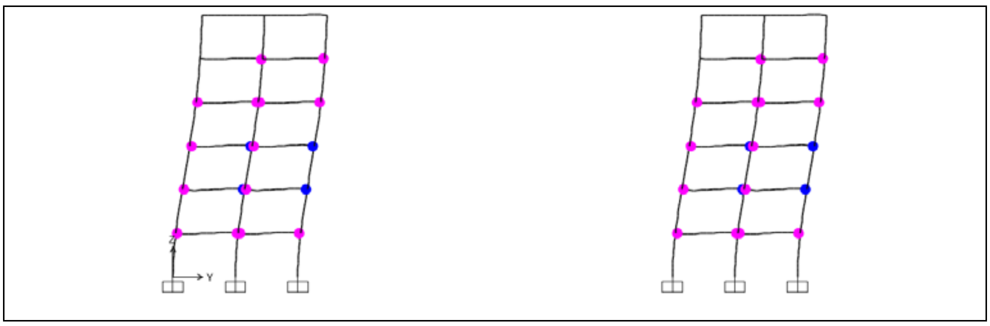

Figure A1.12: Hinge status at performance point, ASCE-41-13, Structure 3, Frame 5.

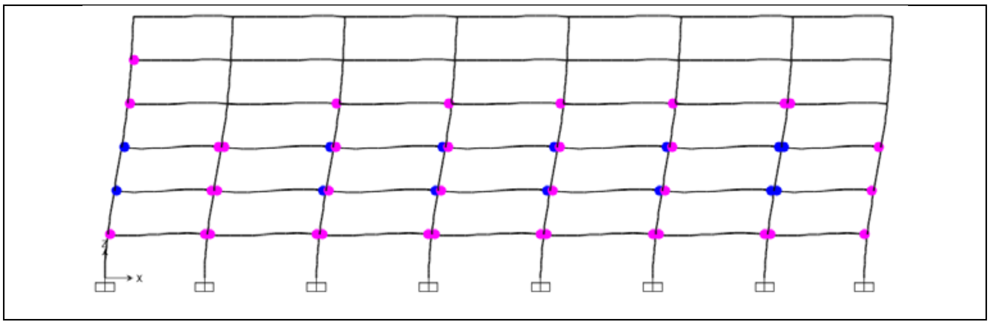

Figure A1.13: Hinge status at performance point, ASCE-41-13, Structure 4,Frame A.

Figure A1.14: Hinge status at performance point, ASCE-41-13, Structure 4,Frame D.

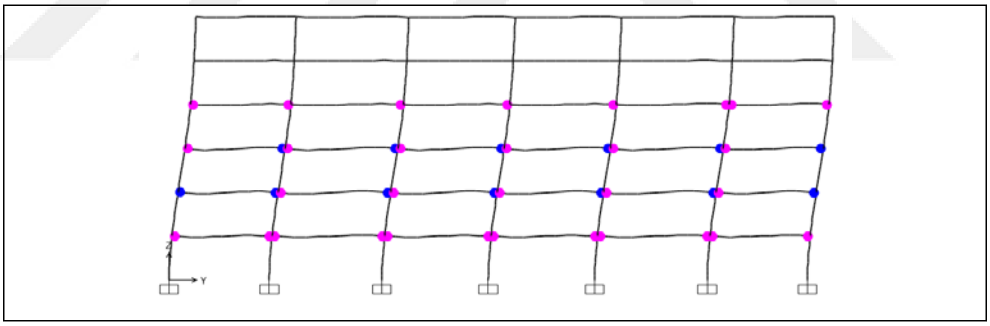

Figure A1.15: Hinge status at performance point, ASCE-41-13, Structure 4, Frame 1.

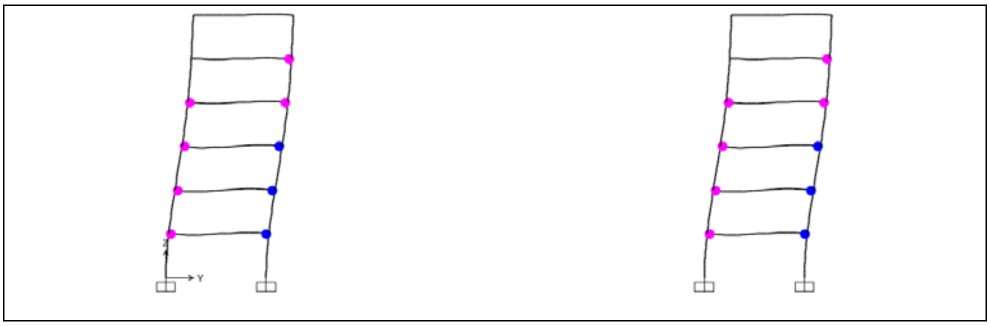

Figure A1.16: Hinge status at performance point, ASCE-41-13, Structure 4, Frame 4.

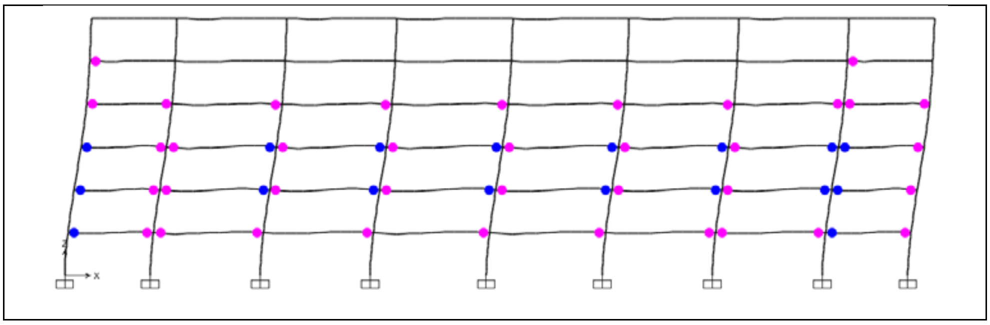

Figure A1.17: Hinge status at performance point, ASCE-41-13, Structure 5,Frame A.

Figure A1.18: Hinge status at performance point, ASCE-41-13, Structure 5,Frame D.

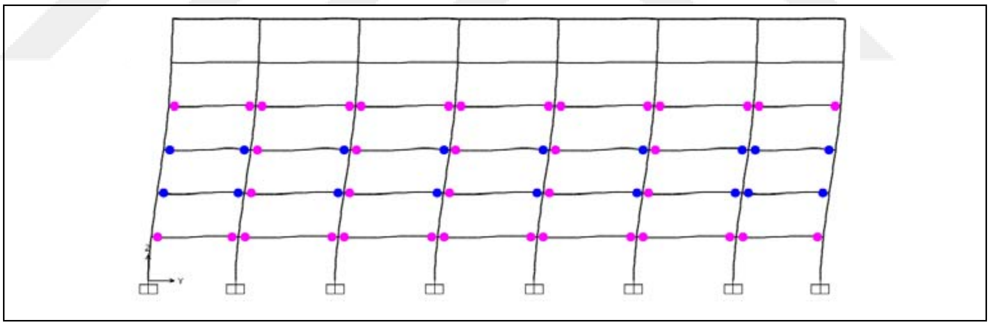

Figure A1.19: Hinge status at performance point, ASCE-41-13, Structure 5, Frame 1.

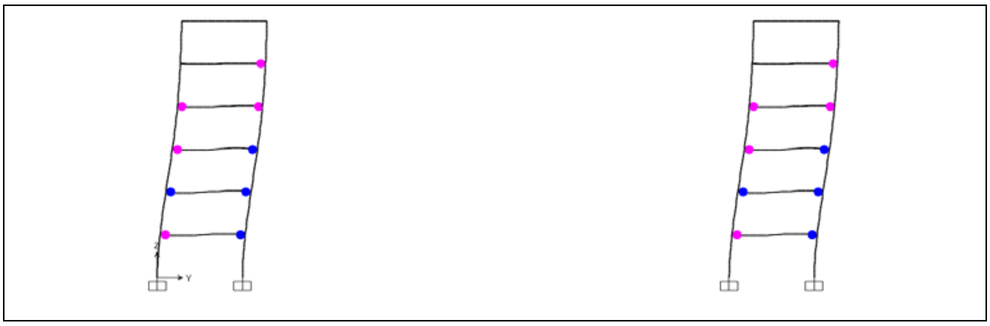

Figure A1.20: Hinge status at performance point, ASCE-41-13, Structure 5, Frame 5.

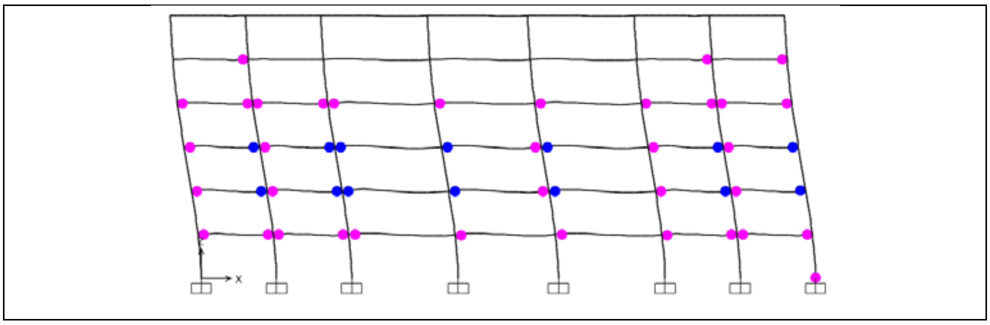

Figure A1.21: Hinge status at performance point, EN 1998-3, Structure 1, Frame B.

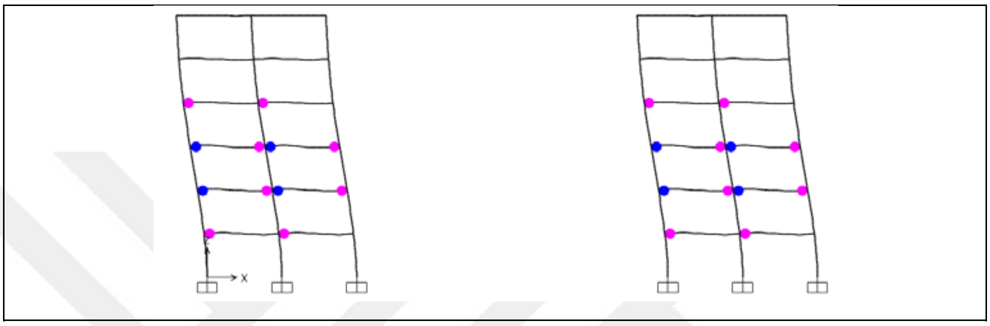

Figure A1.22: Hinge status at performance point, EN 1998-3, Structure 1, Frame D.

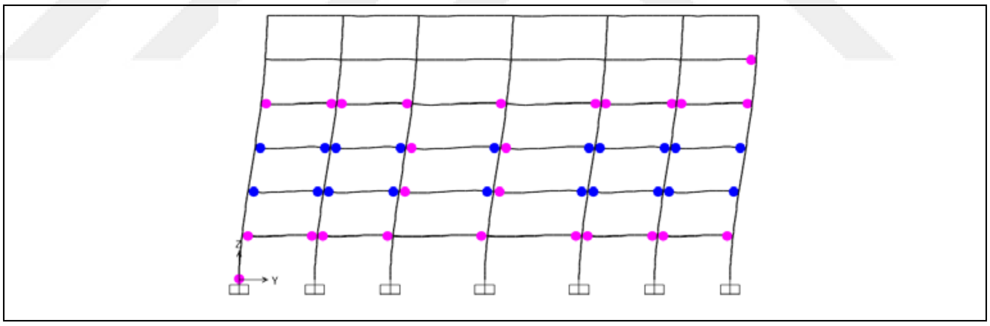

Figure A1.23: Hinge status at performance point, EN 1998-3, Structure 1, Frame 2.

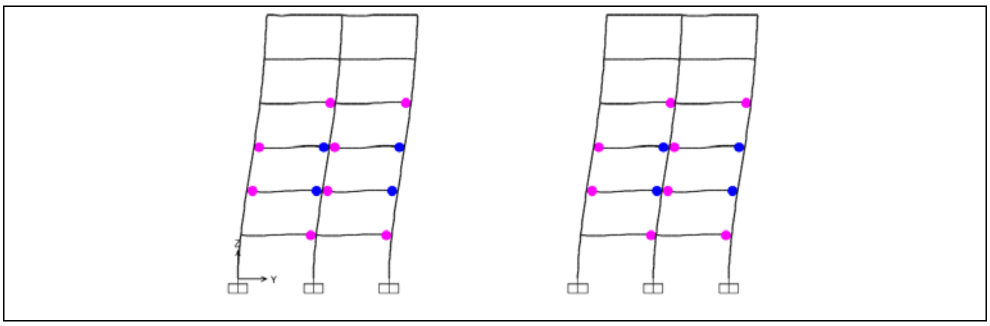

Figure A1.24: Hinge status at performance point, EN 1998-3, Structure 1, Frame 4.

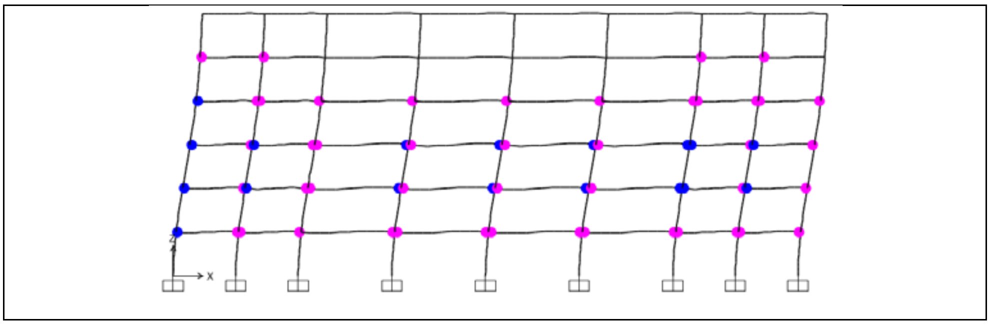

Figure A1.25: Hinge status at performance point, EN 1998-3, Structure 2, Frame B.

Figure A1.26: Hinge status at performance point, EN 1998-3, Structure 2, Frame D.

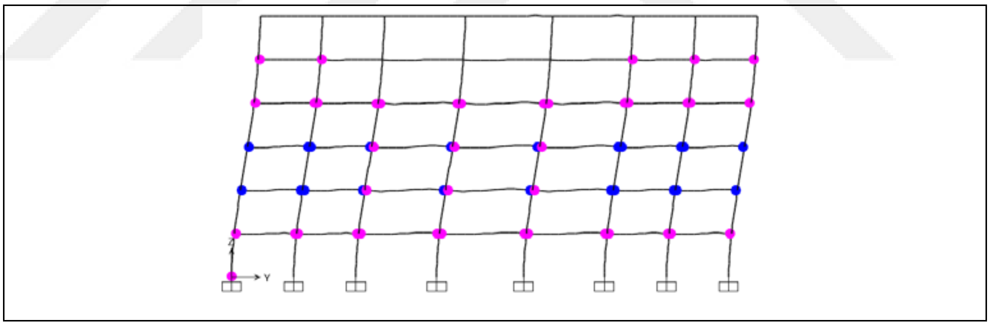

Figure A1.27: Hinge status at performance point, EN 1998-3, Structure 2, Frame 2.

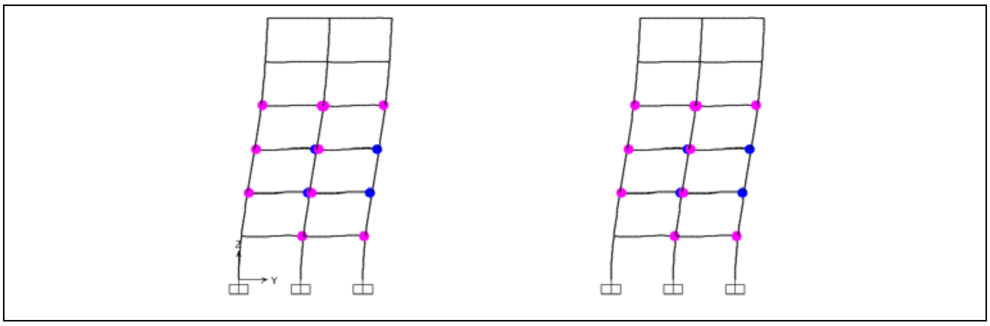

Figure A1.28: Hinge status at performance point, EN 1998-3, Structure 2, Frame 5.

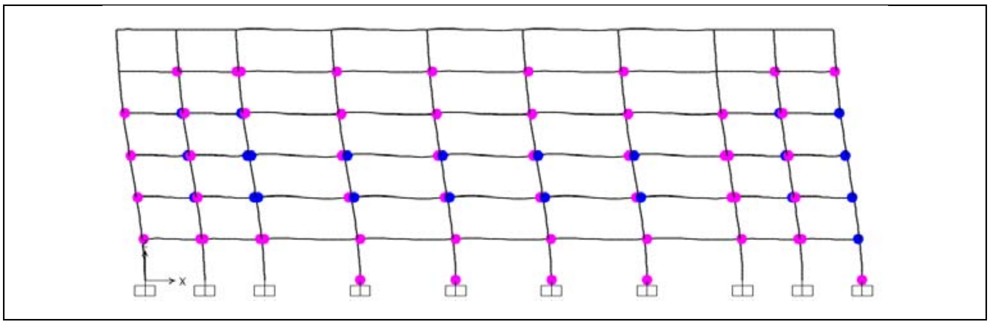

Figure A1.29: Hinge status at performance point, EN 1998-3, Structure 3, Frame B.

Figure A1.30: Hinge status at performance point, EN 1998-3, Structure 3, Frame E.

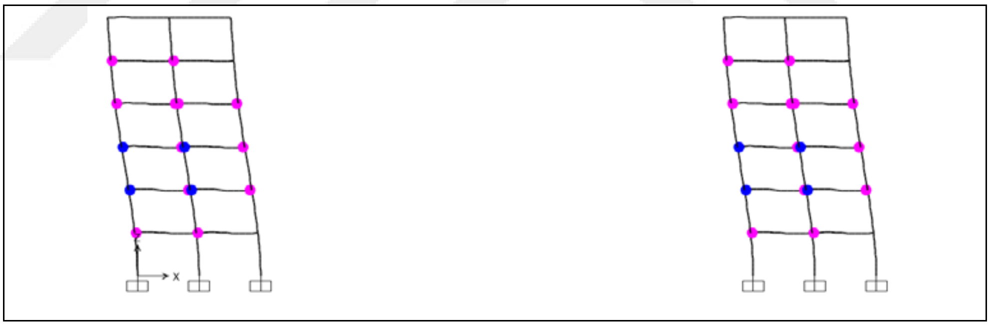

Figure A1.31: Hinge status at performance point, EN 1998-3, Structure 3, Frame 2.

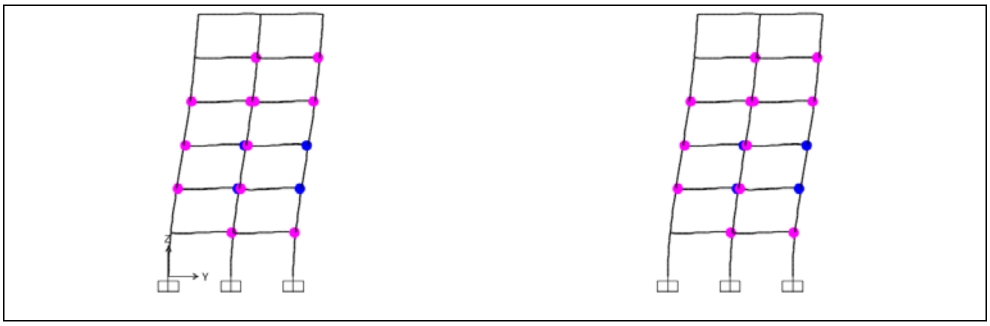

Figure A1.32: Hinge status at performance point, EN 1998-3, Structure, 3, Frame 5.

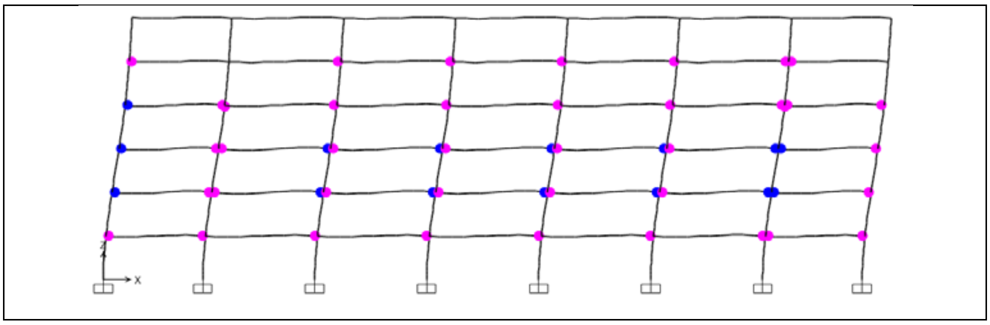

Figure A1.33: Hinge status at performance point, EN 1998-3, Structure 4, Frame A.

Figure A1.34: Hinge status at performance point, EN 1998-3, Structure 4, Frame D.

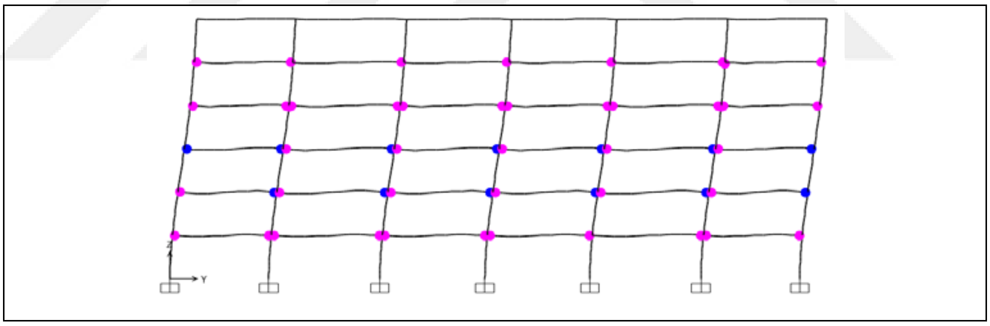

Figure A1.35: Hinge status at performance point, EN 1998-3, Structure 4, Frame 1.

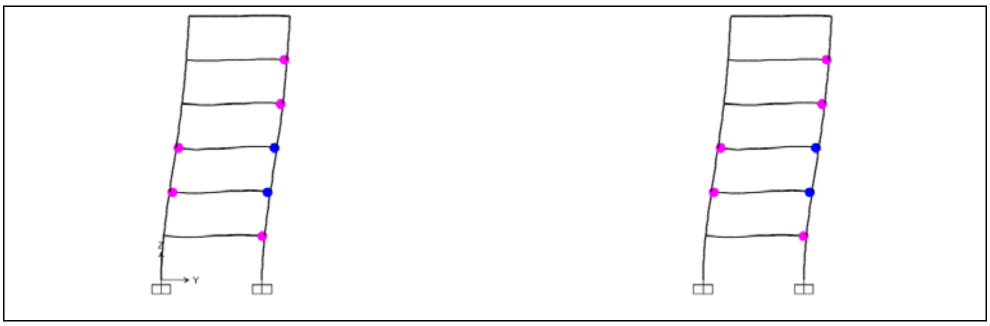

Figure A1.36: Hinge status at performance point, EN 1998-3, Structure, 4, Frame 4.

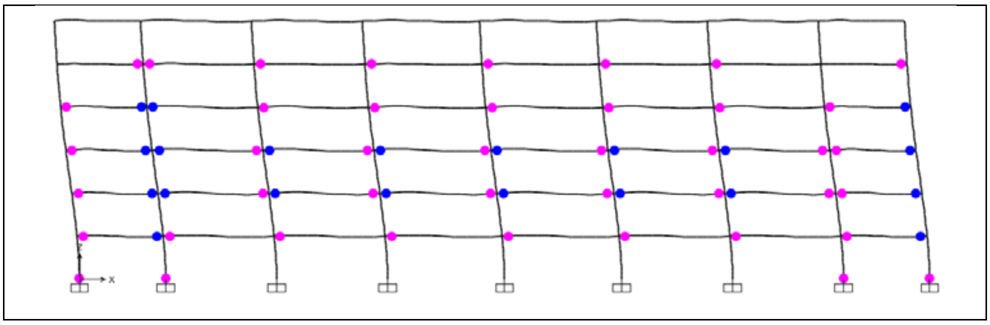

Figure A1.37: Hinge status at performance point, EN 1998-3, Structure 5, Frame A.

Figure A1.38: Hinge status at performance point, EN 1998-3, Structure 5, Frame D.

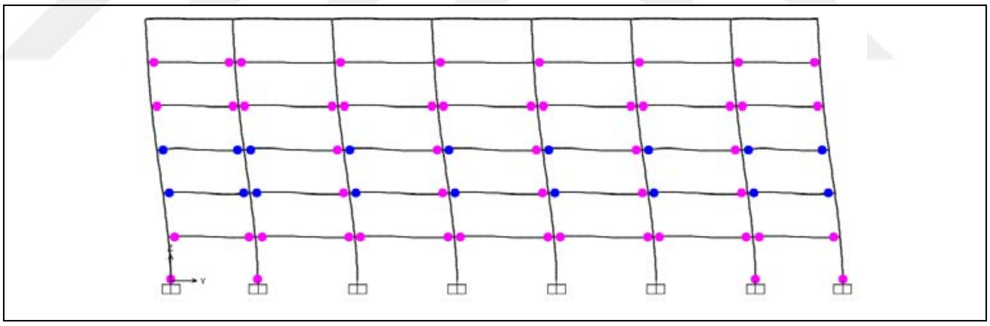

Figure A1.39: Hinge status at performance point, EN 1998-3, Structure 5, Frame 1.

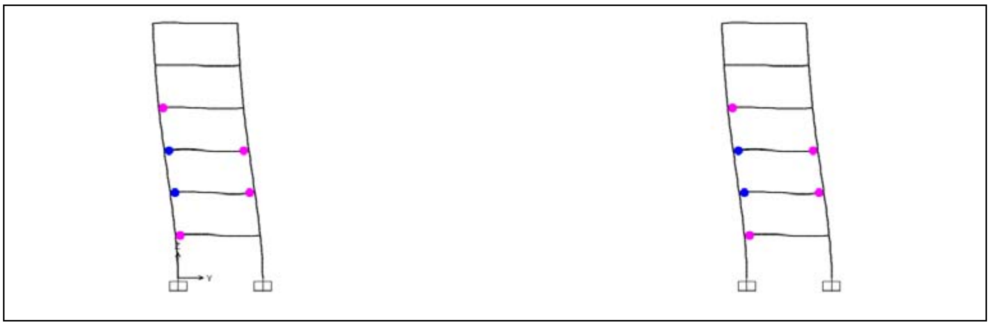

Figure A1.40: Hinge status at performance point, EN 1998-3, Structure, 5, Frame 5.

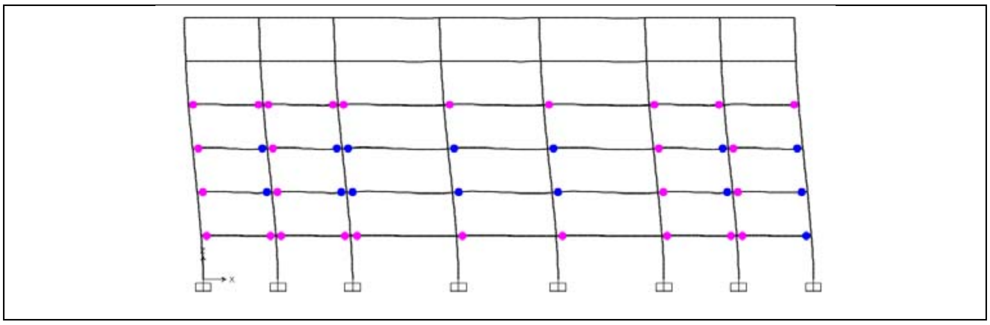

Figure A1.41: Hinge status at performance point, TBDY-16, Structure 1, Frame B.

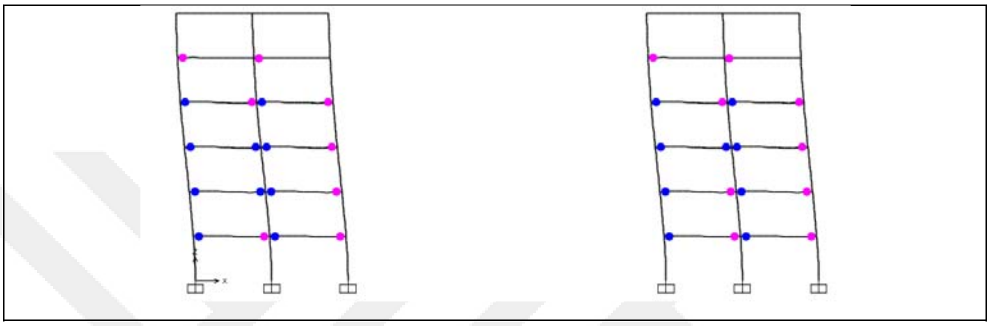

Figure A1.42: Hinge status at performance point, TBDY-16, Structure 1, Frame D.

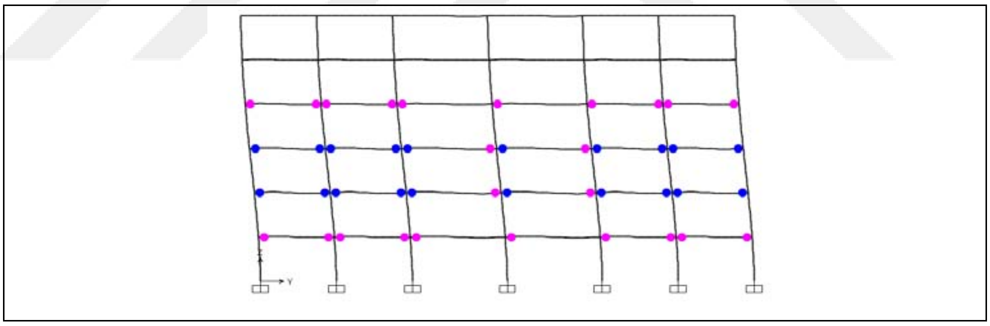

Figure A1.43: Hinge status at performance point, TBDY-16, Structure 1, Frame 2.

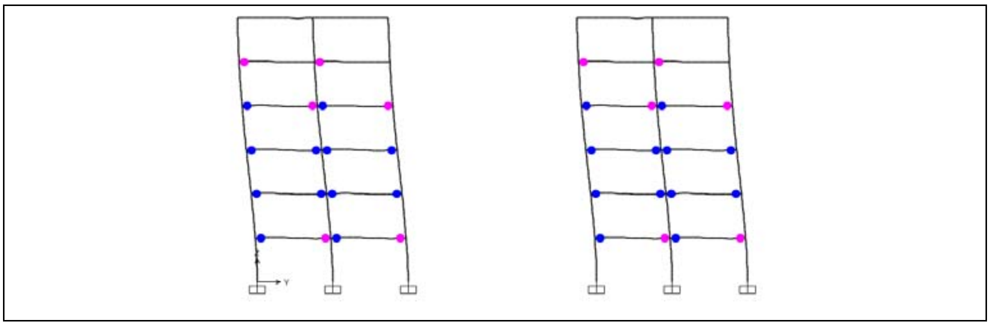

Figure A1.44: Hinge status at performance point, TBDY-16, Structure, 1, Frame 4.

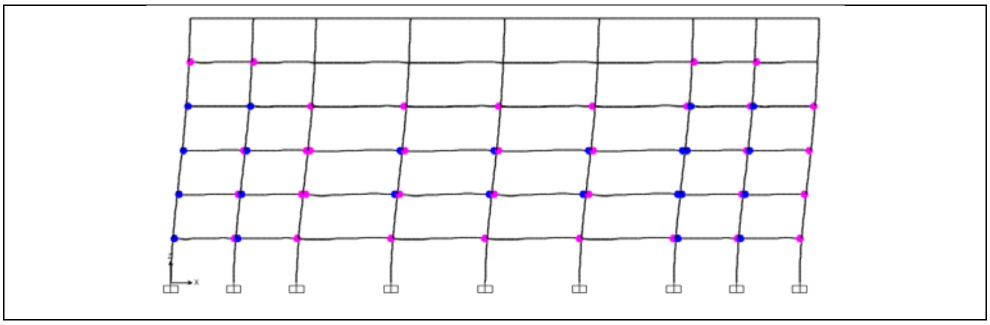

Figure A1.45: Hinge status at performance point, TBDY-16, Structure 2, Frame B.

Figure A1.46: Hinge status at performance point, TBDY-16, Structure 2, Frame D.

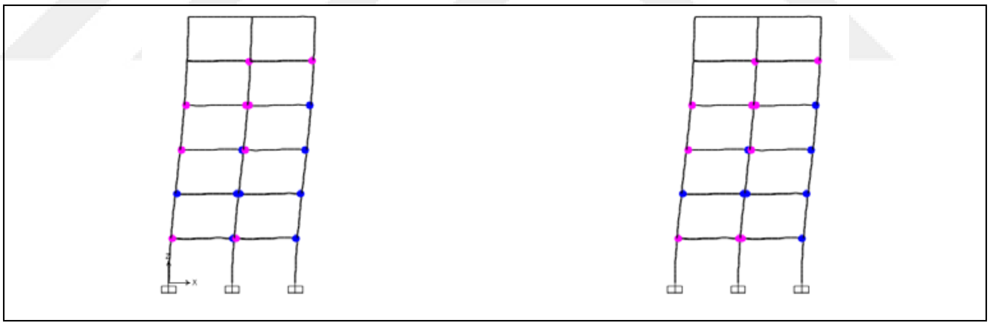

Figure A1.47: Hinge status at performance point, TBDY-16, Structure 2, Frame 2.

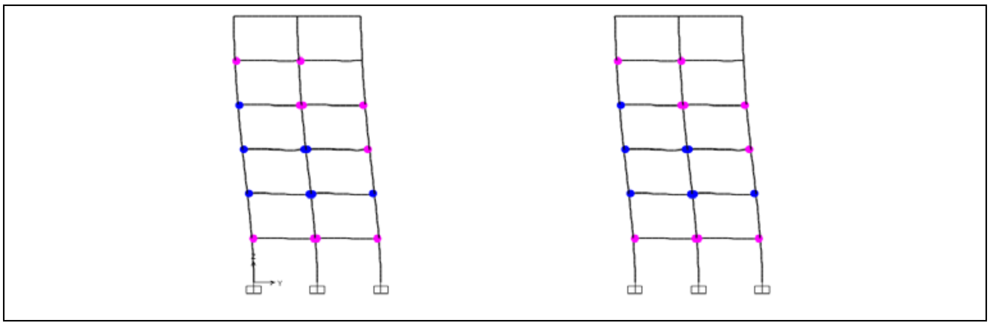

Figure A1.48: Hinge status at performance point, TBDY-16, Structure, 2, Frame 5.

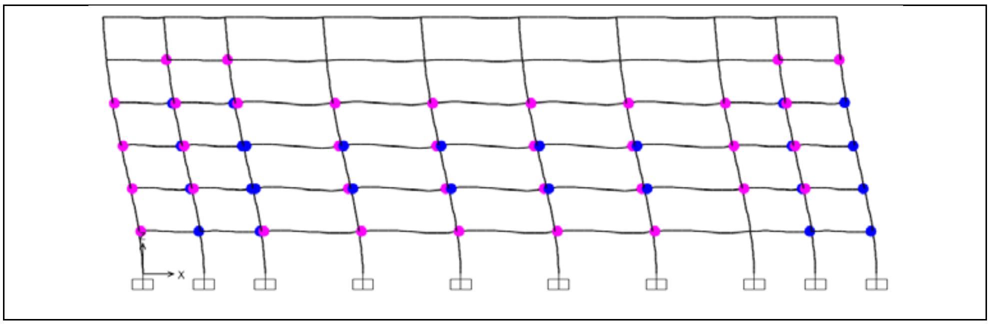

Figure A1.49: Hinge status at performance point, TBDY-16, Structure 3, Frame B.

Figure A1.50: Hinge status at performance point, TBDY-16, Structure 3, Frame E.

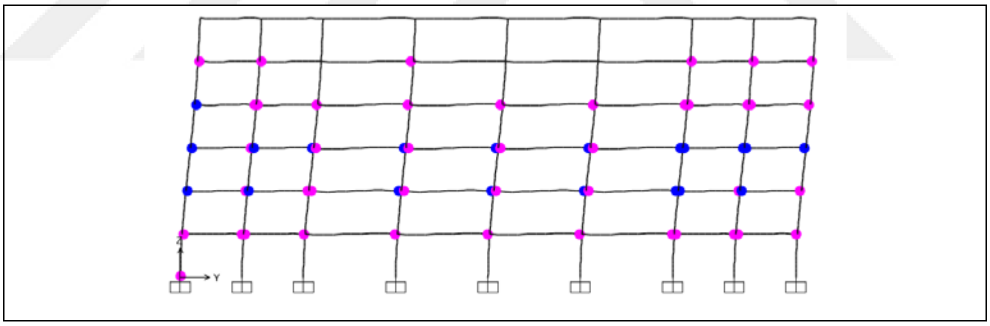

Figure A1.51: Hinge status at performance point, TBDY-16, Structure 3, Frame 2.

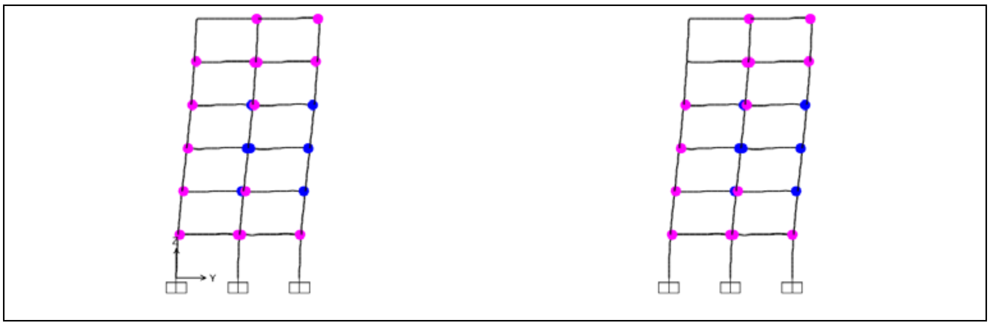

Figure A1.52: Hinge status at performance point, TBDY-16, Structure, 3, Frame 5.

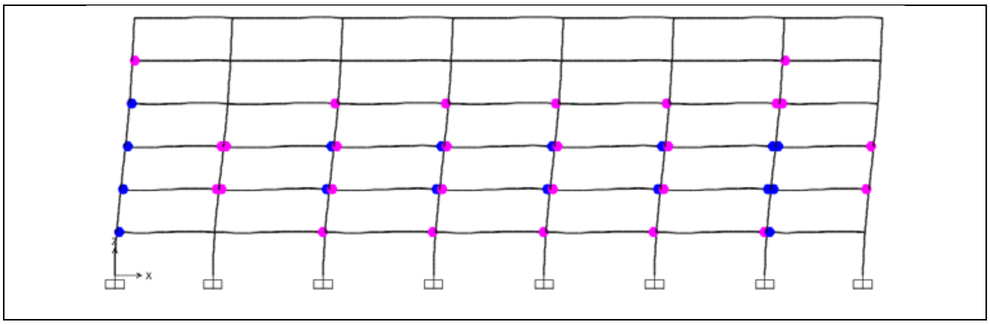

Figure A1.53: Hinge status at performance point, TBDY-16, Structure 4, Frame A.

Figure A1.54: Hinge status at performance point, TBDY-16, Structure 4, Frame D.

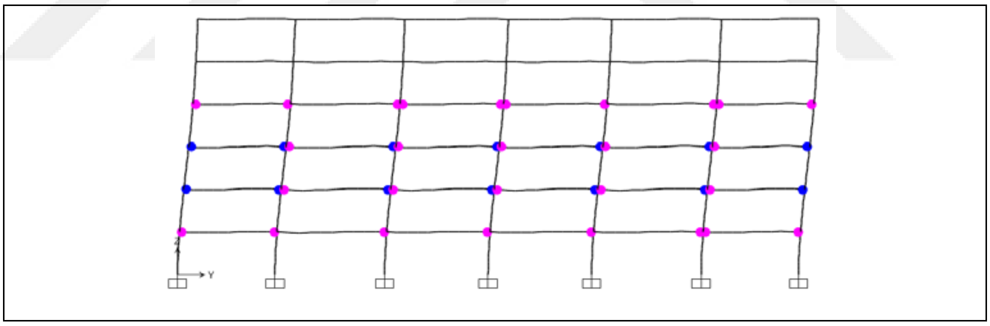

Figure A1.55: Hinge status at performance point, TBDY-16, Structure 4, Frame 1.

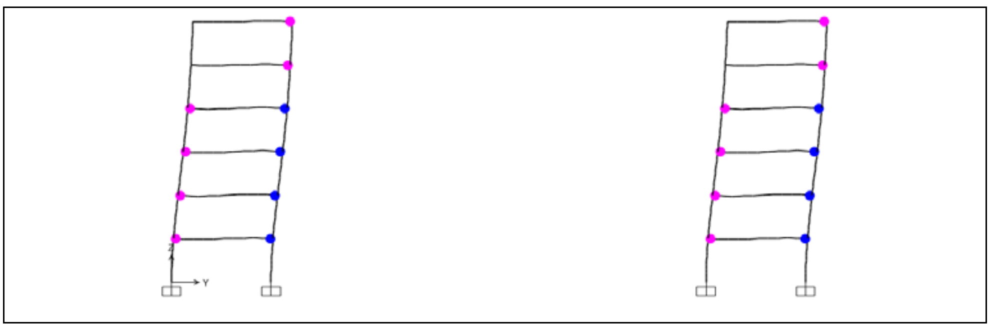

Figure A1.56: Hinge status at performance point, TBDY-16, Structure, 4, Frame 4.

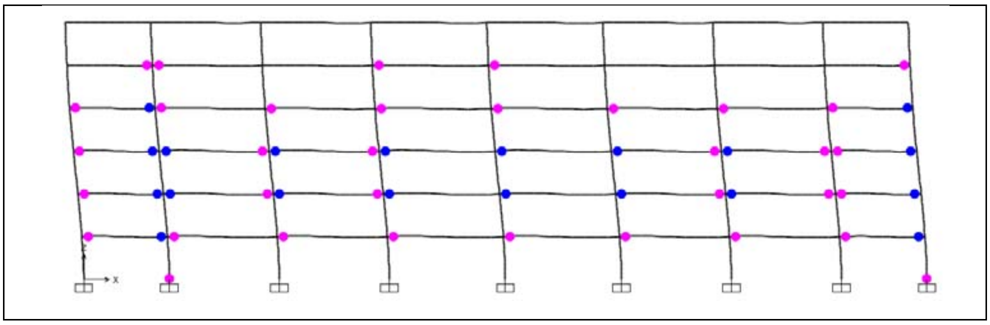

Figure A1.57: Hinge status at performance point, TBDY-16, Structure 5, Frame A.

Figure A1.58: Hinge status at performance point, TBDY-16, Structure 5, Frame D.

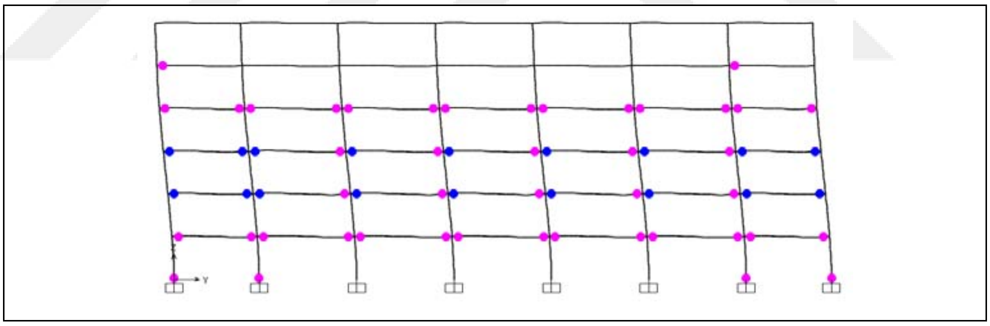

Figure A1.59: Hinge status at performance point, TBDY-16, Structure 5, Frame 1.

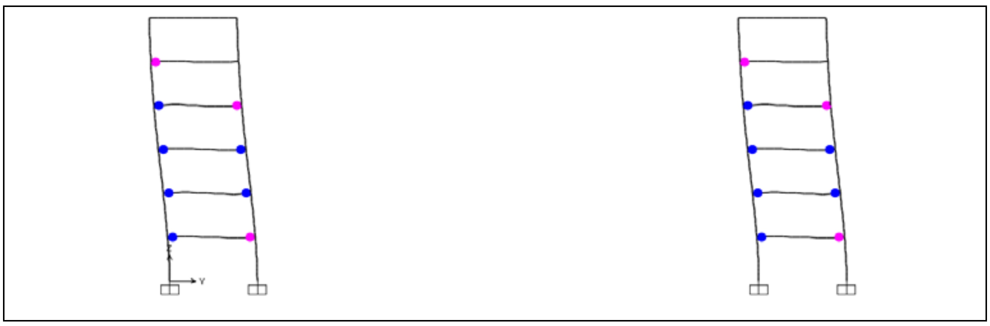

Figure A1.60: Hinge status at performance point, TBDY-16, Structure, 5, Frame 5.